THE OSTEOLOGY OF *BALAUR BONDOC*, AN ISLAND-DWELLING DROMAEOSAURID (DINOSAURIA: THEROPODA) FROM THE LATE CRETACEOUS OF ROMANIA

STEPHEN L. BRUSATTE
Division of Paleontology
American Museum of Natural History, Central Park West at 79th Street, New York, NY 10024
Department of Earth and Environmental Sciences
Columbia University, New York, NY; and
School of GeoSciences
University of Edinburgh, Grant Institute, Edinburgh, Scotland

MÁTYÁS VREMIR
Department of Natural Sciences
Transylvanian Museum Society (EME)
Cluj-Napoca, Romania

ZOLTÁN CSIKI-SAVA
Department of Geology
University of Bucharest, Bucharest, Romania

ALAN H. TURNER
Department of Anatomical Sciences
Stony Brook University, Stony Brook, NY

AKINOBU WATANABE
Department of Biological Science
Florida State University, Tallahassee, FL; and
Richard Gilder Graduate School, American Museum of Natural History

GREGORY M. ERICKSON
Department of Biological Science
Florida State University, Tallahassee, FL

MARK A. NORELL
Division of Paleontology
American Museum of Natural History, and
Department of Earth and Environmental Sciences
Columbia University, New York, NY

BULLETIN OF THE AMERICAN MUSEUM OF NATURAL HISTORY
Number 374, 100 pp., 49 figures, 7 tables
Issued February 13, 2013

Copyright © American Museum of Natural History 2013 ISSN 0003-0090

CONTENTS

Abstract 3
Introduction 3
Institutional acronyms 4
Systematic paleontology 5
  Holotype 5
  Type locality 7
  Diagnosis 11
  Additional material 12
  Locality of additional material 12
  Systematics of additional material 12
Description 14
Axial Skeleton 14
    Dorsal vertebrae 14
    Sacral vertebrae 19
    Caudal vertebrae 21
  Pectoral girdle and forelimb 22
    Sternum 22
    Scapulocoracoid 23
    Humerus 26
    Referred humerus 29
    Ulna 29
    Referred ulna 34
    Radius 34
    Carpometacarpus 34
    Referred manual metacarpal 40
    Manual digits 41
    Manual digit I 42
    Manual digit II 46
    Manual digit III 47
    Referred phalanges 47
  Pelvic girdle 49
    Pelvic crushing 49
    Ilium 54
    Pubis 55
    Ischium 56
  Hind limb 57
    Tibiotarsus 57
    Tarsometatarsus 68
    Pedal digits 72
Histology and growth stage 75
  Holotype specimen 77
  Referred specimen 78
Phylogeny 78
Discussion 79
  The European Late Cretaceous theropod record 79
    Romanian specimens 81
    Hungarian specimens 82
    French specimens 82
  European Late Cretaceous dinosaur biogeography 83
  Balaur: an island-dwelling theropod 88
Acknowledgments 93
References 94

ABSTRACT

The Haţeg Island fauna of the terminal Late Cretaceous (ca. 71–65 million years ago) of Romania is one of the most unusual dinosaur assemblages in the global fossil record. It has long been recognized that many herbivorous dinosaurs from the Haţeg fauna were dwarfed, morphologically aberrant, and/or primitive relative to mainland contemporaries, and these taxa are often considered examples of the so-called island effect: the evolutionary phenomenon by which island-dwelling species are often dwarfed and anatomically modified. Very little, however, is known about the carnivorous dinosaurs that inhabited Haţeg Island, and it is unclear whether they were also dwarfed, aberrant, or primitive. In 2009, the discovery of the first substantially complete theropod from the Late Cretaceous of Europe, the holotype of the Romanian dromaeosaurid *Balaur bondoc*, provided the first clear glimpse at an island-dwelling carnivorous dinosaur. Here we describe and figure this remarkably preserved skeleton in detail. We provide detailed descriptions and photographs of individual bones, and make extensive comparisons with other dromaeosaurids (and other derived coelurosaurian theropods).

This monographic description provides further evidence that *Balaur* is an unusual derived dromaeosaurid, closely related to *Velociraptor*, with a remarkably modified hand and foot skeleton, including a stocky and heavily fused distal hind limb, a double set of hyperextensible pedal claws, and a fused and atrophied hand, which are otherwise unknown among derived coelurosaurian theropods. We present an updated diagnosis of *Balaur* based on additional preparation of the holotype, comparisons with other dromaeosaurids, and careful consideration of postmortem crushing. Histological techniques demonstrate that both the holotype and a referred specimen of *Balaur*, which is approximately 50% larger than the holotype and from a separate locality, belong to mature individuals. Therefore, we remove the referred specimen from *Balaur bondoc* and conservatively consider it *Balaur* sp. We present an updated assessment of the phylogenetic relationships of *Balaur* based on a comprehensive new coelurosaurian cladistic dataset, which corroborates the close relationship between *Balaur*, *Velociraptor*, *Deinonychus*, *Adasaurus*, and *Saurornitholestes*. We review the fossil record of European Late Cretaceous theropods and show that other specimens from the Late Cretaceous of Romania (including the holotype of *Elopteryx*), France, and Hungary either do not belong to *Balaur* (due to the lack of *Balaur* autapomorphies) or cannot be compared to *Balaur* because of a lack of overlapping material. Finally, we discuss the biogeographic history of European terminal Cretaceous dinosaur faunas and comment on the extreme morphological specializations of *Balaur*. We conclude that the phylogenetic position of *Balaur*, a derived dromaeosaurid closely related to Late Cretaceous Laurasian taxa, is inconsistent with previous hypotheses of long-term geographic endemicity of the Romanian island faunas, but argue that the aberrant Bauplan of *Balaur* is similar to that seen in some living and recently extinct mammals and thus likely due to the "island effect."

INTRODUCTION

One of the most bizarre dinosaur faunas of the Mesozoic was the so-called Haţeg Island fauna of the terminal Late Cretaceous (ca. 71–65 million years ago) of Romania. During the terminal Cretaceous, a time of warm temperatures and high sea levels, Europe was fragmented into a series of island archipelagoes (e.g., Csontos and Vörös, 2004). The terrestrial vertebrates inhabiting these islands, especially the "Haţeg Island," are among the most morphologically peculiar dinosaurs in the global fossil record. Dating back to the pioneering studies of Baron Franz Nopcsa, it has been widely recognized that many herbivorous dinosaurs from the Haţeg fauna were dwarfed, morphologically aberrant, and/or strikingly primitive relative to contemporaries from mainland continents (e.g., Nopcsa, 1914; Weishampel et al., 1991; Benton et al., 2010; Weishampel and Jianu, 2011). These fossils are often touted as a prime example of the "island effect": the evolutionary phenomenon where island-dwelling species are often smaller and anatomically distinct compared to close mainland relatives (e.g., Foster, 1964; Van Valen, 1973; Lomolino, 1985, 2005; Lomolino et al., 2006; Benton et al., 2010).

Fossils of herbivorous dinosaurs such as ornithopods and sauropods are fairly common

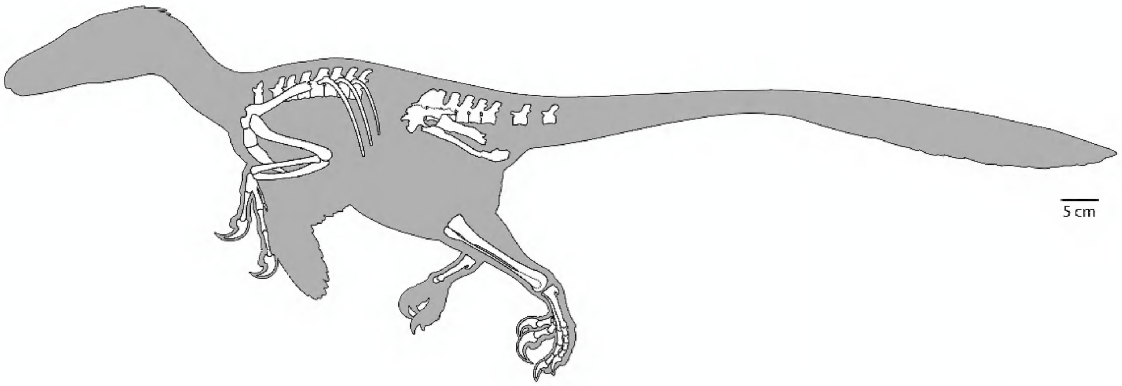

Fig. 1. A sketal drawing of *Balaur bondoc* indicating which bones are represented in the the holotype specimen (EME PV.313). Illustration by Mick Ellison, American Museum of Natural History.

discoveries in the Upper Cretaceous continental units of southern Transylvania (Romania). These specimens have formed the basis for almost all previous discussion of the "island effect" in dinosaur faunas. In contrast, very little is known about the carnivorous dinosaurs that inhabited Haţeg Island, or any other Mesozoic islands, as their fossils are mostly restricted to isolated teeth and other fragmentary remains (Weishampel et al., 2004). It has long been unclear whether island-dwelling predatory dinosaurs were also dwarfed, aberrant, or primitive, or whether the "island effect" had little influence on these animals. The recent discovery of a substantially complete skeleton of a Late Cretaceous Romanian theropod, *Balaur bondoc*, provides the first clear glimpse at an island-dwelling carnivorous dinosaur. This specimen was briefly described in a short paper by Csiki et al. (2010a), who showed that it represented a dromaeosaurid theropod, closely related to *Velociraptor*, which was morphologically aberrant but not primitive and apparently not dwarfed (fig. 1).

Here we describe and figure the remarkably preserved holotype skeleton of *Balaur bondoc* in detail. This monographic description provides further evidence that *Balaur* is an unusual, extremely specialized dromaeosaurid with a remarkably modified hand and foot skeleton, including two hyperextensible pedal claws per foot and a fused and atrophied hand that are otherwise unknown among derived coelurosaurian theropods. We update the diagnosis of *Balaur* based on new preparation of the holotype and comparisons with other dromaeosaurids, and use histological techniques to assess the age and growth stage of both the holotype and putative referred specimens of *Balaur* from another locality in Romania. We also present an updated appraisal of the phylogenetic relationships of *Balaur* based on the comprehensive new coelurosaurian cladistic dataset of Turner et al. (2012). Finally, we review the fossil record of European Late Cretaceous theropods, discuss the biogeographic history of European terminal Cretaceous dinosaur faunas, and comment on the extreme morphological specializations of *Balaur*, which were likely due to the island effect.

INSTITUTIONAL ACRONYMS

The following acronyms are used throughout this work:

AMNH-FARB	American Museum of Natural History, New York, New York
CAGS	Chinese Academy of Geological Sciences, Beijing, People's Republic of China
EME PV.	Vertebrate Paleontology Collection, Transylvanian Museum Society, Cluj-Napoca, Romania
IGM	Institute of Geology, Ulaan Baatar, Mongolia

TABLE 1
Measurements of dorsal and caudal vertebrae (in mm) of the holotype of *Balaur bondoc* (EME PV. 313)

Number	Length	Anterior depth	Anterior width	Posterior depth	Posterior width
Dorsal Vertebrae					
A	12	13	11	?	?
B	?	?	?	?	?
C	14	11	?	10	?
D	16	11	?	10	?
E	15	11	?	12	?
F	14	11	?	12	7
G	11	13	?	12	?
H	12	12	?	12	10
Caudal Vertebrae					
1	?	?	?	?	?
2	17	?	?	10	11
3	19	11	11	10	10
D	22	?	?	11	10
E	26	11	9	12	10

IVPP	Institute of Vertebrate Paleontology and Paleoanthropology, Beijing, People's Republic of China
LPB (FGGUB)	Paleontology Collection, Faculty of Geology and Geophysics, University of Bucharest, Bucharest, Romania
MCF	Museo Carmen Funes, Plaza Huincul, Argentina
MPCA	Museo Provincial Carlos Ameghino, Cipolletti, Argentina
TMP	Royal Tyrrell Museum of Palaeontology, Drumheller, Alberta, Canada
YPM	Yale Peabody Museum of Natural History, New Haven, Connecticut

SYSTEMATIC PALEONTOLOGY

Theropoda Marsh, 1881
Tetanurae Gauthier, 1986
Coelurosauria Huene, 1914
Maniraptora Gauthier, 1986
Paraves Sereno, 1997
Deinonychosauria Colbert and Russell, 1969
Dromaeosauridae Matthew and Brown, 1922
Balaur Csiki et al., 2010
Balaur bondoc Csiki et al., 2010

HOLOTYPE: EME PV. 313. Fragmentary skeleton found partly articulated and belonging to a single individual, including: 8 dorsal vertebrae (7 in articulated series); rib fragments; sacrum and associated caudosacral vertebrae; 4 proximal-middle caudal vertebrae; both left and right scapulocoracoids, humeri, ulnae, and radii; complete right carpometacarpus as well as left metacarpals I and II; complete right manus and complete digits I and II of left manus; articulated pelvis with acetabular region of both ilia together with fragmentary left and right pubes and ischia; left tibiotarsus and fibula, tarsometatarsus, and complete foot in articulation; and almost complete right tarsometatarsus. Associated sternal plates were observed and mapped in the field, but were recovered in a fragmentary state. Neurocentral sutures are closed in all dorsal and caudal vertebrae, suggesting that the holotype individual was mature or nearing skeletal maturity. This is corroborated by histological evidence: the presence of dense Haversian bone and substantially diminished spacing between lines of arrested growth (LAGs) near the periosteal surface suggests that this individual was somatically mature (see below for full explanation of histology), and no less than seven years of age (based on LAGs). A skeletal reconstruction of the holotype is presented

TABLE 2
Measurements of appendicular bones (in mm) of the holotype of *Balaur bondoc* (EME PV. 313)
Asterisk indicates incomplete measurement due to damage.

Humerus (right element)
- Proximodistal length: 117
- Proximal end, anteroposterior: 6
- Proximal end, mediolateral: 31
- Distal end, anteroposterior: 7
- Distal end, mediolateral: 27
- Midshaft, anteroposterior: 10
- Midshaft, mediolateral: 10

Ulna (left element)
- Proximodistal length: 99
- Proximal end, anteroposterior: 12
- Proximal end, mediolateral: 11
- Distal end, anteroposterior: 8
- Distal end, mediolateral: 11
- Midshaft, anteroposterior: 6
- Midshaft, mediolateral: 7

Radius (right element)
- Proximodistal length: 95
- Proximal end, anteroposterior: 12
- Proximal end, mediolateral: 5
- Distal end, anteroposterior: 10
- Distal end, mediolateral: 5
- Midshaft, anteroposterior: 7
- Midshaft, mediolateral: 6

Metacarpal I (right element)
- Proximodistal length: 18
- Distal end, dorsoventral: 6
- Distal end, mediolateral: 9
- Midshaft, dorsoventral: 4
- Midshaft, mediolateral: 10

Metacarpal II (right element)
- Proximodistal length: 41
- Distal end, dorsoventral: 7
- Distal end, mediolateral: 12
- Midshaft, dorsoventral: 5
- Midshaft, mediolateral: 7

Metacarpal III (right element)
- Proximodistal length: 39
- Proximal end, dorsoventral: 9
- Proximal end, mediolateral: 3
- Distal end, dorsoventral: 4
- Distal end, mediolateral: 3
- Midshaft, dorsoventral: 3
- Midshaft, mediolateral: 2

Manual Digit I, Phalanx I-1 (left element)
- Proximodistal length: 40
- Proximal end, dorsoventral: 10
- Proximal end, mediolateral: 11

TABLE 2
Continued

- Distal end, dorsoventral: 6
- Distal end, mediolateral: 5
- Midshaft, dorsoventral: 7
- Midshaft, mediolateral: 9

Manual Digit I, Phalanx I-2 (left element)
- Proximodistal length: 37 (45 mm along the curve)
- Proximal surface, dorsoventral: 15
- Proximal surface, mediolateral: 5

Manual Digit II, Phalanx II-1 (right element)
- Proximodistal length: 31
- Proximal end, dorsoventral: 12
- Proximal end, mediolateral: 10
- Distal end, dorsoventral: 5
- Distal end, mediolateral: 6
- Midshaft, dorsoventral: 9
- Midshaft, mediolateral: 7

Manual Digit II, Phalanx II-2 (right element)
- Proximodistal length: 38
- Proximal end, dorsoventral: 9
- Proximal end, mediolateral: 10
- Distal end, dorsoventral: 4
- Distal end, mediolateral: 6
- Midshaft, dorsoventral: 7
- Midshaft, mediolateral: 9

Manual Digit II, Phalanx II-3 (right element)
- Proximal surface, dorsoventral: 15
- Proximal surface, mediolateral: 5

Manual Digit III, Phalanx III-1 (right element)
- Proximodistal length: 11
- Proximal end, dorsoventral: 4
- Proximal end, mediolateral: 2.5
- Distal end, dorsoventral: 1.5
- Distal end, mediolateral: 1.5

Tibiotarsus (left element)
- Proximodistal length: 153
- Distal end, anteroposterior: 20
- Distal end, mediolateral: 25
- Tibia, proximal end, anteroposterior: 31
- Tibia, proximal end, mediolateral: 17
- Tibia, midshaft, anteroposterior: 12
- Tibia, midshaft, mediolateral: 11
- Fibula, proximal end, anteroposterior: 17
- Fibula, proximal end, mediolateral: 4
- Fibula, midshaft, anteroposterior: 3.5
- Fibula, midshaft, mediolateral: 3

Metatarsal I (left element)
- Proximodistal length: 37

Metatarsal II (right element)
- Proximodistal length: 52
- Distal end, dorsoventral: 8
- Distal end, mediolateral: 12

TABLE 2
Continued

Midshaft, dorsoventral: 6
Midshaft, mediolateral: 10

Metatarsal III (right element)
Proximodistal length: 61
Distal end, dorsoventral: 9
Distal end, mediolateral: 12
Midshaft, dorsoventral: 6
Midshaft, mediolateral: 10

Metatarsal IV (left element)
Proximodistal length: 53
Midshaft, dorsoventral: 6
Midshaft, mediolateral: 8

Metatarsal V (left element)
Proximodistal length: 18

Pedal Digit I, Phalanx I-1 (left element)
Proximodistal length: 23
Proximal end, mediolateral: 9

Pedal Digit I, Phalanx I-2 (left element)
Proximodistal length: 33
Proximal end, mediolateral: 9

Pedal Digit II, Phalanx II-1 (left element)
Proximodistal length: 13

Pedal Digit II, Phalanx II-2 (left element)
Proximodistal length: 22
Proximal end, dorsoventral: 10
Distal end, dorsoventral: 9
Distal end, mediolateral: 8

Pedal Digit II, Phalanx II-3 (left element)
Proximodistal length: 42
Proximal end, dorsoventral: 15

Pedal Digit III, Phalanx III-1 (left element)
Proximodistal length: 21

Pedal Digit III, Phalanx III-2 (left element)
Proximodistal length: 15

Pedal Digit III, Phalanx III-3 (left element)
Proximodistal length: 19
Distal end, dorsoventral: 7
Distal end, mediolateral: 7

Pedal Digit III, Phalanx III-4 (left element)
Proximodistal length: 24
Proximal end, dorsoventral: 11

Pedal Digit IV, Phalanx IV-1 (left element)
Proximodistal length: 14

Pedal Digit IV, Phalanx IV-2 (left element)
Proximodistal length: 11

Pedal Digit IV, Phalanx IV-3 (left element)
Proximodistal length: 11

TABLE 2
Continued

Pedal Digit IV, Phalanx IV-4 (left element)
Proximodistal length: 12

Pedal Digit IV, Phalanx IV-5 (left element)
Proximodistal length: 19

in figure 1 and measurements of individual elements are presented in tables 1–2.

TYPE LOCALITY: The holotype was collected by M.V. (September 2009) from red floodplain mudstones of the lower-middle part of the Late Cretaceous (late early Maastrichtian) Sebeş Formation, exposed at the Sebeş-Glod locality (figs. 2–3). The Sebeş-Glod locality (abbreviated as SbG/A-D) encapsulates a suite of restricted outcrops located 1.5 to 3.0 km north of Sebeş city (SW Transylvanian Basin, Alba county, Romania), downstream along the Sebeş River (fig. 2) (Codrea et al., 2010; Csiki et al., 2010a). These outcrops expose a roughly 50 m thick profile from the mid-lower section of the Sebeş Formation (SBF), 300 to 350 m below the major middle-Miocene (Badenian) unconformity that caps the Sebeş Formation at its type section (Râpa Roşie/Red Cliff), and approximately 100 m above the top of the conformably underlying marine Bozeş Formation (late Santonian–lowermost Maastrichtian), which is well exposed at the nearby Petreşti-Arini (PT) section (Vremir, 2010). The Sebeş Formation succession is dominated by coarse, mainly cross-bedded channel fills (gravels, sandy gravels, cross-laminated sandstones) with occasional interbeds of finer grained red or brownish-red overbank and floodplain associations (fine laminated sandstones, silty claystones, massive mudstones), all of which was formed by a high-sinuosity fluvial system.

The SbG/B site is a small waterlogged riverbed outcrop, exhibiting a 6 m thick profile that dips slightly eastward (figs. 2, 4). The basal channel association is built up by fining upward, medium-to-coarse, occasionally pebbly, light pinkish-gray sandstones, grouped in progressively thinner trough cross-laminated sets (dunes) that show internal truncation (St/Sp), characterizing a lateral accretional facies (LA). The progressive abandonement and lateral migration of the

Fig. 2. Photographs of the type locality of *Balaur bondoc*, where the holotype specimen (EME PV.313) was discovered by MV in 2009 in Upper Cretaceous (Maastrichtian) red floodplain mudstones of the Sebeş Formation. This site, known as the Sebeş-Glod (SbG/A) locality, is located approximately 2.5 km north of Sebeş town, downstream and along the Sebeş River, in Alba County, Romania.

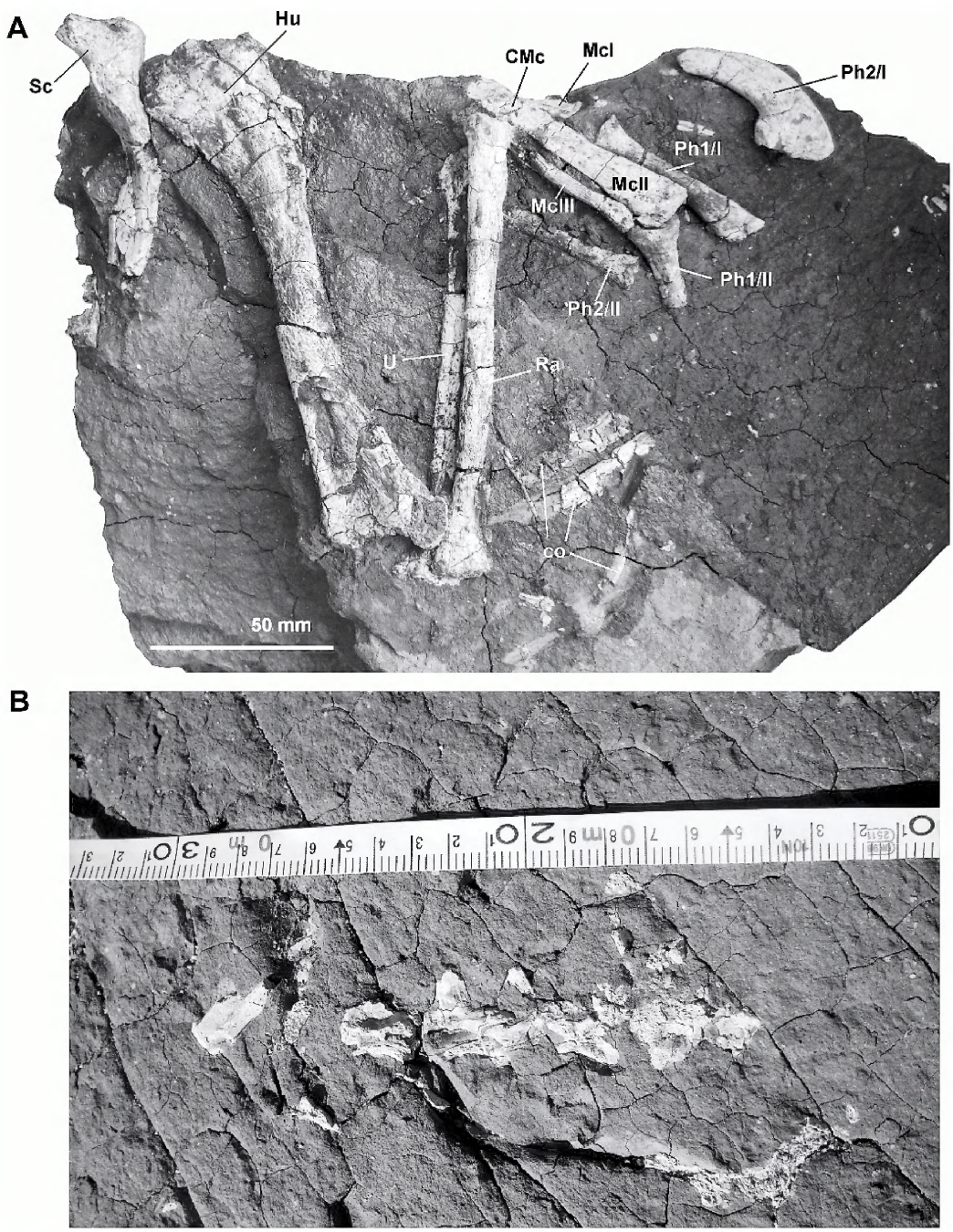

Fig. 3. Photographs of the holotype of *Balaur bondoc* (EME PV.313) as exposed in the field. Photograph of right forearm and pectoral girdle (**A**) and caudosacral region (**B**), with scale bars as indicated in the images. Abbreviations: **CMc,** carpometacarpus; **co,** ribs; **Hu,** humerus; **Mc,** metacarpal; **Ph,** phalanx; **Ra,** radius; **Sc,** scapulocoracoid; **U,** ulna. Numbers of individual phalanges denoted as phalanx number/digit number.

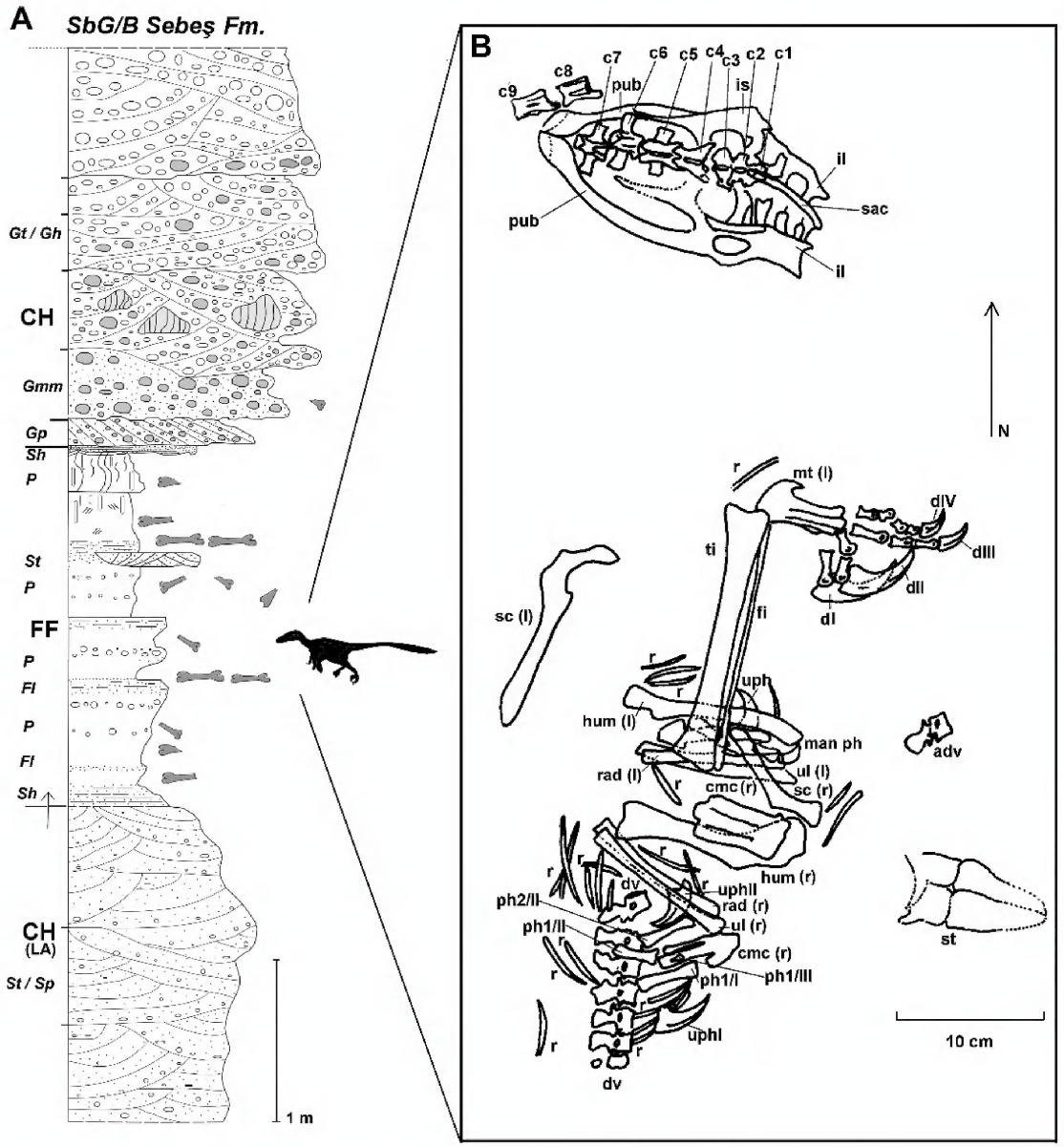

Fig. 4. Stratigraphic log of the holotype locality of *Balaur bondoc* (the Sebeş-Glod locality) (**A**) and quarry map showing how the individual elements of the holotype of (EME PV.313) were discovered in the field (**B**). Abbreviations for A are given in the text. The dromaeosaurid silhouette denotes the level where the *Balaur* holotype was recovered. Abbreviations for B: **adv,** anterior dorsal vertebra; **c 1–9,** caudal vertebrae; **cmc,** carpometacarpus; **d,** digit; **dv,** dorsal vertebrae; **fi,** fibula; **hum,** humerus; **il,** ilium; **is,** ischium; **man ph,** manual phalanx; **mt,** metatarsus; **ph,** phalanx; **pub,** pubis; **r,** rib; **rad,** radius; **sac,** sacrum; **sc,** scapulocoracoid; **st,** sternum; **ti,** tibia; **ul,** ulna; **uph,** ungual phalanx. The designations (l) and (r) denote left and right elements, respectively.

channel is marked by fine, horizontally laminated, sand-silt-clay deposits, with occasional scour-fill features and flute marks, indicating minor crevasses (Sh/Fl), grading into a reddish sandy-silty claystone and mudstone dominated proximal floodplain association (OF). The fossiliferous layers are grouped into a 2.2 m thick dark-red, calcareous, silty-claystone

sequence, which exhibits thinly laminated and lenticular sandy interbeddings (crevasses) likely related to periodic flooding events, and several pedogenic calcitic horizons containing nodules. Bone fragments are common troughout the whole overbank sequence, but more complete elements and associated and/or articulated skeletal parts (such as the *Balaur* holotype: fig. 3) are found immediately above the sandy crevasses, covered by fine sediments. The top of the overbank facies is represented by massive dark-red mudstone, which exhibits abundant tubular burrowings and rhysolites, marking the incipient topsoil horizon. A conglomerate channel fill complex, which is several meters thick and comprised of poorly sorted massive, plannar, or concoid cross-laminated multistoried conglomerates (Gmm, Gp/Gh), covers the whole sequence, bounded by a fifth-order flat lower surface. In the basal lag deposits, large cobble and boulder size, red claystone-mudstone intraformational subangular clasts are common, originating from the ancient undercut riverbank.

The multistory complex CH fills, dominated upward by truncated cross-bedded sets (Gh), may indicate mobile, broad, and shallow channels more common in braided fluvial settings. An unstable and dynamic environment, with frequent reactivations and flow-direction changes, is often present in these settings. Since its discovery in 1999 (Vremir, 2010), the SbG/B site has yielded a large number of vertebrate fossils, which originate entirely from the red overbank deposits. Most specimens are fragmentary isolated bones; complete bones, and especially closely associated and partially articulated skeletons, are comparatively rare. The vertebrate record from this site is comprised of various ornithopod (*Zalmoxes*, *Telmatosaurus*), sauropod (titanosaurs) and theropod (*Balaur*) dinosaurs, as well as abundant cryptodiran (*Kallokibotion*) and rare pleurodiran ("*Muehlbachia*") turtles, small crocodylomorphs, rare pterosaurs (medium-sized azhdarchids), and birds.

The sedimentological and taphonomic evidence suggests a general attritional and trampled taphofacies of largely isolated and evenly distributed bone fragments. Many preserved bones suffered long-term subaerial biodegradation, disarticulation, effects of scavenging (possibly from crocodylomorphs), and prefossilization weathering (weathering stage 3–5), including occasional insect-related surficial modifications. Most insect marks may be assigned to coleopterans (Dermestidae?) and isopterans (termites), pointing to long-term subaerial exposure of bones, a low water table, a sparsely vegetated environment, and relatively dry conditions. Episodic flood-related fine sediment input then covered the drifted and partially degraded carcasses. As indicated by the bone map (fig. 4B), the partially decayed *Balaur* carcass (probably still bearing some soft tissues) was probably transported in a low-energy current during a waning flood, then subaerially exposed (weathering stage 1–2), partially disarticulated, and finally buried due to additional sediment input. As suggested by the quarry map, lithological profile, and sedimentological analysis, more extensive excavations at the site may lead to the recovery of some remaining bones of the *Balaur* holotype, particularly hind-limb elements, or eventually the neck region and skull. The distal caudal series, however, was destroyed and washed away by recent fluvial erosion.

DIAGNOSIS: Dromaeosaurid theropod with the following autapomorphies (asterisk denotes autapomorphies unique among all theropods, other characters unique among dromaeosaurids): hypertrophied coracoid tubercle*; sinuous ridge on lateral surface of distal humerus extends for 1/3 of the length of the bone*; prominent ridge on medial surface of distal half of humerus*; anterior surface of ulna flattened and bisected by longitudinal ridge*; fused carpometacarpus; reduced, splintlike metacarpal III; metacarpal III contacting metacarpal II distally, buttressed by overhanging ridge on metacarpal II*; distal articular surface not extending onto plantar surfaces of metacarpals I and II; manual ungual II with Y-shaped lateral and medial grooves*; phalanges of manual digit III reduced to small nubbins without condylar articulations; ischial obturator tuberosity expressed as enlarged, thin flange that contacts or nearly contacts pubis ventrally*; tarsometatarsus substantially wider (1.5×) than distal tibiotarsus*; fused metatarsus (metatarsals II–V fused proximally and possibly along parts of their shafts); robust

ridges on extensor surfaces of metatarsals II–IV*; metatarsals II and III not ginglymoid; articular region of metatarsals II–III narrower than entire distal end*; first digit of pes with enlarged phalanges but small metatarsal I*; and short, hooklike metatarsal V (emended from Csiki et al., 2010a).

Two pelvic characters that Csiki et al. (2010a) originally considered as autapomorphies of *B. bondoc*—a laterally everted pubic peduncle and the reorientation of the lateral surface of the pubis to face ventrally—are here reinterpreted as artifacts of crushing. Reexamination and additional preparation of the holotype pelvis indicates that the specimen has been subjected to extensive dorsoventral crushing, which has caused the ilium to break along the margins of the cuppedicus fossa (making it seem as if the pubic peduncle is laterally everted) and the pubis to artificially rotate ventrally. This crushing, which is described in further detail below, fully explains the presence of the two supposed autapomorphies, which we no longer consider valid. Furthermore, a third autapomorphy listed by Csiki et al. (2010a), extremely retroverted pubes and ischia whose long axes are nearly horizontal, is here considered only potentially valid because it may also be explained partially, or entirely, by crushing.

Additional Material: LPB (FGGUB) R.1580, incomplete left humerus; R.1581, left ulna; R.1585, incomplete left metacarpal II; R.1583, proximal fragment of right manual phalanx I-1; R.1582, proximal fragment of left? manual phalanx I-1 or II-1; and R.1584, distal fragment of left manual phalanx II-2, all from the same locality (see below) and possibly from the same individual. Histological analysis suggests that FGGUB R.1581 belongs to a skeletally mature individual, no less than six years of age. Measurements of the referred material is presented in table 3.

Locality of Additional Material: The Tuştea (also referred to as Oltoane Hill) nesting site, north of the Tuştea locality, Haţeg Basin, Hunedoara County, Romania. The nesting site is located in a 1 m thick, red silty mudstone bed overlying a thin, medium-grained crevasse splay sandstone, and covered by a thick, poorly sorted conglomerate-sandstone unit locally showing tabular or trough cross-bedding, as well as graded bedding. According to the local stratigraphic framework, the nesting site is placed in the unnamed middle subunit (member) of the Densuş-Ciula Formation, a continental detritic-volcanoclastic unit of Maastrichtian age (Bojar et al., 2011); more detailed information on the sedimentology and paleoenvironmental setting of the Tuştea site is given by Bojar et al. (2005), Grigorescu et al. (1994, 2010), and Therrien (2005).

Besides egg clutches and hatchling bones, usually attributed to the basal hadrosaur *Telmatosaurus transsylvanicus* (see Grigorescu et al., 1994, 2010; but see Weishampel and Jianu, 2011, and discussion therein), a large number of skeletal remains were also recovered from the fossiliferous mudstone, representing several taxa. Although most of these fossils are found disarticulated, several instances of associated (even articulated) remains have also been recorded (e.g., Csiki et al., 2010b, Martin et al., 2010). All of the *Balaur* referred material was discovered during the same excavation season (1997), and all the bones were spread across a small area roughly along the same stratigraphic level within the fossiliferous bed. No futher postcranial remains referrable to *Balaur* or close relatives were subsequently discovered at the Tuştea site, despite continuous excavations. Moreover, all referred *Balaur* material belongs to the forelimb, all elements are commensurate in size, and all show the same peculiar surface texture, a characteristic feature of *Balaur* (see below). Based on these circumstances, it is probable that these elements belong to the same individual, whose skeleton was scattered and almost completely destroyed after its death and before its final burial in a well-drained floodplain environment undergoing pedogenesis.

Systematics of Additional Material: The referred specimens uniquely share characters with the holotype of *B. bondoc* that are not seen in any other theropod dinosaurs. First, all bones of the referred specimens possess the characteristic rugose surface texture of the *Balaur* holotype (this is also present in other isolated theropod bones from Romania). Second, the humerus exhibits a sinuous ridge on the lateral surface of the distal end, which extends for approximately 1/3 of the length of the bone, as well

TABLE 3
Measurements of appendicular bones (in mm) of additional referred specimens of *Balaur* sp.
Asterisk indicates incomplete measurement due to damage.

Humerus (left element – LPB (FGGUB) R.1580)
Proximodistal length: 157* (estimated at 170 mm)
Midshaft, anteroposterior: 15
Midshaft, mediolateral: 17

Ulna (left element – LPB (FGGUB) R.1581)
Proximodistal length: 133* (estimated 163 mm)
Midshaft, anteroposterior: 9
Midshaft, mediolateral: 10

Metacarpal II (left element – LPB (FGGUB) R.1585)
Proximodistal length: 46.2* (as preserved)
Distal end, dorsoventral: 11.6* (dorsally abraded)
Distal end, mediolateral: 15.7
Midshaft, dorsoventral: 7.3
Midshaft, mediolateral: 10.1

Manual Digit I, Phalanx I-1 (right element – LPB (FGGUB) R.1583)
Proximodistal length: 59.2* (minimum estimate, based on mold)
Proximal end, dorsoventral: 15.2
Proximal end, mediolateral: 16.4
Distal end, dorsoventral: –
Distal end, mediolateral: 13.2* (minimum estimate, based on mold)
Midshaft, dorsoventral: 8.9
Midshaft, mediolateral: 8.4

Manual Digit II, Phalanx II-2 (left element – LPB (FGGUB) R.1584)
Proximodistal length: 54.5* (minimum estimate, based on mold)
Proximal end, dorsoventral: –
Proximal end, mediolateral: 11.9* (minimum estimate, based on mold)
Distal end, dorsoventral: 12.8
Distal end, mediolateral: 9.4
Midshaft, dorsoventral: 7.7
Midshaft, mediolateral: 6.7

as a prominent ridge on medial surface of distal half. Third, the ulna possesses a flat anterior surface that is bisected by a longitudinal ridge. Fourth, metacarpal II possesses a distal ridge that laterally overhangs metacarpal III, as well as a distal articular surface that does not extend onto the plantar surface (the latter an autapomorphy of *Balaur* among dromaeosaurids but not among all theropods). Therefore, these specimens can be united with the holotype of *B. bondoc* based on synapomorphies, and for this reason, Csiki et al. (2010a) considered them to represent a referred specimen of *B. bondoc*.

Although these specimens share unique derived characters with the *B. bondoc* holotype, Csiki et al. (2010a) noted a peculiar fact: the referred material is substantially larger than the holotype. The referred humerus is 1.45 times the length of the holotype humerus, whereas the referred ulna is 1.65 times larger. Csiki et al. (2010a) suspected that the holotype of *B. bondoc* was a mature individual, because of extensive fusion across the skeleton, but were unable to provide a histological estimate of absolute age and growth stage because of extensive fungal damage to the interior regions of the long bones commonly used for these estimates. As part of this monograph we attempted to take further histological samples and were able to obtain samples from the holotype fibula and referred ulna. As detailed below, these

samples indicate that both specimens were skeletally mature (i.e., full or nearly fully grown) and of similar numerical age.

It seems unusual that two mature and slow-growing adults of the same species would vary in size to the degree noted between the two specimens of *Balaur*. It is difficult to test whether this may be the case in other dinosaur species, because sample sizes are usually too low to permit histological examination of large numbers of individuals. Sander and Klein (2005) did find that fully grown individuals of the basal sauropodomorph *Plateosaurus* may differ in size by up to 50%, but it is worth noting that this determination is based on specimens from a single locality (not multiple localities like the two specimens of *Balaur*) and hinges on a single outlier specimen that is much larger than a tight cluster of several similarly sized mature individuals (Sander and Klein, 2005: fig. 3B). Furthermore, *Plateosaurus* is distantly related to dromaeosaurids, is hypothesized to have had a less active metabolism than the birdlike dromaeosaurids, and its great variability in adult body size is hypothesized to have been related to local environmental conditions (Sander and Klein, 2005). In summary, it is not clear whether the case study of *Plateosaurus* growth and variability is applicable to dromaeosaurids in general or the case of the two *Balaur* specimens in particular.

Because it seems unusual for two mature specimens to differ so greatly in size, and because there is no clear evidence that adult theropod dinosaurs varied in size to this degree, we take the conservative step and here remove the referred material from the species-level taxon *Balaur bondoc*. We emphasize, however, that this removal is based on a biological argument (the improbability of a biological species varying in adult size to this degree) and not an anatomical argument (a lack of synapomorphies). Indeed, the two specimens share several unique derived characters and are therefore hypothesized to be close relatives, and surely sister taxa among all currently known theropods. Because these shared characters are autapomorphies of *Balaur*, we now assign the referred material to *Balaur* sp., with the prediction that it belongs to a larger species closely related to *B. bondoc*. Therefore, the size differences between the holotype and referred specimen should not be used as evidence that a single dinosaur species can vary greatly in adult body size or continue growing after extensively fusing its skeleton. Fowler et al. (2011) recently used *Balaur* as an example of the latter phenomenon, and thus as support for their hypothesis that some tyrannosaurids may also undergo dramatic size changes after fusing portions of their skeleton. We strongly caution against this line of argument.

It is also possible that the extreme adult size difference between the two *Balaur* specimens is the result of sexual dimorphism, but this proposition is difficult to test because of low sample size and the difficulty of distinguishing male and female dinosaurs. Intriguingly, the recently extinct moa was sexually dimorphic to an extreme degree, with adult females up to 280% larger than adult males (Bunce et al., 2003). Such marked dimorphism cannot be ruled out for *Balaur*, and it is hoped that this possibility can be tested as more specimens become available. In the meantime, we consider removing the referred specimen from *B. bondoc* and referring to it as *B.* sp. to be the most conservative course of action.

DESCRIPTION

Axial Skeleton

Dorsal Vertebrae: Portions of eight dorsal vertebrae are preserved, including an isolated anterior dorsal (fig. 5) and an articulated series of seven mid-posterior dorsals (figs. 6–7). Because their exact position in the dorsal column is uncertain, these vertebrae are here referred to as dorsals A–H, with alphabetical notation corresponding to relative position on the trunk. The first vertebra in the articulated series (dorsal B) is represented by a small fragment, but the six remaining elements are well preserved, especially the two posteriormost vertebrae (dorsals G–H). The neurocentral suture is closed in all dorsal vertebrae in which this region is visible and well preserved.

The single anterior dorsal vertebra (dorsal A) is embedded in matrix and exposed in right lateral view (fig. 5). The right lateral side of the neural spine has been broken from

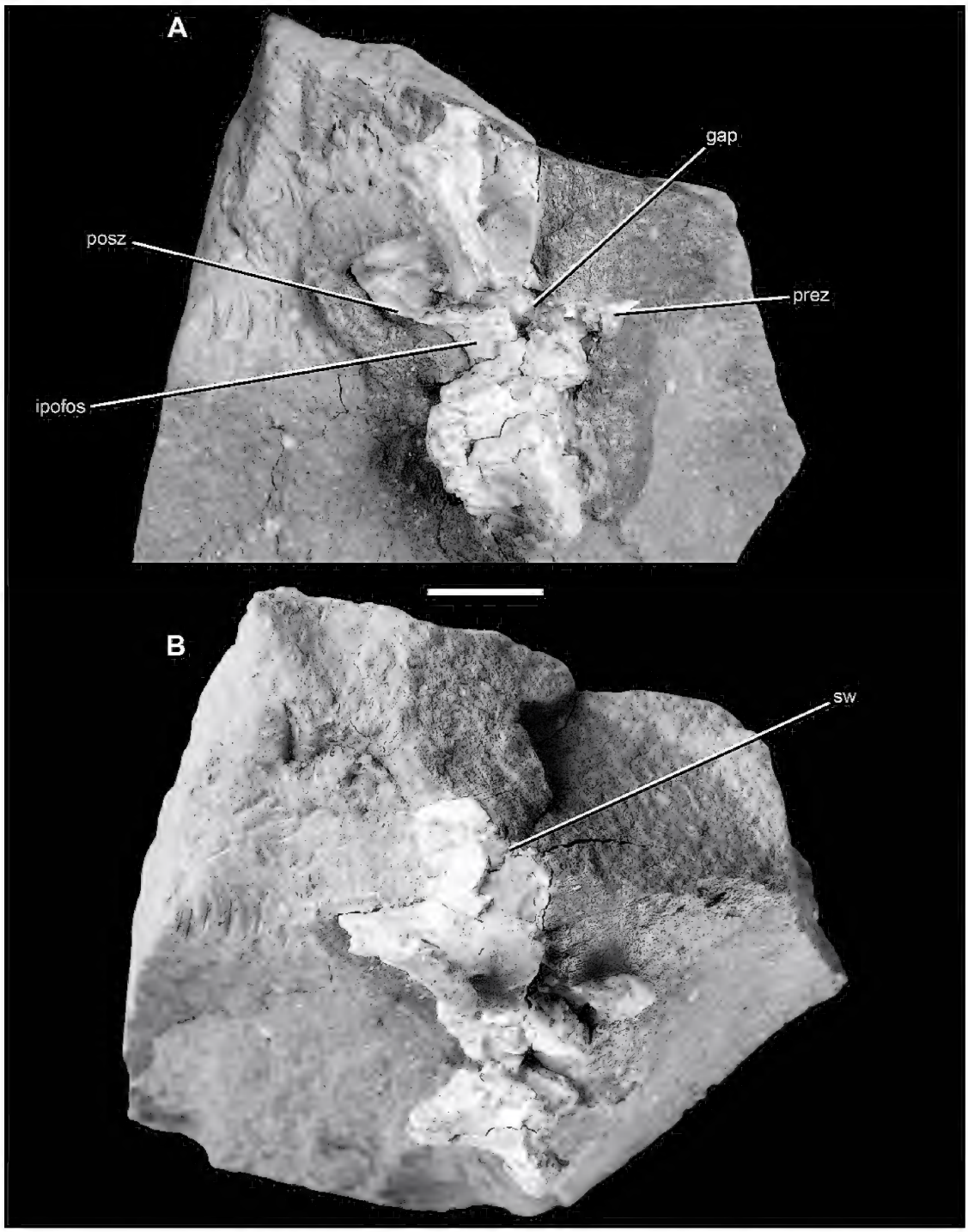

Fig. 5. Dorsal vertebra A of *Balaur bondoc* (EME PV.313) in right lateral (**A**) and oblique dorsolateral (**B**) views. Abbreviations: **gap,** artificial gap between centrum and neural arch, caused by breakage; **ipofos,** infrapostzygapophyseal fossa; **prez,** prezygapophysis, **posz,** postzygapophysis; **sw,** dorsal swelling on neural spine. Scale bar equals 1 cm.

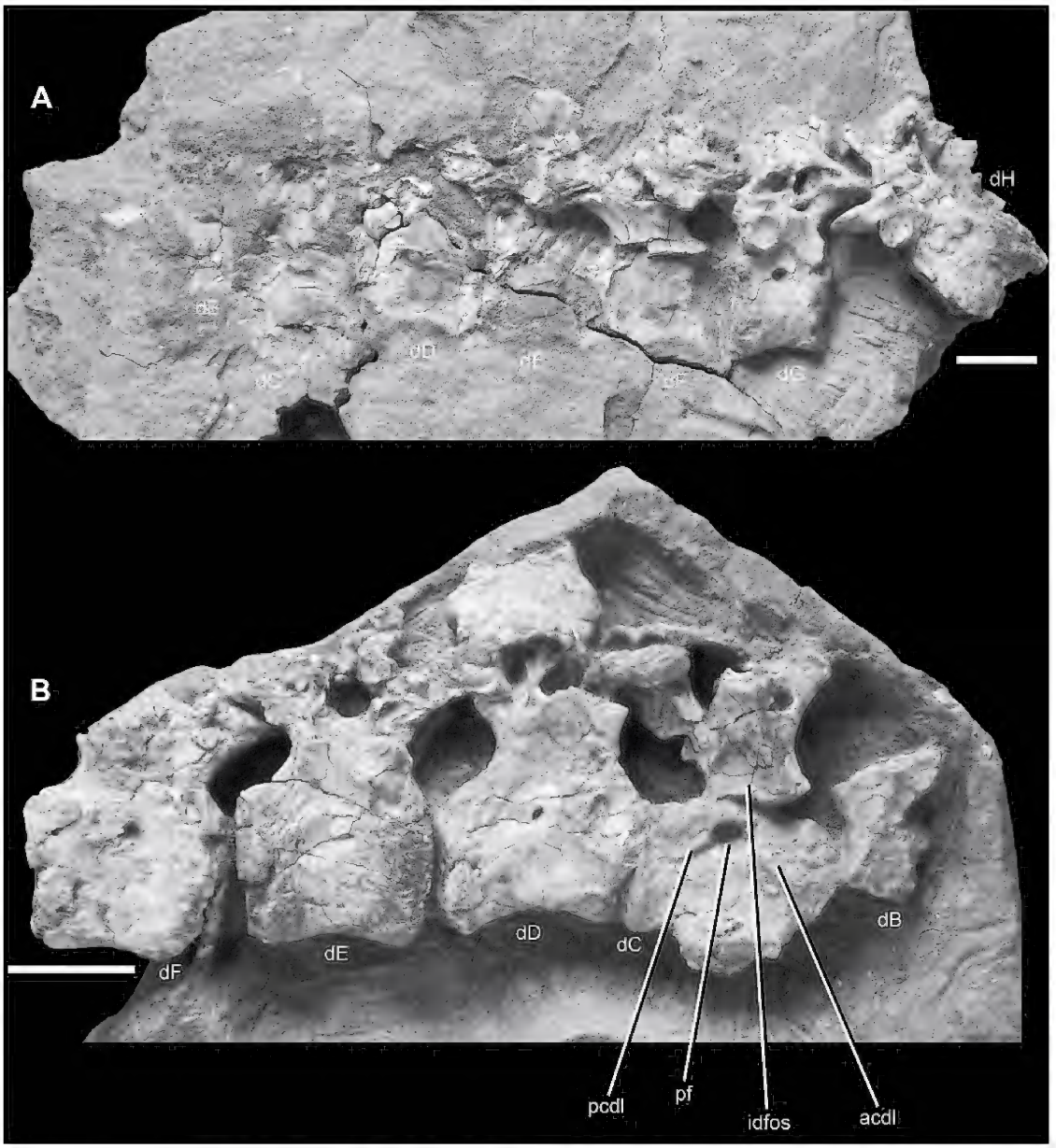

Fig. 6. Dorsal vertebrae B–H of *Balaur bondoc* (EME PV.313) in left lateral (**A**) and right lateral (**B**) views. Abbreviations: **acdl,** anterior centrodiapophyseal lamina; **idfos,** infradiapophyseal fossa; **pcdl,** posterior centrodiapophyseal lamina; **pf,** pneumatic foramen. dB–H designates the relative position of the vertebrae in sequence (see text for details). Scale bars equal 1 cm.

the remainder of the vertebra and displaced dorsally, exposing a large artificial gap and exaggerating the dorsoventral height of the bone (fig. 5: gap). This specimen is the only dorsal vertebra that preserves large portions of the neural spine. The anterior margin of the spine is eroded, but the posterior and dorsal margins are swollen relative to the rest of the spine (fig. 5: sw). Such swelling is indicative of a rugose spine table at the apex of the neural spine, as is also seen in the velociraptorines *Deinonychus* (Ostrom, 1969),

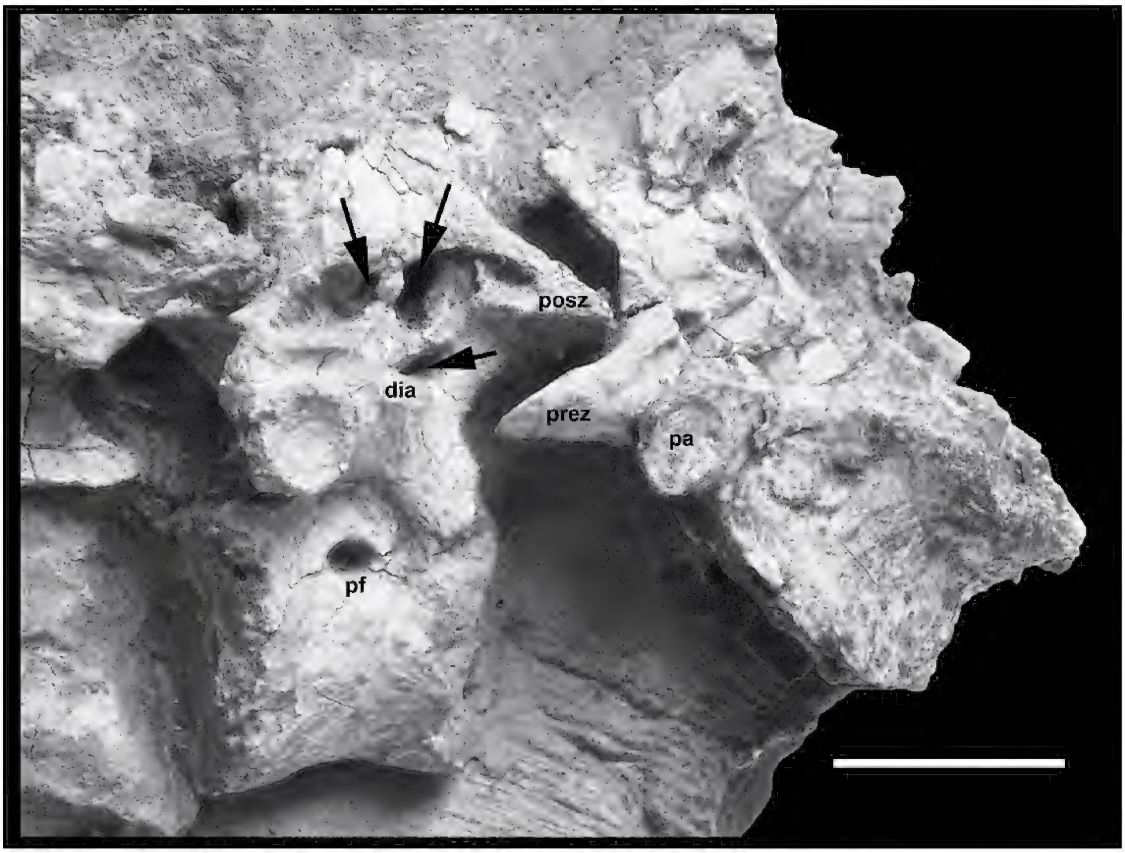

Fig. 7. Closeup of dorsal vertebrae G–H *Balaur bondoc* (EME PV.313) in left lateral view. Abbreviations: **dia,** diapophysis; **pa,** parapophysis; **pf,** pneumatic foramen; **posz,** postzygapophysis; **prez,** prezygapophysis. Scale bar equals 1 cm. Arrows point to internal pneumatic recesses exposed due to the erosion of the lateral surface of the vertebra.

Velociraptor (Norell and Makovicky, 1999), and *Saurornitholestes* (TMP 67.20.36), as well as the unenlagiines *Unenlagia* (Novas and Puerta, 1997) and *Austroraptor* (Novas et al., 2009). Several laminae and fossae are also visible on this specimen. Anterior and posterior centrodiapophyseal laminae are present but mostly eroded ventrally, as is the infradiapophyseal fossa. The infrapostzygapophyseal fossa is deep and widely exposed in lateral view (fig. 5: ipofos), whereas the infraprezygapophyseal fossa is reduced in size, but very deep, and faces almost entirely anteriorly. A prespinal fossa is visible on the small region of the anterior surface of the neural spine that is exposed, bound laterally by the prespinal lamina. A spinoprezygapophyseal lamina connects the neural spine to the prezygapophysis, which is placed at approximately the same horizontal level as the postzygapophysis.

The series of articulated mid-posterior dorsal vertebrae (dorsals B–H) is embedded in matrix (fig. 6). Some vertebrae are split and exposed on a slab and counterslab; the anterior vertebrae are best exposed in right lateral view and the more posterior elements are exposed in left lateral view. The individual centra become progressively shorter anteroposteriorly and deeper dorsoventrally along the dorsal column (table 1). Where well preserved and visible, the anterior and posterior faces are ovoid, taller than wide, with subtly concave articular surfaces. They extend only slightly ventrally relative to the centrum midpoint and are slightly swollen such that they stand out laterally from the smooth and inset lateral surface of the

centrum. The lateral and ventral surfaces of the centrum smoothly merge with each other and are not separated by a discrete angle. Anteriorly, the ventral surface is sharp and mediolaterally thin, but it funnels out to become mediolaterally wider as it continues posteriorly. Distinct ridges or grooves are not visible on any of the exposed ventral surfaces.

The line of fusion between the neural arches and centra is visible on most individual dorsals as a thin, slightly raised rim. The parapophysis is well preserved only on the two posteriormost dorsals (dorsals G–H; fig. 7: pa), but eroded surfaces mark its position on the five additional dorsals in the block. Anteriorly, in dorsals C–D, the parapophysis is located at the juncture of the centrum and neural arch, whereas in the posterior dorsals G–H it is located solely on the arch (fig. 7: pa). In these two posterior dorsals the parapophysis is a large structure offset laterally on a pronounced stalk, a characteristic dromaeosaurid feature (e.g., Norell and Makovicky, 1999; Turner et al., 2007a). Here, the lateral articular surface of the parapophysis is large and circular, with a diameter of approximately 4 mm, and deeply excavated as a smooth fossa.

The transverse processes are broken on all dorsal vertebrae, but their preserved bases indicate that they became more horizontally oriented posteriorly along the dorsal column. The anterior and posterior centrodiapophyseal laminae linking the transverse processes to the centrum are visible on most of the mid-posterior dorsals, and are best preserved on dorsal C (fig. 6: acdl, pcdl). Here, the two laminae are approximately equally developed, and the infradiapophyseal fossa between them is deep and triangular (fig. 5: idfos). In more posterior dorsals, it is clear that the posterior lamina becomes progressively thicker and more prominently offset than the anterior lamina, in concert with the dorsal migration of the parapophysis onto the neural arch. Unfortunately, details of the infrapre- and infrapostzygapophyseal fossae are visible only on dorsal C, where these depressions are much smaller than the infradiapophyseal fossa, only marginally visible in lateral view, and face primarily anteriorly and posteriorly, respectively.

The zygapophyses are eroded on most specimens but are well preserved on some mid-posterior vertebrae. The prezygapophysis is most complete on dorsal H, where it has a flat articular surface that expands anteriorly into a spatulate bulb (fig. 7: prez). This surface faces mostly dorsally, but is also oriented somewhat medially and posteriorly. Between the prezygapophysis, parapophysis, and diapophysis of dorsal H is a deep, mostly dorsally and posteriorly facing fossa, which is almost entirely concealed in lateral view. This is the infraprezygapophyseal fossa (= *hapidocoel* of Ostrom, 1969), which is a broader fossa in more anterior dorsals (e.g., dorsal C), but takes the form of a deep notch here because it occupies less space due to the dorsal migration of the parapophysis. The postzygapophysis is best preserved on dorsal G, where it is in near articulation with the prezygapophysis of dorsal H (fig. 7: posz). It is smaller than the adjoining prezygapophysis, has a flat articular surface, and is linked to the base of the transverse process by a sharp lamina. Spinoprezygapophyseal and spinopostzygapophyseal laminae are present at the base of the neural spines where dorsals G and H articulate, and here the lateral surfaces of the spine bases are smooth and slightly concave.

Pneumatic features are visible on all well-preserved dorsals, suggesting that pneumaticity extended throughout the entire dorsal column, unlike in *Velociraptor* (IGM 100/985, IGM 100/986) but similar to *Deinonychus* (Ostrom, 1969; see also Benson et al. 2012). Large pneumatic foramina ("pleurocoels") are clearly visible on the lateral centrum surfaces of dorsals C, E, F, G, and H (figs. 6–7: pf). The size, shape, and position of the foramina are highly variable along the column and between the left and right sides of a single vertebra (dorsal F, the only vertebra exposed on both lateral sides). The left foramen of dorsal F is ovoid, much deeper, and larger (3.5 mm anteroposteriorly by 3 mm dorsoventrally) than the more circular right foramen (1.5 mm by 2 mm). Furthermore, the foramen on dorsal C is large and deep (3 mm anteriorposteriorly by 2 mm dorsoventrally), whereas that on dorsal D is a tiny circle (diameter of 0.75 mm), and some foramina are positioned immediately below the neurocentral suture (e.g., dorsals C, D) whereas others are positioned further

ventrally (e.g., dorsal F). Pneumatic features are also present on the neural arch. Above the lamina linking the postzygapophysis and transverse process of dorsal G is a collapsed region that exposes large internal chambers, which would have been covered laterally in life (fig. 7, denoted by arrows). Other broken surfaces, especially on dorsals C, D, and H, also reveal extensive hollow internal cavities. Therefore, it is clear that both the centra and neural arches of all preserved dorsals were considerably pneumatized.

Sacral Vertebrae: A portion of the fused sacrum is preserved in articulation with the pelvis (fig. 8). Four sacral vertebrae are preserved, based on the presence of four clearly observable sacral ribs (fig. 8, denoted by arrows). However, the anteriormost preserved sacral has a broken anterior articular surface, and the rib of this vertebra reaches the broken anterior end of the ilium, making it difficult to determine whether additional sacral vertebrae may have been present anteriorly. As all other dromaeosaurids have at least five sacrals (e.g., Turner et al., 2007a), it is likely that at least some additional anterior sacrals were present in *Balaur*.

The length of the sacrum as preserved is approximately 100 mm. Although eroded, the anterior face of the first preserved sacral vertebra is approximately circular, with a diameter of 12 mm. Posteriorly, at the level of the third preserved sacral vertebra, the sacrum expands to 16 mm in mediolateral width. The lateral surface of the first preserved sacral bears a deep, smooth fossa. This depression, which is present on both sides of the vertebra, may be pneumatic in origin, but this remains equivocal since there is no pneumatic foramen ("pleurocoel") that penetrates into the interior of the centrum. The lateral depressions are not present on more posterior sacral vertebrae, so if the sacrum is pneumatic then there is little external evidence of this morphology. This is not unexpected for a dromaeosaurid, as pneumatic foramina are also absent on the sacral vertebrae of *Velociraptor* (Norell and Makovicky, 1997), *Buitreraptor* (Makovicky et al., 2005), *Unenlagia* (Novas and Puerta, 1997), and *Mahakala* (Turner et al., 2007a). They are, however, present in an anterior sacral element of *Saurornitholestes langstoni* (TMP 67.20.36) and in the anterior sacrals of *Adasaurus* (IGM 100/20).

The ventral surface of the first preserved sacral is rounded and convex anteriorly, whereas those of the second, third, and fourth vertebrae are marked by a longitudinal groove. Longitudinal grooves are also present in most other dromaeosaurids, including *Mahakala*, *Saurornitholestes*, and *Velociraptor* (e.g., Norell and Makovicky, 1999; Turner et al., 2007a). The ventral groove starts on the second sacral in *Velociraptor* as well, but is present only on the third sacral in *Bambiraptor* (Burnham, 2004), whereas in *Mahakala* it is only feebly developed on the posterior half of the second sacral vertebrae to the posterior end of the fourth vertebra (Turner et al., 2011).

Unfortunately, the neural spines of all sacral vertebrae have been eroded, and details of the zygapophyses are not visible due to obscuring matrix.

The right sacral rib corresponding to the first preserved vertebra is visible in ventral view. It is a thin sheet that twists anteroventrally as it extends laterally, such that its anterior surface faces mostly ventrally where it meets the ilium along a broad contact. The rib expands in anterposterior length to form this expansive articulation. The second rib is not well preserved on the right side but is nearly complete on the left side. It extends laterally as a sheet, but unlike the first rib it does not twist anteroventrally where it contacts the ilium. Therefore, its anterior surface faces anteriorly across its entire length. The third rib, which is preserved on both sides, has a similar morphology as the second rib. Its anterior surface, which is well visible on the left side in anterior view, is smooth and concave; the concavity appears to be very deep, but this may be exaggerated by crushing. The third rib contacts the ilium immediately anterior to the level of the acetabulum and expands in anteroposterior length as it continues laterally to meet the ilium. The fourth rib is preserved on both sides and extends laterally, without twisting. It is clearly shallower dorsoventrally than the third rib, and hence is not as greatly expanded where it meets the ilium. The fourth rib is the longest of the sacral series in the mediolateral dimension, and as a result

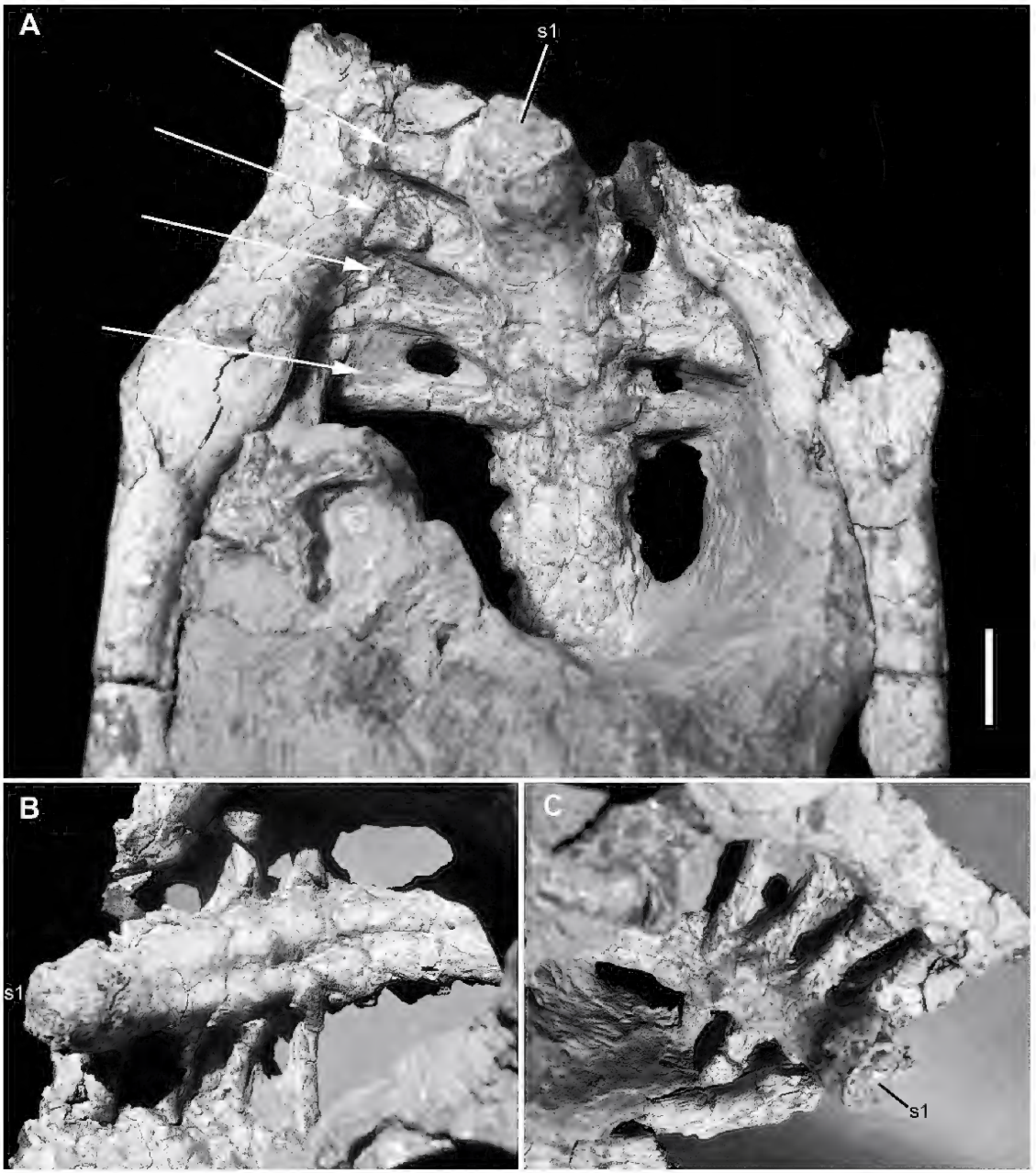

Fig. 8. The sacrum of *Balaur bondoc* (EME PV.313) in three slightly different anteroventral views. The arrows in part A denote the four preserved sacral ribs. Abbreviations: **s1,** first sacral vertebra. Scale bar in A equals 1 cm.

the sacral vertebrae and ilium are widely separated in this region, as in *Velociraptor* (Norell and Makovicky, 1999: fig. 17) and *Microraptor zhaoianus* (Hwang et al., 2002). In dorsal and ventral views there are large, ovoid fenestrae between the sacral ribs; these openings are bounded medially by the sacral vertebrae and laterally by the ilium.

There is a series of three articulated and coossified caudosacral vertebrae, which are fused to the sacrum (fig. 8). None of these preserve clearly observable sacral ribs, but

there are broken regions on some of them that may represent the bases of ribs. We conservatively refer to these as caudosacrals, and note that if some or all of them are proper sacrals, then the sacrum of *Balaur* contained at least 5–7 vertebrae. Furthermore, there is an unfused single vertebra between the fused sacrum-plus-caudosacral block and the first caudal vertebra. We also refer to this as a caudosacral vertebra, based on comparison to *Velociraptor*, in which the first caudal is located between the postacetabular blades of the ilium and becomes incorporated into the sacrum late in ontogeny (Norell and Makovicky, 1999). In *Balaur*, this vertebra is morphologically similar to the first caudal and possesses clear zygapophyses, supporting its identity as a caudal vertebra.

Caudal Vertebrae: Five anterior caudals are present, including the first two caudals that are embedded in the pelvic block, the third caudal that was discovered in articulation with the first two caudals but was removed during preparation, and two more posterior caudals that come from the anterior portion of the tail but whose exact position is unknown (referred to here as caudals D–E) (figs. 8–9). These latter two vertebrae are identified as anterior caudals because they retain transverse processes, which disappear posterior to caudal 11 in *Deinonychus* (Ostrom, 1969) and *Velociraptor* (Norell and Makovicky, 1997, 1999). In comparison with *Deinonychus* (Ostrom, 1969), caudal E of *Balaur* appears to be approximately equivalent to caudal 8–9, due to the fact that the transverse process is reduced to a thin longitudinal ridge and the neural spine to a sharp, anteroposteriorly short ridge that also appears to have been dorsoventrally short in life.

The caudal centra lengthen posteriorly and their anterior and posterior articular faces, where well preserved, are concave. The ventral surfaces of caudals 3, D, and E are excavated by a longitudinal groove that is deepest at its center and shallows anteriorly and posteriorly before abruptly terminating at the articular face. Unfortunately, the ventral surfaces of caudals 1 and 2 are embedded in matrix and are not visible. The lateral surfaces of the caudal vertebrae are smoothly and slightly depressed, but there are no pneumatic foramina or other features of obvious pneumatic origin. The centrum and neural arch are coossified in all specimens and their suture has been obliterated.

The anteriormost four preserved caudal vertebrae possess large, winglike transverse processes that extend horizontally and posteriorly, and slightly expand distally into a spatulate swelling (fig. 9: tvp). In caudal E, however, the transverse process is reduced to a longitudinal ridge on the lateral surface of the neural arch (fig. 9: tvpr). This ridge extends along the entire anteroposterior length of the centrum, whereas the discrete transverse processes of the four more anterior caudals are centered on the centrum. The neural spine is incomplete on all caudal vertebrae and preserved only at its base. On caudals 1 and 2 the base is very thin, less than 1 mm in transverse width, but anteroposteriorly elongate. In contrast, the spine base of caudals 3, D, and E is shortened anteroposteriorly, suggesting that the neural spine was progressively reduced in size posteriorly along the tail before disappearing altogether, as in *Deinonychus* and *Velociraptor* (Ostrom, 1969; Norell and Makovicky, 1997, 1999).

The zygapophyses are poorly preserved on most caudal vertebrae. The postzygapophyses of the first caudal are preserved in articulation with the prezygapophyses of the second caudal, and this contact is unfused. In more posterior caudal vertebrae the zygapophyses are mostly broken, but the prezygapophysis is well preserved on both sides of caudal E (fig. 9: prez). These structures are elongate, extending approximately 3 mm anterior to the anterior articular face, and diverge from each other when seen in dorsal view. The anterior end of the prezygapophysis is swollen relative to its neck, and the articular surface is smooth, concave, and faces mostly medially but also slightly dorsally. The postzygapophysis is well preserved on the right side of caudal D. It is shorter than the prezygapophysis and extends only slightly posterior to the posterior articular face. The articular surface is smooth and flat, and faces mostly laterally but also slightly ventrally. There is a sharp lamina, preserved only on small regions of caudals D and E, that extends from the prezygapophysis

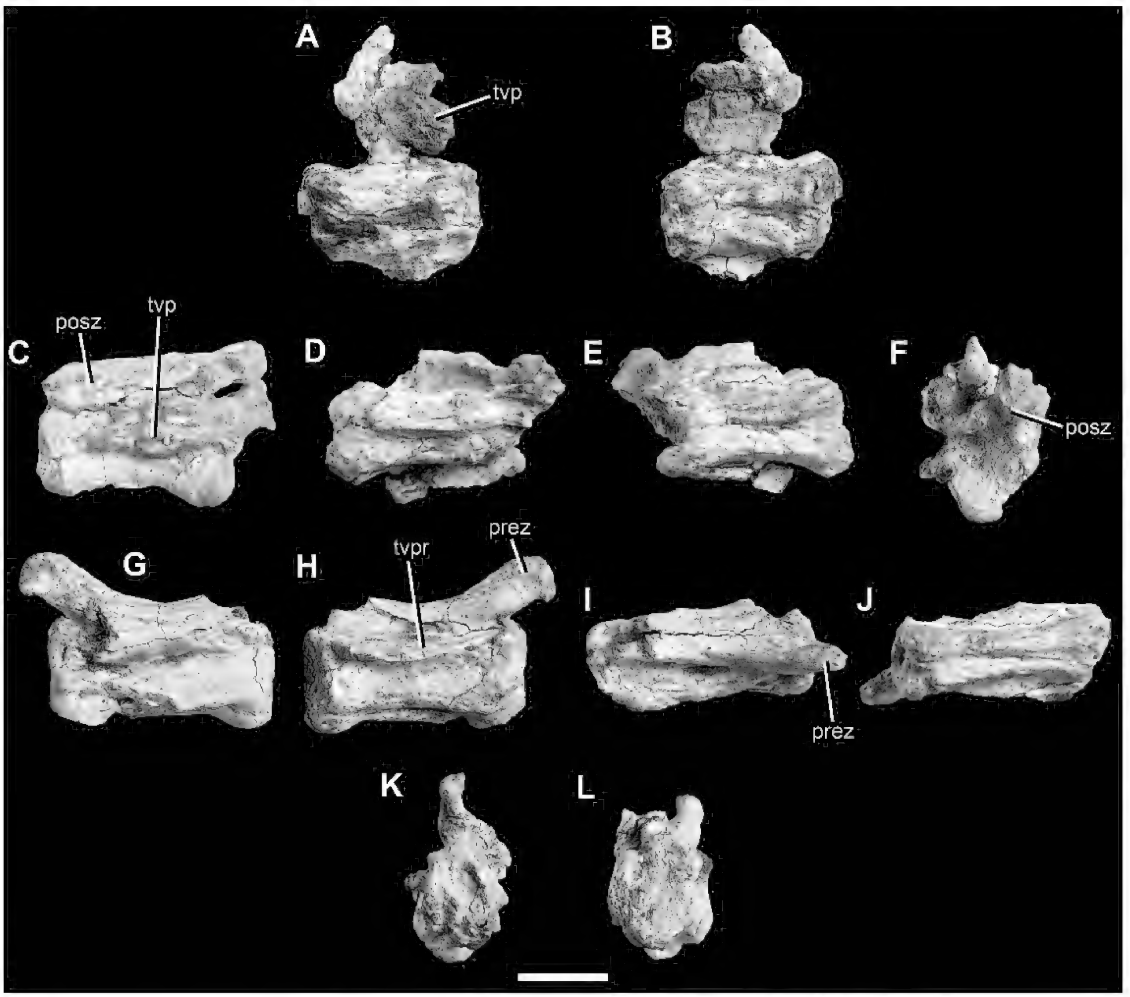

Fig. 9. Caudal vertebrae of *Balaur bondoc* (EME PV.313). Caudal 3 (**A–B**), caudal D (**C–F**), caudal E (**G–L**) in dorsal (**A, D, I**), ventral (**B, E, J**), right lateral (**C, H**), posterior (**F, L**), left lateral (**G**), and anterior (**K**) views. Abbreviations: **posz,** postzygapophysis; **prez,** prezygapophysis; tvp, transverse process; **tvpr,** transverse process reduced to a ridge. Scale bar equals 1 cm.

to the postzygapophysis along the lateral surface of the vertebra. Because all five caudal vertebrae of *Balaur* are from the anterior region of the tail, none preserves the elongate prezygapophyses of the middle-posterior caudal vertebrae that are characteristic of derived dromaeosaurids (e.g., Ostrom, 1969; Norell and Makovicky, 1997, 1999; Hwang et al., 2002).

Pectoral Girdle and Forelimb

Sternum: Ossified sternal plates were discovered with the specimen but were so poorly preserved that they could not be conserved (see fig. 4B for a drawing of the specimen as it was excavated). As a result, few details of sternal morphology are apparent. However, it is clear that the two sternal plates are separate and unfused on the midline, as in *Velociraptor* (Norell and Makovicky, 1997, 1999) and most other dromaeosaurids for which sterna are known (Xu et al., 2003; Turner et al., 2007a), and that the articular facet for the coracoid is positioned along the anterior edge of the sternum, as is present in most coelurosaurs (Xu et al., 1999; Turner et al., 2007a).

SCAPULOCORACOID: Portions of both the left and right scapulocoracoids are present, including a nearly complete left bone (fig. 10) and a small fragment of the glenoid region of the right element (fig. 11). The left scapulocoracoid is 94 mm long anteroposteriorly as preserved, but it is eroded posteriorly and would have been considerably longer in life. The scapula and coracoid are completely fused on both sides and the suture between them has been obliterated. Such fusion is also present in *Velociraptor* (Norell and Makovicky, 1999), *Microraptor* (Xu et al., 2000, 2003; Hwang et al., 2002), and *Adasaurus* (IGM 100/20), but the scapula and coracoid are unfused in most dromaeosaurids, including *Achillobator* (Perle et al., 1999), *Buitreraptor* (Makovicky et al., 2005), *Deinonychus* (Ostrom, 1969), *Sinornithosaurus* (Xu et al., 1999), and *Unenlagia* (Novas and Puerta, 1997). It is possible that scapulocoracoid fusion is ontogenetically variable, but its presence in multiple *Velociraptor* and *Microraptor* specimens of different sizes (Norell and Makovicky, 1999; Hwang et al., 2002) and in the diminutive paravian *Pneumatoraptor* (Ősi et al., 2010) suggests that this feature is not solely characteristic of large-bodied taxa or adults.

The glenoid is formed by both the scapula and coracoid, but the relative contributions of each bone are uncertain because their suture is not visible. Unfortunately, the glenoid is preserved only on the right specimen, where it is heavily eroded (fig. 11: gl). However, it is clear that the glenoid faces mostly ventrally but also slightly laterally, as the smooth articular surface continues onto the lateral surface of the bone. This feature is characteristic of paravians, including other dromaeosaurids and avialans (e.g., Turner et al., 2007a, 2012), and allows increased humeral abduction, a necessary component of the avian flight stroke (Gauthier and Padian, 1985). The glenoid of *Balaur* is bounded anteriorly and posteriorly by enlarged, swollen rims.

The **coracoid** is incomplete in both specimens, and only the region near the glenoid and the base of the ventral process are preserved. As in paravians generally, the coracoid is L-shaped, due to a discrete ventral process that is inflected medially to articulate with the anterior margin of the sternum (e.g., Norell and Makovicky, 1999; Hwang et al., 2002; Turner et al., 2007a, 2012). The ventral process is large and robust, and measures 28 mm long as preserved on the more complete left coracoid, but its anterior edge is broken and it would have been larger in life (figs. 10–11: cvp). Anteroventral to the glenoid, on the posterolaterally facing surface of the ventral process, is a shallow subglenoid fossa (figs. 10–11: sgf). This triangular fossa is present in other paravians, as well as some ornithomimosaurs (e.g., Norell and Makovicky, 1999; Turner et al., 2007a, 2012). Compared to the morphology of other dromaeosaurids the subglenoid fossa of *Balaur* appears to be shallowly inset, but this may be an artifact of poor preservation. The fossa of *Tsaagan* is also described as shallow, however, so there may be phylogenetically informative variation in the depth of the fossa among dromaeosaurids (Norell et al., 2006).

The coracoid tubercle (sometimes referred to as the biceps tubercle) is autapomorphically enlarged in *Balaur* (figs. 10–11: ct) The tubercle is located immediately anterior to the glenoid and projects far laterally from the coracoid as a discrete, convex, rugose bulge. When the scapulocoracoid is held in life position the tubercle forms the anterolateral corner of the bone, which is most apparent in dorsal view, where it is seen to project as a pronounced, rounded corner. The large size of the tubercle is also evident in lateral view, as it rises above the floor of the coracoid foramen to obscure this small opening in lateral view. Although the coracoid tubercle of other dromaeosaurids is large (e.g., *Velociraptor*: Norell and Makovicky, 1999; *Buitreraptor*: Makovicky et al., 2005), *Balaur* is unusual in possessing a discrete, conical, rugose tuber that projects far laterally and obscures the floor of the coracoid foramen in lateral view.

Only the ventral margin of the coracoid foramen is present, and it is preserved as a smooth, concave notch that is 5 mm long anteroposteriorly (fig. 11: cf). The foramen is positioned 10 mm directly medial to the coracoid tubercle and is located at approximately the same dorsoventral level as the midpoint of the glenoid, as in other dromaeosaurids (e.g., Norell and Makovicky,

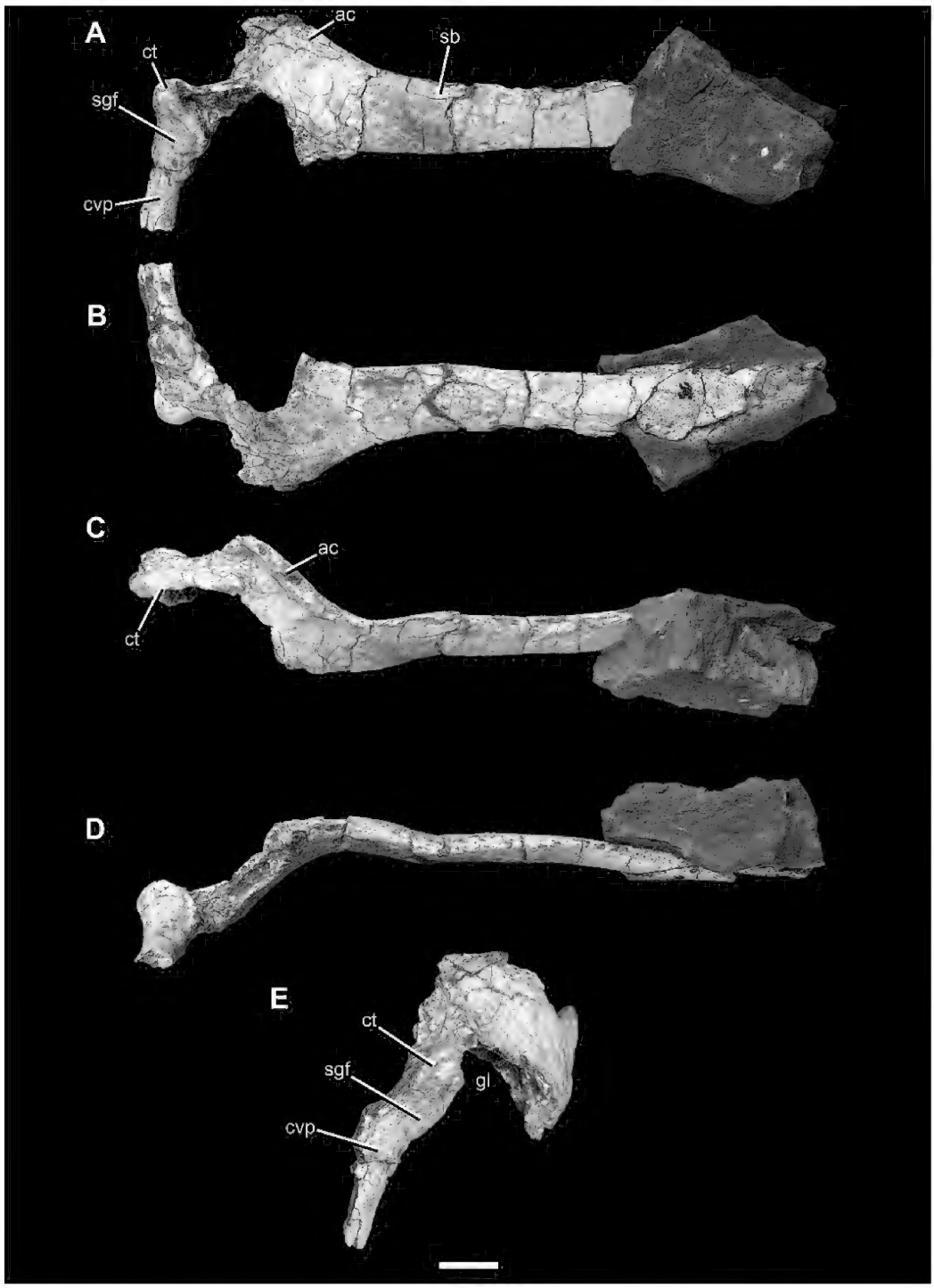

Fig. 10. Left scapulocoracoid of *Balaur bondoc* (EME PV.313) in lateral (**A**); medial (**B**), dorsal (**C**), ventral (**D**), and anterior (**E**) views. Abbreviations: **ac,** acromion; **ct,** coracoid tubercle; **cvp,** coracoid ventral process; **gl,** glenoid (articular surface eroded on this specimen); **sb,** scapula blade; **sgf,** subglenoid fossa. Scale bar equals 1 cm.

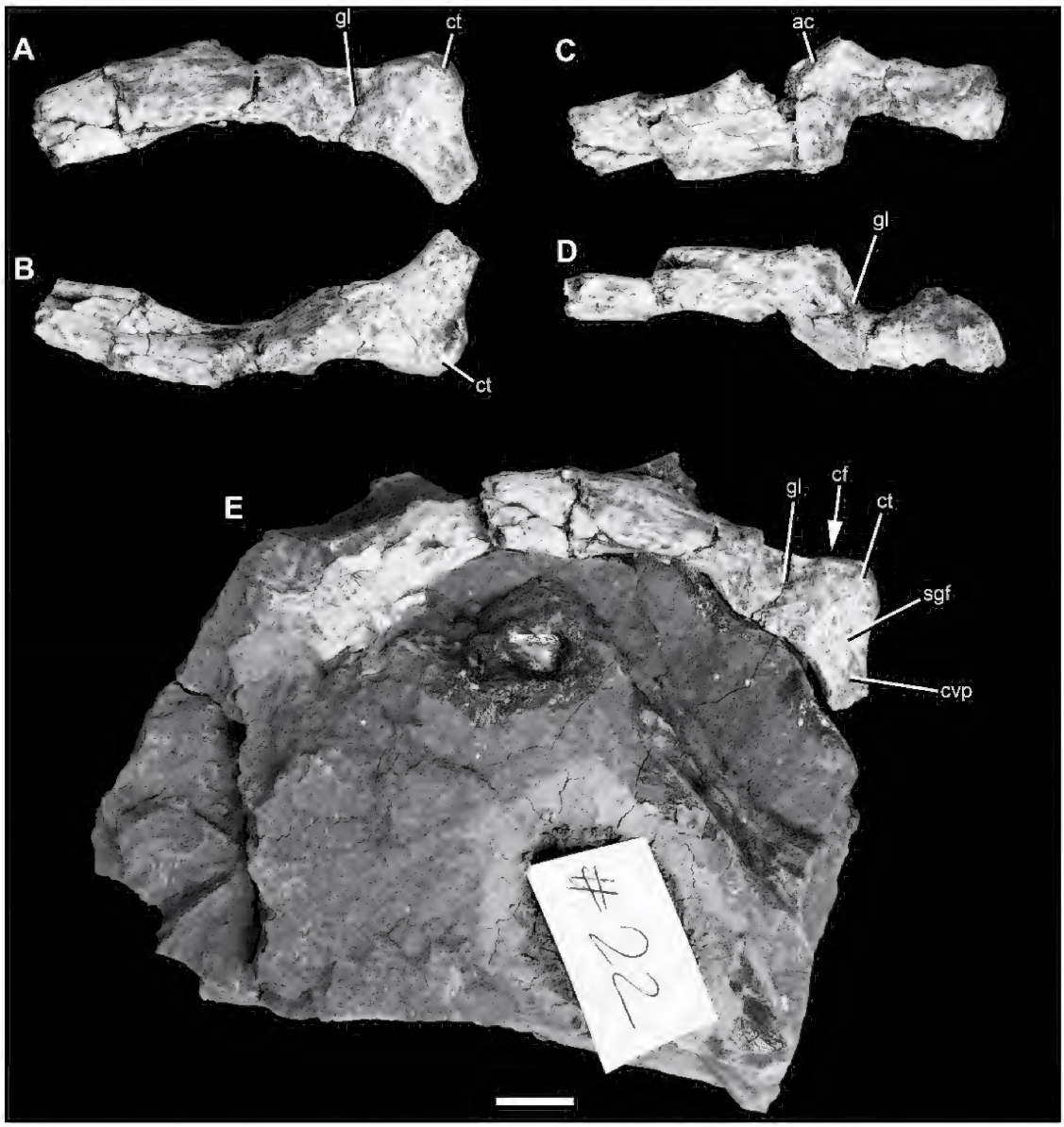

Fig. 11. Right scapulocoracoid of *Balaur bondoc* (EME PV.313) in lateral (**A, E**), medial (**B**), dorsal (**C**), and ventral (**D**) views. E shows lateral view of specimen as it was discovered, with an additional piece of the distal scapular blade. Abbreviations: **ac,** acromion; **cf,** coracoid foramen (arrow pointing to location of foramen, which is obscured in lateral view by coracoid tubercle); **ct,** coracoid tubercle; **cvp,** coracoid ventral process; **gl,** glenoid; **sgf,** subglenoid fossa. Scale bar equals 1 cm.

1999; Norell et al., 2006). Additionally, as in *Tsaagan* and *Deinonychus*, the foramen appears to form a small channel, which trends dorsomedially-ventrolaterally through the interior of the coracoid (Norell et al., 2006). In contrast, the coracoid foramen of most theropods is a larger aperture that opens straight laterally-medially (e.g., Madsen, 1976; Colbert, 1989; Madsen and Welles, 2000; Brochu, 2003; Brusatte et al., 2008). Although not explicitly mentioned by Norell et al. (2006) when they described this unusual

feature, *Velociraptor* also appears to possess this morphology (IGM 100/986).

The **scapula** is much better preserved and more complete on the left specimen, but its blade is broken posteriorly at the point where it begins to expand in dorsoventral depth. The blade is 9 mm deep by 4 mm wide mediolaterally at its midshaft, and is 13 mm deep at the posterior broken margin. The acromion expands at least 10 mm dorsally relative to the blade, but its dorsal margin is broken. Because the acromion is a very thin and large structure in better preserved dromaeosaurid scapulae, it may have been much larger in life in *Balaur*.

The scapula blade is long and gracile, with approximately parallel dorsal and ventral edges that begin to diverge slightly from each other posteriorly (fig. 10: sb). The lateral surface of the blade is flat or shallowly convex across most of its length, but becomes more strongly convex anteriorly as the scapula curves medially ventral to the acromion to articulate with the coracoid. The medial surface, on the other hand, is flat anteriorly and becomes convex posteriorly, and there is no medial ridge as present in many theropods (e.g., Brochu, 2003). The acromion is broken dorsally, but the entire preserved portion has a smoothly concave lateral surface, as is characteristic of dromaeosaurids such as *Velociraptor* (Norell and Makovicky, 1999) (fig. 10: ac). Furthermore, the acromion is clearly everted, such that it projects anteromedially relative to the parasagittal long axis of the scapular blade, which is readily apparent in dorsal view. As a result, the lateral surface of the acromion faces not only laterally but also anteriorly as well. Such eversion is a characteristic feature of paravians and is present in other dromaeosaurids (e.g., Ostrom, 1969; Norell and Makovicky, 1999; Burnham et al., 2000; Hwang et al., 2002; Norell et al., 2006), troodontids (e.g., Xu et al., 2002), and avialans (Clarke and Norell, 2002; Zhou and Zhang, 2002, 2003; Clarke et al., 2006). The medial surface of the acromion of *Balaur* is also concave, but much shallower than the lateral surface concavity.

HUMERUS: Both the left and right humeri are known, and the right is nearly complete and better preserved (fig. 12; table 2). This bone is straight in anterior and posterior views, but sigmoidally curved, with a concave anterior surface and convex posterior surface, in lateral and medial views. Bowed humeri are also present in most dromaeosaurids, including *Austroraptor* (Novas et al., 2009), *Deinonychus* (Ostrom, 1969), *Microraptor* (Hwang et al., 2002), and *Velociraptor* (Norell and Makovicky, 1999). In contrast, the humeri of *Buitreraptor* (Makovicky et al., 2005) and *Unenlagia* (Calvo et al., 2004) are straight in lateral and medial view, with parallel anterior and posterior margins. Unfortunately, because both scapulae are incomplete, it is unclear whether the humerus of *Balaur* was longer than the scapula, as is the case in avialans and most, but not all, dromaeosaurids (Turner et al., 2007a, 2012).

The proximal portion of the humerus is expanded relative to the shaft. The proximal margin is approximately straight in anterior and posterior views, as is characteristic of paravians (e.g., Ostrom, 1969; Norell and Makovicky, 1999; Burnham et al., 2000; Currie and Dong, 2001; Hwang et al., 2002; Calvo et al., 2004), but contrasting with the highly convex or laterally sloped margins of more basal theropods (e.g., Madsen, 1976; Currie and Chen, 2001; Brochu, 2003; Carpenter et al., 2005; Zanno, 2006). The anterior surface of the proximal end is deeply excavated by a smooth fossa (fig. 12: pfos), bordered laterally by the deltopectoral crest and medially by the large internal tuberosity. A nearly identical fossa is also present in other dromaeosaurids (e.g., Ostrom, 1969; Burnham et al., 2000; Calvo et al., 2004) and troodontids (Currie and Dong, 2001). In *Balaur*, both the lateral and medial margins of the fossa are demarcated by a slight crest that separates the convex anterior surfaces of the deltopectoral crest and internal tuberosity from the fossa itself. The medial crest becomes thinner and sharper proximally where it merges with the base of the internal tuberosity, and its pronounced morphology may represent a unique feature of *Balaur* (fig. 12: mpc). However, similar, albeit weaker, crests are also present in *Bambiraptor* (Burnham et al., 2000), *Deinonychus* (Ostrom, 1969), and *Velociraptor* (IGM 100/985), and we hesitate to regard a subtle

Fig. 12. Humeri of *Balaur bondoc* (EME PV.313). Left humerus (**A–F**) and right humerus (**G–L**) in anterior (**A, G**), posterior (**B, H**), lateral (**C, I**), medial (**D, J**), proximal (**E, K**), and distal (**F, L**) views. Abbreviations: **brid,** ridge bisecting fossa on anterior surface of distal end; **dfos,** fossa on anterior surface of distal end; **dpc,** deltopectoral crest; **ec,** ectepicondyle; **en,** entepicondyle; **et,** external tuberosity; **gr,** groove between humeral head and internal tuberosity; **hh,** humeral head; **it,** internal tuberosity; **lrid,** ridge on lateral surface of distal end; **mpc,** medial crest on anterior surface of proximal end, demarcating proximal fossa; **mrid,** ridge on medial surface of distal end; **pfos,** fossa on anterior surface of proximal end; **rc,** radial condyle; **slc,** sinuous crest on lateral surface continuous with deltopectoral crest. Scale bars equal 1 cm. Smaller scale bar on left for anterior, posterior, lateral, and medial views. Larger scale bar on right for proximal and distal views.

feature of the medial crest morphology as an autapomorphy of *Balaur*.

The proximal articular surface is somewhat eroded in both humeri, but several important details are apparent. The humeral head is missing on the right humerus and only half remains on the left, but it is clear that it is bulbous and strongly overhangs the posterior, but not the anterior, surface of the humerus (fig. 12: hh). This is also the case in other dromaeosaurids such as *Bambiraptor* (Burnham, 2004), *Deinonychus* (Ostrom, 1969), and *Velociraptor* (IGM 100/985). Medial to the head, and separated from it by a groove on the posterior surface, is an enlarged internal tuberosity (fig. 12: it). The elongate morphology of the internal tuberosity is characateristic of dromaeosaurids (e.g., Ostrom, 1969; Novas and Puerta, 1997; Burnham et al., 2000; Calvo et al., 2004; Makovicky et al., 2005) and is also present in other coelurosaurs (e.g., Choiniere et al., 2010). The enlarged nature of the tuberosity is readily apparent in medial view, in which the internal tuberosity appears as a convex, bulbous structure that is expanded anteriorly and posteriorly. Lateral to the head there is a small tuberosity on the proximal surface, which projects proximally as a discrete, conical structure, but is not expanded anteriorly or posteriorly (fig. 12: et). This tuber likely corresponds to the external tuberosity, but comparison with other dromaeosaurids is difficult due to poor preservation in most taxa.

The deltopectoral crest extends for approximately 30% of the length of the humerus, a comparable ratio to that seen in other dromaeosaurids (e.g., Ostrom, 1969; Novas and Puerta, 1997; Burnham et al., 2000; Calvo et al., 2004; Xu and Wang, 2004; Makovicky et al., 2005). The crest extends straight anteriorly, such that in proximal view it is approximately perpendicular to the long axis of the proximal surface of the humerus (fig. 12: dpc). This is also the case in most other dromaeosaurids, but the deltopectoral crests of the unenlagiines *Austroraptor* (Novas et al., 2009), *Buitreraptor* (Makovicky et al., 2005), and *Unenlagia* (Calvo et al., 2004) project anteriorly and laterally, and hence form an obtuse angle relative to the proximal surface. Proximally the crest is thin and sheetlike, with a mediolateral width of 2 mm, but distally it thickens and expands in width to 5 mm. The humeral shaft immediately distal to the deltopectoral crest is marked by a sinuous crest following the edge where the posterior and lateral surfaces meet (fig. 12: slc). This crest parallels the lateral margin of the bone for 22 mm. Medial to the crest, on the posterior surface of the humerus, is a deep and elongate groove. A nearly identical crest and groove are present in *Bambiraptor* (Burnham et al., 2000), *Deinonychus* (Ostrom, 1969), *Linheraptor* (Xu et al., 2010), and *Velociraptor* (Norell and Makovicky, 1999), and likely represents a derived character shared by these taxa. A ridge is also present in *Buitreraptor* (MPCA 245) and *Unenlagia* (Calvo et al., 2004), but it is located more proximally, such that it follows the trend of the deltopectoral crest itself, and does not demarcate a groove (Calvo et al., 2004: figs. 9–10).

The humeral shaft is circular in cross section at its midpoint. However, all four surfaces gradually flatten distally, especially the anterior and posterior surfaces. A subtle protuberance is present along the medial margin of the posterior surface, near the midshaft region of the bone. This delicate feature is difficult to assess in other dromaeosaurids but does not appear to be present in *Velociraptor* (IGM 100/985). A much larger tuberosity, referred to in the literature as a "spur," is present in this region in some derived therizinosauroids (Zanno, 2006), and likely is a site of muscle attachment.

The distal end is expanded relative to the shaft and is excavated by a large triangular fossa on its anterior surface (fig. 12: dfos). The fossa, which extends approximately 25% of the proximodistal length of the humerus, is bordered laterally and medially by pronounced crests, which originate from the proximal tips of the ectepicondyle and entepicondyle, respectively (fig. 12: ec, en). The medial ridge is oriented straight proximodistally, extends to the midpoint of the humeral shaft, and gradually becomes sharper and more prominent as it continues proximally (fig. 12: mrid). At its most proximal position, before abruptly merging with

the shaft, the ridge forms a sheetlike shelf that overhangs the medial surface. The lateral crest is oriented obliquely, proximomedially-distolaterally, and is shorter than the medial crest. Where it terminates proximally it merges with a third ridge, which extends straight proximodistally to bisect the fossa (fig. 12: brid). This ridge does not separate the fossa into two equal partitions, but is located closer to the medial margin and terminates distally at the proximal tip of the ulnar condyle. A deep fossa, demarcated by lateral and medial ridges, is present in other dromaeosaurids and troodontids (e.g., Ostrom, 1969; Burnham et al., 2000; Currie and Dong, 2001; Calvo et al., 2004). However, the prominent, shelflike morphology and extreme proximal extent of the medial ridge are autapomorphic for *Balaur*.

Much of the distal articular surface is eroded on both humeri of *Balaur*, including the entirety of the ulnar (medial) condyle. However, portions of the radial (lateral) condyle are present, and these poorly preserved regions indicate that this structure was located on the anterior surface of the humerus (fig. 12: rc). This is unique among dromaeosaurids, which otherwise have the normal theropod condition of a distally placed radial condyle, but is also seen in therizinosauroids and often is considered a diagnostic feature of that clade (e.g., Zanno, 2006). The ectepicondyle is mostly eroded on both humeri, but is clearly present as a discrete structure, separated from the radial condyle (fig. 12: ec). The entepicondyle is preserved on the right humerus and takes the form of a robust ridge that is oriented proximodistally and extends for a total length of 10 mm (fig. 12: en). It is separated from the base of the ulnar condyle by a groove on the anterior surface of the humerus; although the ulnar condyle is missing, the groove itself is well preserved. A subtle fossa is present immediately medial to the entepicondyle, but it does not extend further proximally than the entepicondyle itself. In general, the morphology of the distal humerus is extremely similar to *Deinonychus* in overall morphology (Ostrom, 1969).

An unusual feature is present on the lateral surface of the distal end. Beginning near the distal termination of the humerus is a thin, sharp, sinuous ridge that continues proximally for 1/3 of the length of the bone (fig. 12: lrid). This ridge is not present in *Bambiraptor* (Burnham et al., 2000), *Buitreraptor* (Makovicky et al., 2005), *Deinonychus* (Ostrom, 1969), *Unenlagia* (Calvo et al., 2005), or *Velociraptor* (IGM 100/985), and is therefore an autapomorphy of *Balaur*. A ridge is present on the lateral surface of the distal end in *Bambiraptor*, but this is simply the ridge defining the lateral margin of the anterior fossa, as described above, which is somewhat reoriented relative to other dromaeosaurids such that it is also visible in lateral view (Burnham et al., 2000: fig. 3).

Referred Humerus: A left humerus, approximately 1.45 times the size of the holotype humeri, is among the referred specimens here assigned to *Balaur* sp. (LPB [FGGUB] R.1580) (fig. 13; table 3). It can be referred to *Balaur* based on the possession of autapomorphies, including the sinuous crest on the lateral surface of the distal end (fig. 13: lrid) and the elongate and shelflike medial crest demarcating the anterior fossa on the distal end (fig. 13: mrid). Additionally, it has a radial condyle located on the anterior surface of the distal end, which is also present in the holotype but otherwise unknown among dromaeosaurids (fig. 13: rc). Finally, it possesses dromaeosaurid features such as the groove distal to the deltopectoral crest and the deep fossa on the anterior surface of the distal end. Although this bone can be referred to *Balaur* it does exhibit some differences compared to the much smaller holotype humeri. For instance, on the posterior surface of the proximal end there is a distinct oblique crest that rises to the base of the head, which is absent in the holotype. Furthermore, on the anterior surface of the proximal end there is a ridge bisecting the deep fossa, whereas there is no median ridge in the holotype. Finally, the detailed morphology of the fossa differs between the two specimens: the entire fossa is excavated as a smooth concavity in the holotype, but in the referred specimen the region between the novel bisecting ridge and the medial ridge is convex.

Ulna: Left and right ulnae are present in the holotype and both bones are generally well preserved (fig. 14). The ulna is bowed, as is usual for maniraptorans (Gauthier, 1986),

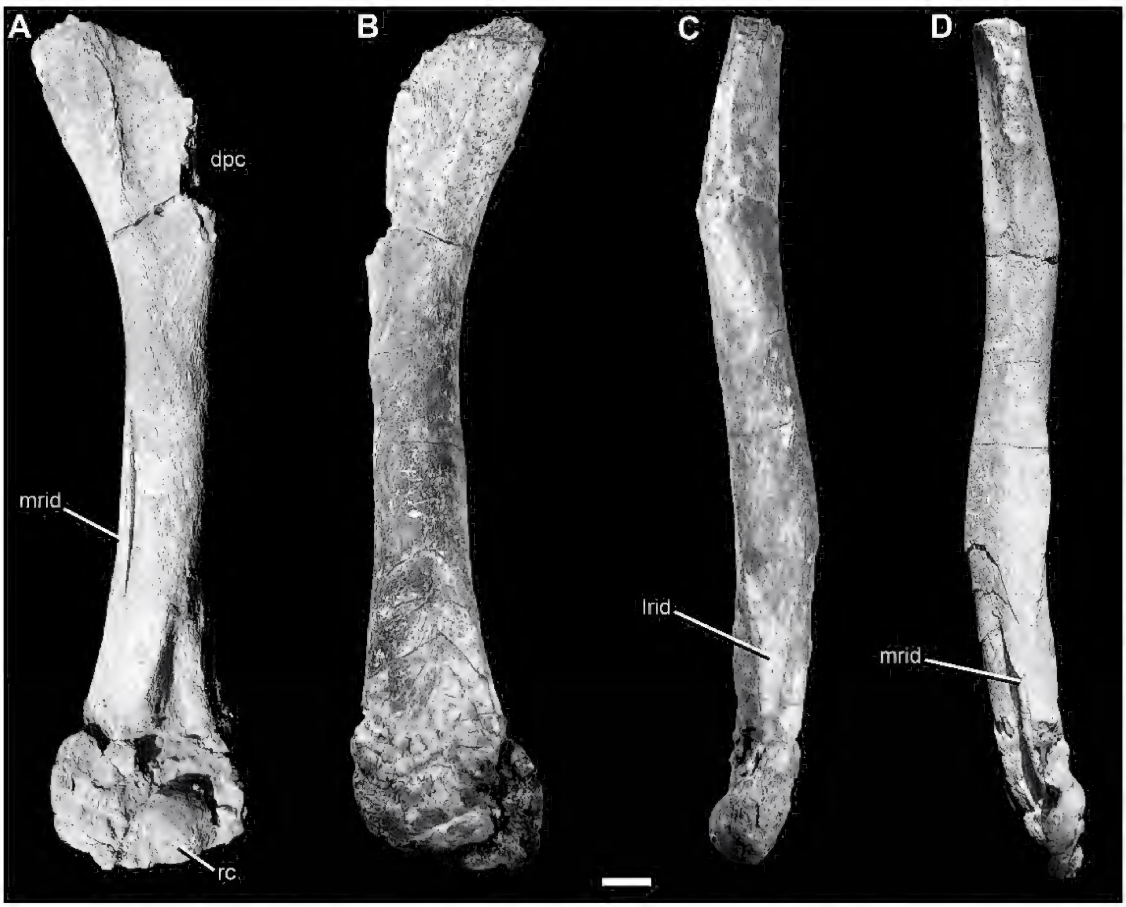

Fig. 13. Referred humerus of *Balaur* sp. (LPB [FGGUB] R.1580). Left humerus in anterior (**A**), posterior (**B**), lateral (**C**), and medial (**D**) views. Abbreviations: **dpc,** region of deltopectoral crest (broken in this specimen); **lrid,** ridge on lateral surface of distal end; **mrid,** ridge on medial surface of distal end; **rc,** radial condyle. Scale bar equals 1 cm.

and is of approximately the same gracile proportions as the radius (table 2). The ulna and radius are of approximately the same build in close relatives of *Balaur*, such as *Bambiraptor* (Burnham, 2004; Senter, 2006), *Deinonychus* (Ostrom, 1969; Senter, 2006), and *Velociraptor* (IGM 100/982). In contrast, the ulnae of more distantly related dromaeosaurids such as *Microraptor* (Hwang et al., 2002), *Rahonavis* (Forster et al., 1998), and *Sinornithosaurus* (Xu et al., 1999) are approximately twice as thick as the corresponding radius. The ulna of *Balaur* is relatively longer (compared to humeral length) than in close relatives such as *Deinonychus* and *Saurornitholestes*, but is more similar in proportions to the ulnae of the microraptorines *Microraptor* (CAGS 20-8-001; Hwang et al., 2002) and *Graciliraptor* (Xu and Wang, 2004) (table 4; see also figs. 42–43). In *Bambiraptor* (Burnham, 2004), and especially *Mahakala* (Turner et al., 2007a), the ulna is even more proportionally elongated than in *Balaur*.

The proximal end is triangular in proximal view. Its medial surface is excavated by a deep, ovoid fossa (fig. 14: pfos) and its lateral surface bears a large coronoid process that fits against the medial surface of the radius (fig. 14: cp). The coronoid process is continuous with a long, sharp crest that extends for 32 mm proximodistally and is only 2 mm thick anteroposteriorly at its midpoint (fig. 14: cpr). It is bordered both anteriorly and

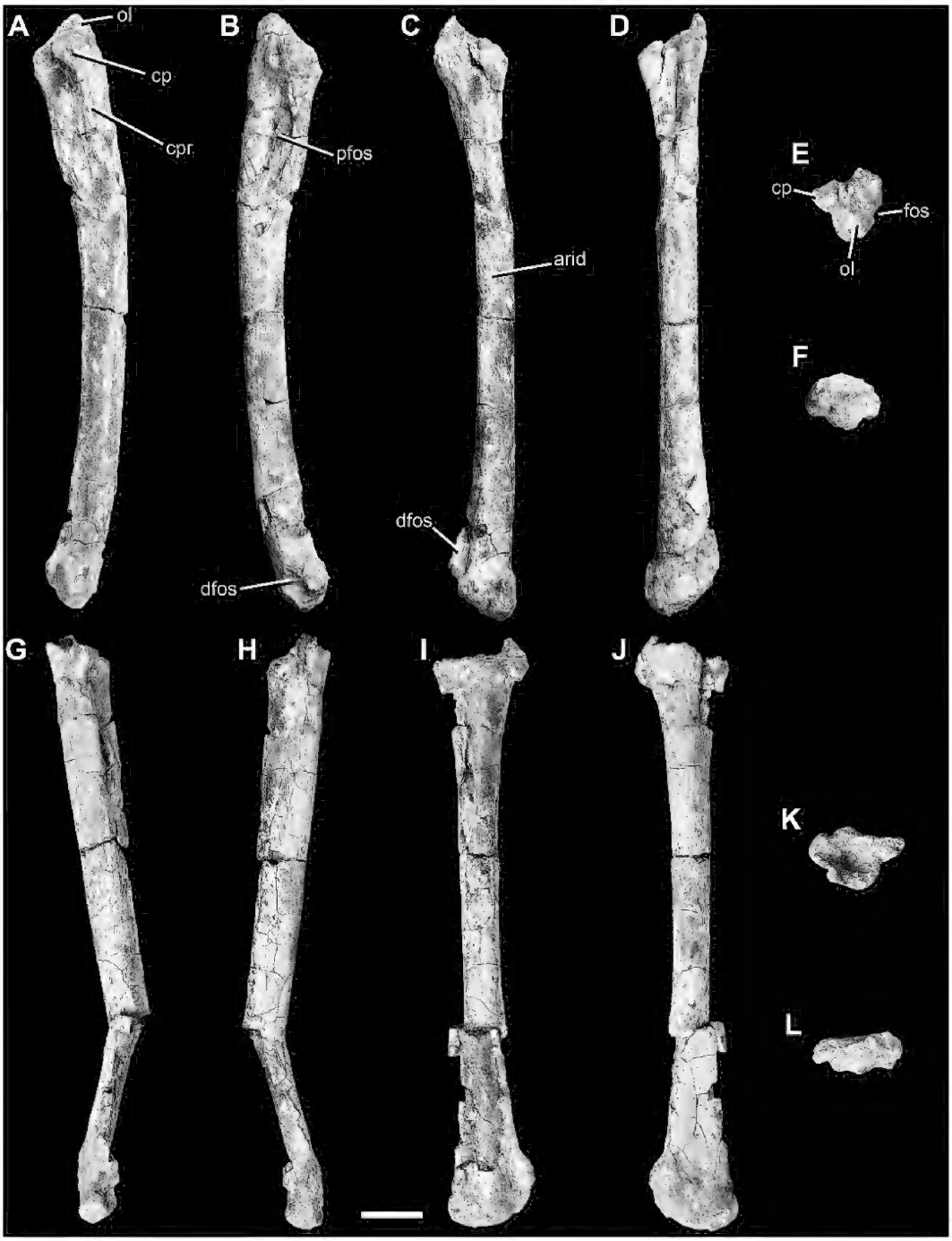

Fig. 14. Ulnae of *Balaur bondoc* (EME PV.313). Left ulna (**A–F**) and right ulna (**G–L**) in lateral (**A, G**), medial (**B, H**), anterior (**C, I**), posterior (**D, J**), proximal (**E, K**), and distal (**F, L**) views. Abbreviations: **arid,** ridge on anterior surface; **cp,** coronoid process; **cpr,** ridge extending distally from coronoid process; **dfos,** fossa on the medial surface of the distal end, abutting the articular condyles; **fos,** fossa; **ol,** olecranon process; **pfos,** fossa on the medial surface of the proximal end. Scale bar equals 1 cm. Proximal end toward top in lateral, medial, anterior, and posterior views.

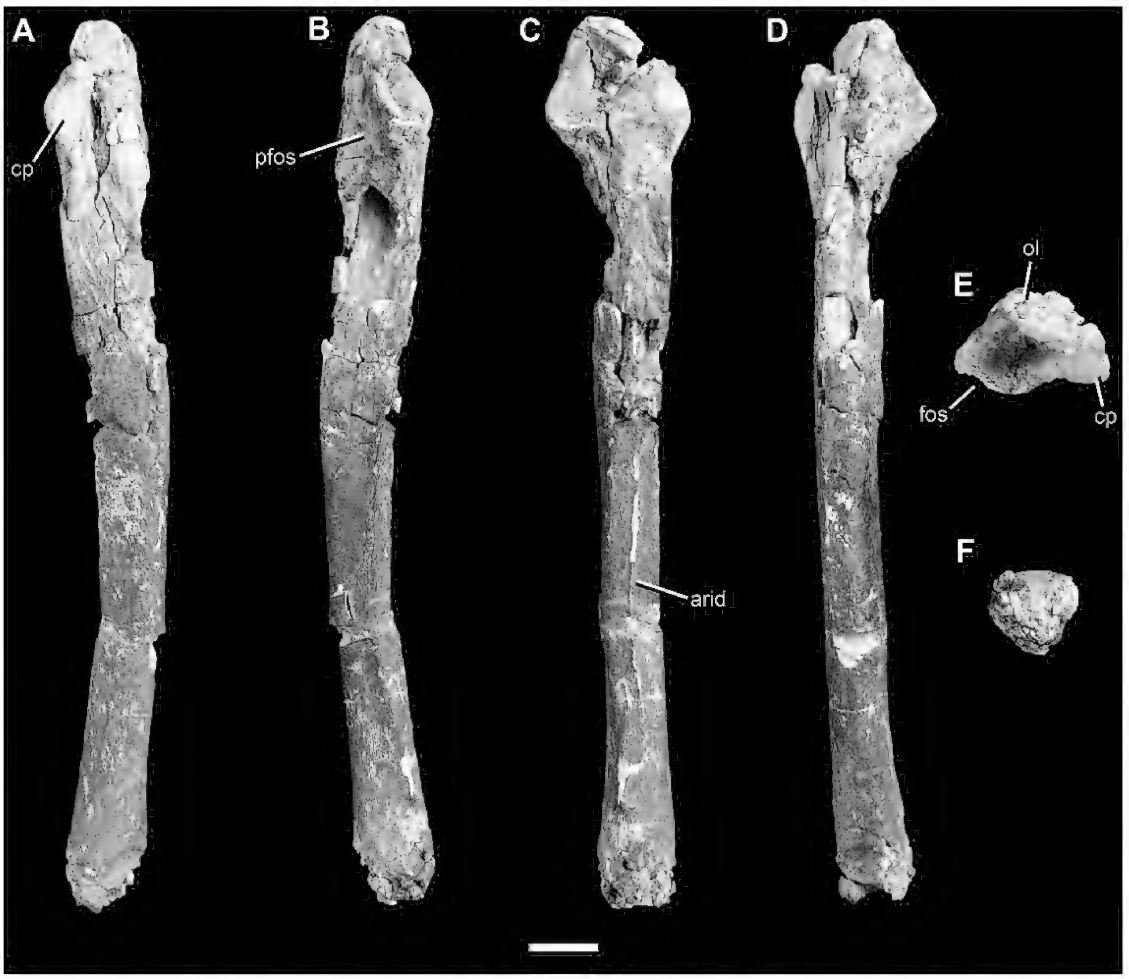

Fig. 15. Referred ulna of *Balaur* sp. (LPB [FGGUB] R.1581). Left ulna in lateral (**A**), medial (**B**), anterior (**C**), posterior (**D**), proximal (**E**), and distal (**F**) views. Abbreviations: **arid,** ridge on anterior surface; **cp,** coronoid process; **fos,** fossa; **ol,** olecranon process; **pfos,** fossa on the medial surface of the proximal end. Scale bar equals 1 cm. Proximal end toward top in lateral, medial, anterior, and posterior views.

posteriorly by shallow fossae that parallel the crest across its entire length. A similar morphology is present in *Deinonychus* (Ostrom, 1969), but is difficult to assess in other dromaeosaurids because many specimens lack ulnae or because the ulna is often preserved flattened on slab specimens (especially in the Chinese Jehol material). The olecranon process of *Balaur* is mostly eroded (fig. 14: oc), but was clearly large, distinct, and conical, as in other dromaeosaurids (e.g., Ostrom, 1969; Forster et al., 1998; Norell and Makovicky, 1999; Hwang et al., 2002; Turner et al., 2007a).

The ulnar shaft is highly convex laterally and posteriorly, flat to slightly convex medially, and flattened anteriorly. As a result, it is somewhat D-shaped in cross section. Furthermore, the lateral and medial margins of the bone, where the flat anterior surface meets the more convex lateral and medial surfaces, are defined as sharp ridges due to the abrupt change of surface orientation. The flat anterior surface is bisected by an elongate, sharp ridge that is oriented proximodistally (fig. 14: arid). The ridge begins proximally at the level of the distal termination of the coronoid process and

TABLE 4
Measurements of forelimb elements (in mm) of dromaeosaurid theropods
Asterisk indicates incomplete measurement due to damage or poor preservation.

Taxon	Humerus	Ulna	MC I	MCII	MCIII
Balaur bondoc EME PV.313	117	99	18	41	39
Balaur sp. LPB (FGGUB) (see table 3)	157*	133*	–	46.2*	–
Deinonychus antirrhopus YPM 5206 (Ostrom, 1969)	–	–	45.8	93.7	82
Deinonychus antirrhopus MCZ 4371 (Ostrom, 1976)	254	208	–	90*	90
Deinonychus antirrhopus AMNH FARB 3015 (Ostrom, 1976)	237	186	35.5	–	73.5
Velociraptor mongoliensis IGM 100/982	–	–	19.2	50.8	45
Saurornitholestes langstoni MOR 660	178	135	30	–	67
Linheraptor exquisitus IVPP V16923	157	110	25.3	64.4	53.1
Bambiraptor feinbergorum AMNH FARB FR 30556	104.1	94	17.3	47.1	43.7
Buitreraptor gonzalezorum MPCA 245	136	112.2	–	20.1	–
Microraptor zhaoianus CAGS 20-7-004	61.3	53.8	7.8	31.3*	29.8*
Graciliraptor lujiatunensis IVPP V13474					
Sinornithosaurus millenii IVPP V12811	–	109.9	17.8	61.8	–
Mahakala onmogovae IGM/1033	37	40	–	18	–

extends distally before terminating against an eroded surface 31 mm from the distal end of the bone. However, based on the morphology of the referred ulna (see below), it is likely that the ridge continued to the distal end of the bone. The flat anterior surface and bisecting ridge together comprise an autapomorphy of *Balaur*, as the anterior ulna is more convex and lacks a sharp, elongate ridge in other dromaeosaurids (e.g., Ostrom, 1969; Burnham, 2004). Unfortunately, surface preservation is not fine enough to assess the presence or absence of quill knobs for the attachment of secondary flight feathers, as are present in extant avialans and have been identified in the dromaeosaurids *Rahonavis* (Forster et al., 1998) and *Velociraptor* (Turner et al., 2007b). It is clear, however, that there was no pronounced bicipital tuberosity on the anterior surface of the proximal end of the shaft.

At approximately the midpoint of the anterior surface of the shaft there are distinct crests paralleling the lateral and medial margins of the bone, the latter of which is thicker and more prominent. Together these ridges enclose a subtle fossa. Farther distally, on the medial surface of the bone, is a deep fossa bordered anteriorly by the medial crest described above and distally by the raised, convex distal articular surface (fig. 14: dfos). The distalmost portion of the fossa is invaginated, as it is laterally enclosed by the distal articular surface itself. This fossa may be a unique feature of *Balaur*, as it is not present in some other dromaeosaurids (e.g., Ostrom, 1969; Burnham, 2004), but we hesitate to regard it as an autapomorphy

here because comparable, well-preserved distal ulnae are not known for most dromaeosaurid taxa. The distal articular surface itself is mostly eroded in both ulnae, but preserved regions indicate that it was a convex, single surface and was not separated into multiple condyles.

Referred Ulna: A left ulna, approximately 60% larger than that of the holotype, is among the referred specimens assigned to *Balaur* sp. (LPB [FGGUB] R.1581) (fig. 15; table 3). It can be referred to *Balaur* based on the possession of the autapomorphic flat anterior surface bisected by a sharp proximodistal ridge (fig. 15: arid). The preserved portion of the referred ulna is 133 mm long proximodistally, but comparison with the holotype indicates that the complete bone would have measured approximately 163 mm. If the referred humerus and ulna belong to the same individual, as we argue above, then the referred ulna is proportionally larger relative to the humerus than in the holotype (table 4).

Radius: Left and right radii, both generally well preserved, are present in the holotype (fig. 16; table 2). The radius is gracile and nearly straight, as is normal for dromaeosaurids (Ostrom, 1969; Forster et al., 1998; Norell and Makovicky, 1999; Hwang et al., 2002; Burnham, 2004; Xu et al., 2010). The proximal surface is ovoid in proximal view and smoothly concave to articulate with the humerus. The posterior region of the proximal surface is thickened, and although somewhat eroded, clearly raised above the level of the more anterior region.

The slender shaft has a highly convex medial surface, which is so strongly convex at the midpoint of the bone that the entire surface resembles a swollen ridge. Here, the radius would have fit against the ulna. Proximally, there is an elongate fossa along the anterior edge of the medial surface (fig. 16: fos). Although somewhat exaggerated by erosion in the right radius, this fossa is undeformed on the left bone, where it measures 12 mm in proximodistal length and is demarcated posteriorly by a thin ridge. This smooth depression would have articulated against the coronoid process (and its associated elongate crest) of the ulna. The lateral surface of the shaft is flat proximally but becomes concave distally, where it is bisected by a proximodistally oriented ridge. This ridge, which measures 6 mm in length, is well preserved on both specimens. Two oblique muscle attachment ridges are present on the lateral surface proximal to midshaft.

The distal surface is ovoid and divided into two convex condyles to articulate with the semilunate carpal. The posterior condyle is much larger, and the two are separated by a smooth, concave trochlear surface. A double articular surface is normal for maniraptorans and is present in other dromaeosaurids, including *Bambiraptor* (Burnham, 2004) and *Deinonychus* (Ostrom, 1969). The medial surface of the distal end is concave for articulation with the distal ulna.

Carpometacarpus: The manus of *Balaur* is remarkably modified relative to other dromaeosaurids, and indeed, other dinosaurs in general (fig. 17). Notably, the three metacarpals (I–III) and at least some distal carpals are fused into a carpometacarpus (figs. 17–18), which is unknown among other dromaeosaurids and is otherwise present only in derived alvarezsauroids (e.g., Perle et al., 1994), perhaps in *Avimimus* (Vickers-Rich et al., 2002), and in derived avialans. The number of fused carpals is difficult to determine due to the extreme fusion of the carpometacarpus, which has obliterated sutures between individual bones. Similarly, the morphology of the carpals cannot be described in detail. The metacarpals themselves are fused proximally but diverge from each other distally, and much of their morphology is visible. Despite the heavy fusion, the first two metacarpals of *Balaur* are similar to those of other dromaeosaurids and show no affinity with the stocky metacarpals of alvarezsauroids (Perle et al., 1994; Choiniere et al., 2010) or the avialan condition in which metacarpals II and III are fused proximally and distally and metacarpal I is reduced to a nubbin. In the *Balaur* holotype, the right carpometacarpus is essentially complete (figs. 17–18), whereas only fragments of the left metacarpals I and II are present, broken and separated from each other (fig. 19). Fusion between metacarpals I and II proceeds farther distally than that between II and III, but these latter two metacarpals do

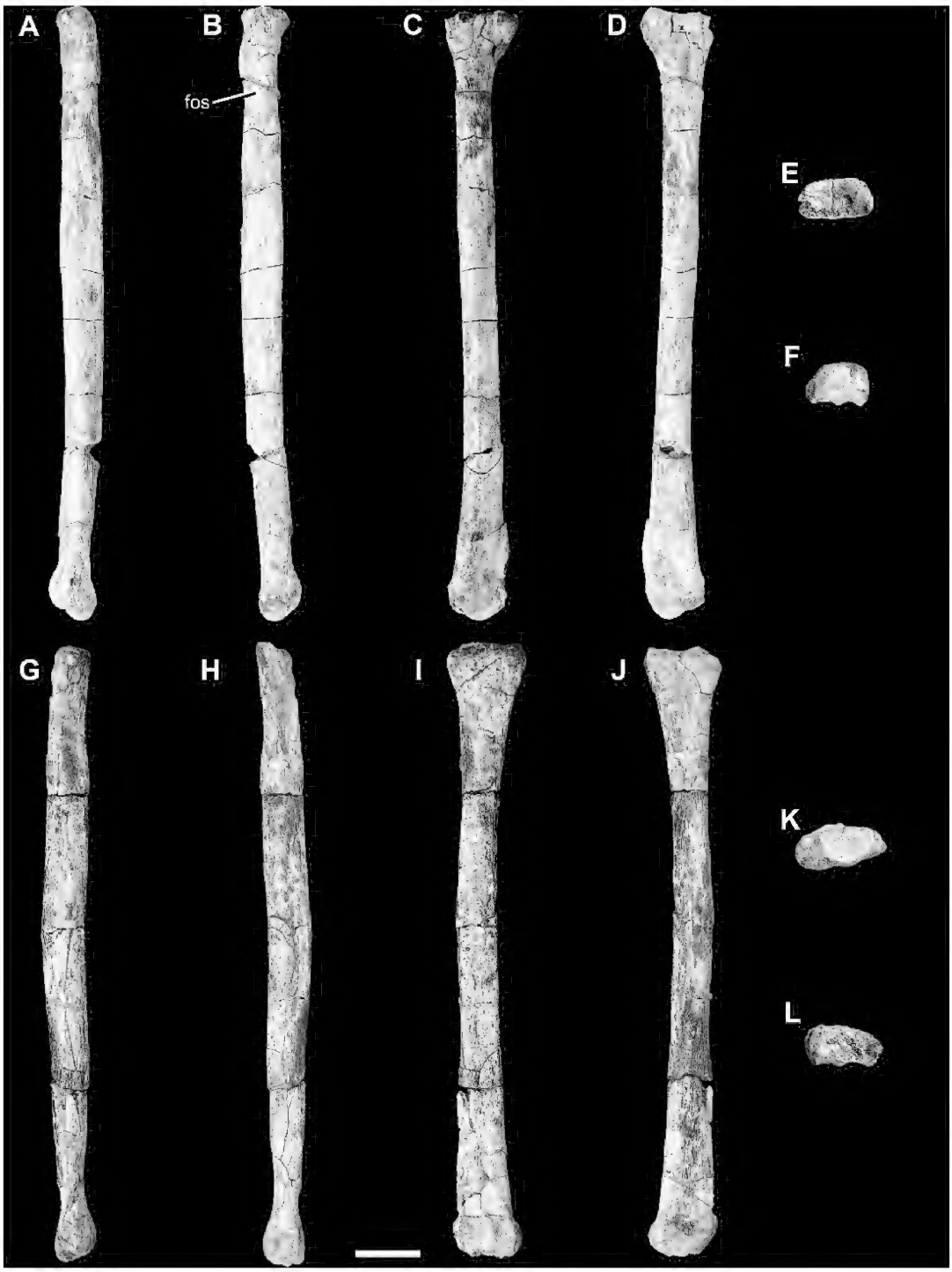

Fig. 16. Radii of *Balaur bondoc* (EME PV.313). Left radius (**A–F**) and right radius (**G–L**) in lateral (**A, G**), medial (**B, H**), anterior (**C, I**), posterior (**D, J**), proximal (**E, K**), and distal (**F, L**) views. Abbreviations: **fos,** fossa on proximal end of medial surface. Scale bar equals 1 cm. Proximal end toward top in lateral, medial, anterior, and posterior views.

Fig. 17. Right carpometacarpus and digits of *Balaur bondoc* (EME PV.313) in extensor view (unguals in medial view). Scale bar equals 1 cm.

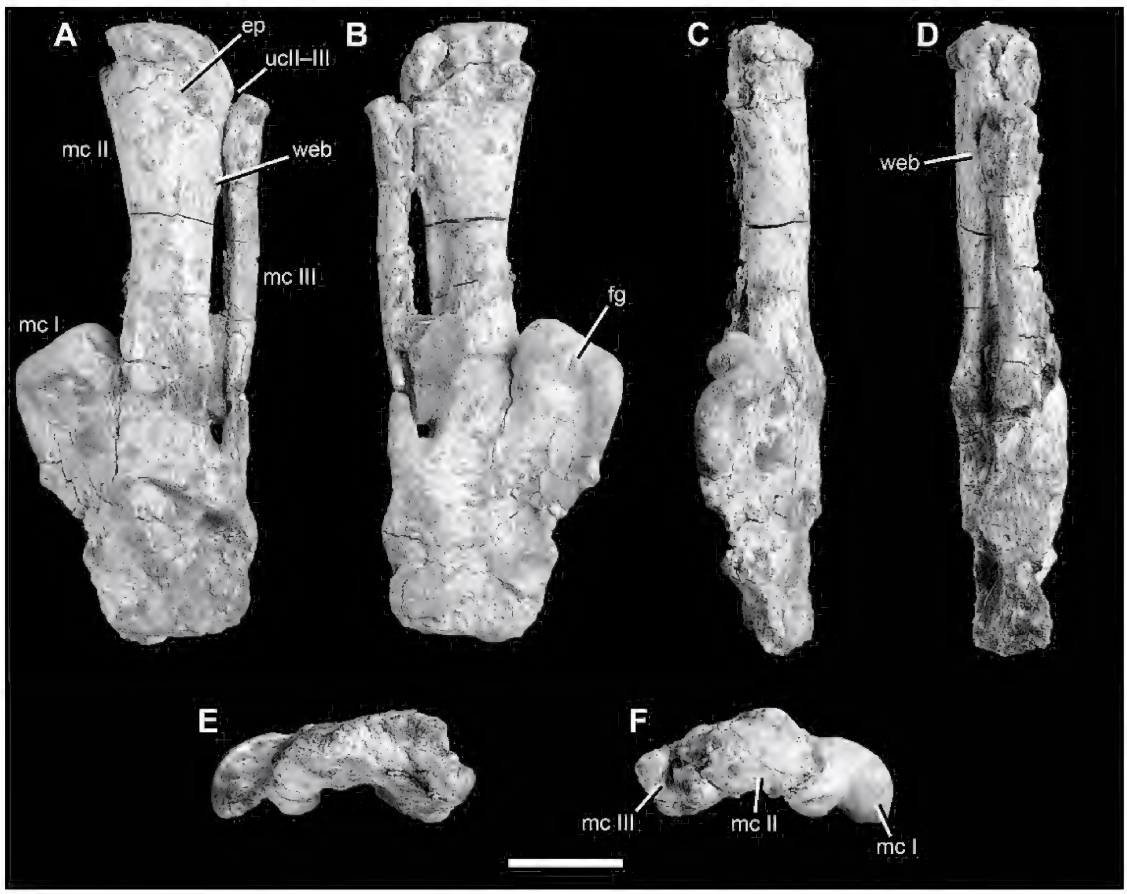

Fig. 18. Right carpometacarpus of *Balaur bondoc* (EME PV.313) in extensor (**A**), flexor (**B**), medial (**C**), lateral (**D**), proximal (**E**), and distal (**F**) views. Abbreviations: **ep,** extensor pit; **fg,** flexor groove; **mc I–III,** individual metacarpals; **ucII–III,** distal unfused contact between metacarpals II and III; **web,** web of bone along the lateral edge of the extensor surface of metacarpal II. Scale bar equals 1 cm.

contact each other distally at an unfused contact, which is an autapomorphy among dromaeosaurids.

The metacarpus is shortened in *Balaur*, compared to the condition in most other dromaeosaurids (table 4; see also fig. 44). Metacarpal II represents about 35% of humeral length and 41% of ulnar length, compared to over 45% and 50%, respectively, in basal velociraptorines (*Bambiraptor*: Burnham, 2004), and in microraptorines (*Microraptor*: Hwang et al., 2002; *Graciliraptor*: Xu and Wang, 2004; *Sinornithosaurus*: IVVP V12811). Velociraptorines that are more closely related to *Balaur*, including *Linheraptor* (Xu et al., 2010) and *Deinonychus* (Ostrom, 1969), exhibit similar, but still larger, ratios than those recorded in *Balaur*.

Metacarpal I is small compared to metacarpals II and III, but nevertheless relatively longer (compared to metacarpal II) than in *Velociraptor* (IGM 100/982), more basal velociraptorines such as *Linheraptor* (Xu et al., 2010) and *Bambiraptor* (Burnham, 2004; AMNH FR 30556), and especially in microraptorines such as *Microraptor* (Hwang et al., 2002) and *Sinornithosaurus* (IVVP V12811). The relative degree of metacarpal I elongation in *Balaur* is most closely comparable to *Deinonychus* (YPM 5205), which has a metacarpal I that is slightly proportionally longer than in *Balaur* (table 4; see also fig. 44).

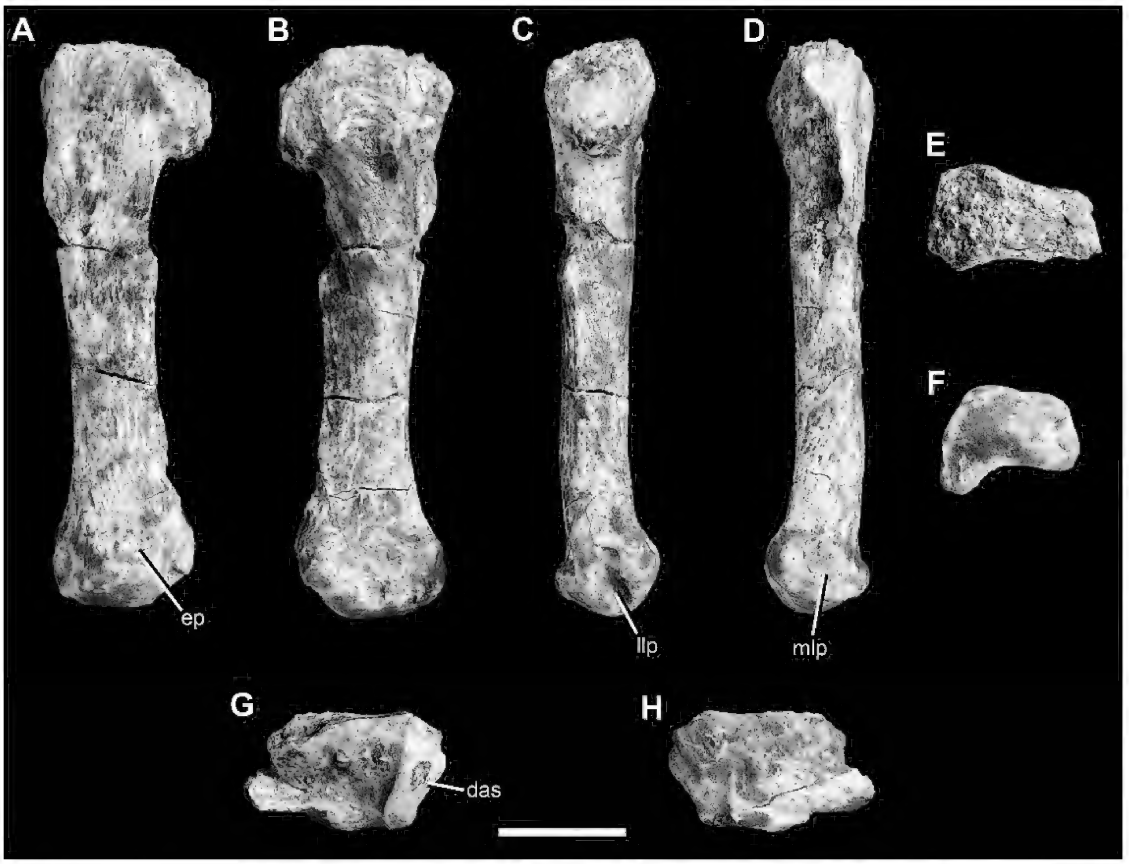

Fig. 19. Left carpometacarpus of *Balaur bondoc* (EME PV.313). Metacarpal II (**A–F**) and metacarpal I (**G–H**) in extensor (**A, G**), flexor (**B, H**), lateral (**C**), medial (**D**), proximal (**E**), and distal (F) views. Abbreviations: **das,** distal articular surface; **ep,** extensor pit; **llp,** lateral ligament pit; **mlp,** medial ligament pit. Scale bar equals 1 cm. Note that these two bones would have been fused in life but have been broken apart postmortem.

In *Balaur*, metacarpal I diverges medially relative to the remainder of the hand and has a lateral surface that abuts the medial surface of metacarpal II along a broad, flat contact, as is normal for theropod dinosaurs. Unfortunately, the proximal and lateral surfaces cannot be observed due to fusion, but the medial surface is subtly concave. Distally, there is no medial ligament pit, but the lateral ligament pit is large, deep, and ovoid. The flexor (ventral) surface is concave across its entire length, and this concavity is deepest distally where it smoothly merges with the flexor groove.

The distal articular surface is convex and asymmetrical, as is normal for theropods, allowing the phalanges to diverge medially relative to digit II. Posteriorly the distal surface divides into two condyles. The medial condyle is an elongate oval, with a long axis oriented ventromedially, which tapers posteriorly to a rounded point. The lateral condyle is smaller, more strongly convex distally, and has a long axis that is oriented closer to straight dorsoventrally (extensor-flexor direction). The condyles continue onto the flexor (ventral) surface and are separated by a deep flexor groove (fig. 18: fg), which excavates both the distal and flexor surfaces of the articular region. However, separate condyles do not extend onto the extensor (dorsal) surface, and in extensor view the distal margin appears as a slightly convex, continuously rounded margin. This is an autapomorphy among dromaeosaurids, and is associated with more limited manual extension relative

to closely related taxa. In contrast, dromaeosaurids such as *Deinonychus* (Ostrom, 1969), *Graciliraptor* (Xu and Wang, 2004), and *Velociraptor* (Norell and Makovicky, 1999; IGM 100/982) possess a metacarpal I with distal condyles that extend onto the extensor surface, and are clearly apparent in extensor view as discrete structures separated by a concave margin. In *Balaur*, the reduced condyles are associated with the lack of an extensor pit on the extensor surface immediately proximal to the distal articular region, which is present in the other dromaeosaurids listed above.

Metacarpal II is the longest bone in the hand. Its extensor surface is flat proximally, becomes convex near the midpoint, and then is concave distally due to a large extensor pit (fig. 18: ep). Both medial and lateral ligament pits are present distally (fig. 19: mlp, llp). The distal articular surface is divided into two condyles of equal size, which are separated by an obtuse angle. As with metacarpal I, the condyles extend onto the flexor surface of the bone but are not apparent as discrete structures in extensor view. Furthermore, the groove between the condyles is present only on the flexor surface and does not extend onto the distal articular surface itself. However, the articular surface does extend onto the extensor surface, but does so as a single rounded convexity, and it is bordered by an extensor pit proximally (fig. 19: ep). Therefore, limited manual extension was possible. The flexor surface of the bone is concave proximally as a triangular fossa, then convex at midlength, and finally becomes concave again distally at the flexor groove. It is crossed obliquely by a weak ridge, stretching between the proximolateral corner, where it begins immediately distal to the fusion with metacarpal III and the edge of the medial condyle.

Unusually, there is a raised web of bone along the margin where the lateral and extensor surfaces meet (fig. 18: web). This begins proximally immediately distal to the fused contact of metacarpals II and III, and here it is located precisely at the dorsolateral corner of the bone. Further distally it curves ventrally (i.e., toward the flexor direction), and in doing so defines a flat, triangular facet dorsal to it (i.e., toward the extensor direction). This facet articulates against the distal end of metacarpal III. Between their proximal fused contact and distal unfused articulation (fig. 18: ucII–III), the two metacarpals parallel each other and are separated by approximately 2 mm. The web on metacarpal II is most pronounced at approximately one third of the length of the shaft, where it is visible in extensor view as a rugose crest that projects laterally, and in lateral view as a thickened ridge that is dorsally convex (toward the extensor direction). Although the web is prominent here, it directly articulates with metacarpal III only further distally, where it is weaker.

Metacarpal III is the most unusual element in the carpometacarpus, as it is extremely reduced in thickness relative to other dromaeosaurids such that it resembles a thin splint. In most theropods metacarpal III is more gracile than the first two metatarsals, but in *Balaur* it is only 30% as thick as metacarpal II. In contrast, metacarpal III is approximately 50% of the mediolateral thickness of metacarpal II in *Velociraptor* (IGM 100/982), and a similar ratio is seen in other dromaeosaurids (e.g., Ostrom, 1969; Hwang et al., 2002; Burnham, 2004; Xu and Wang, 2004; Senter, 2006). Therefore, the extremely reduced metacarpal III is an autapomorphy of *Balaur*. That said, metacarpal III of *Balaur* is not reduced in its anteroposterior length. In fact, it is slightly more elongated, compared to metacarpal II, than in closely related velociraptorines, and is comparable in relative length to the third metacarpals of microraptorines such as *Microraptor* (CAGS 20-7-004; Hwang et al., 2002), *Graciliraptor* (Xu and Wang, 2004), or *Sinornithosaurus* (IVVP V12811) (table 4; see also fig. 44).

Metacarpal III is thickest anteroposteriorly at its proximal fused end, but abruptly thins distally into a splint with an ovoid cross section. On the flexor surface, the proximal fused region is projected below the remainder of the metacarpus and extends to approximately the same level as the lateral edge of metacarpal I. Together, these two ventrally projected regions define a deep depression between them, which covers the entirety of the flexor surface of the proximal portion of metacarpal II and much of the flexor surfaces

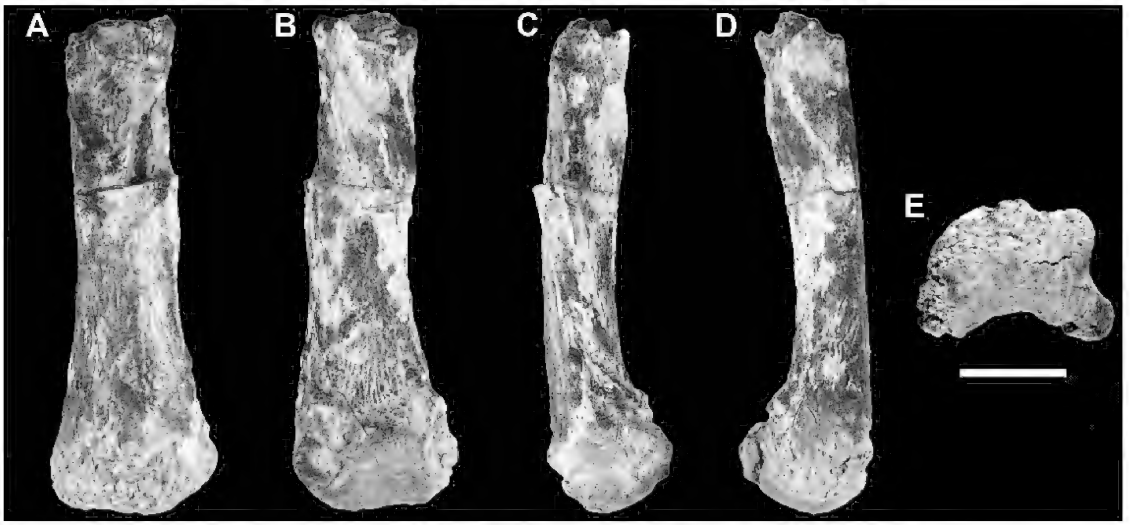

Fig. 20. Referred metacarpal II of *Balaur* sp. (LPB [FGGUB] R.1585). Left metacarpal II in extensor (**A**), flexor (**B**), lateral (**C**), medial (**D**), and distal (**E**) views. Scale bar equals 1 cm. Proximal end toward top in lateral, medial, anterior, and posterior views.

of the proximal regions of metacarpals I and III. Distally, the articular surface of metacarpal III is a single, rounded structure that is not divided into separate condyles. This is an unusual condition, departing from the double condyles present in other dromaeosaurids (e.g., Ostrom, 1969; Norell and Makovicky, 1999; Burnham, 2004; Xu and Wang, 2004), and is related to the atrophied morphology of the phalanges of the third digit (see below).

Referred Manual Metacarpal: A distal fragment of left metacarpal II (LPB [FGGUB] R.1585) is included within the referred material of *Balaur* sp. (fig. 20). The shaft and distal articular end are essentially complete and well preserved, but the proximal region, where the bone was likely coossified with metacarpals I and III, is missing. Furthermore, the extensor margin of the distal articular surface is largely abraded, as is the distalmost extremity of the flexor surface of the medial condyle, exposing cancellous bone texture.

Despite its fragmentary nature, this bone exhibits several features shared with the holotype of *B. bondoc* (EME PV.313). These include: the restriction of the intercondylar groove to the flexor surface of the distal end, so that the distal articular end is straight in extensor view; the widely divergent distal condyles on the flexor surface; and, especially, the unique raised web that would have overhung metacarpal III distally. As this referred specimen is disarticulated from the remainder of the (presumably) fused carpometacarpus, it also reveals some details of the lateral and medial surfaces that are hidden in the holotype by the closely appressed metacarpals I and III.

On the lateral edge of the extensor surface, the proximal part of the overhanging web is broken off, but its preserved distal part suggests it was also prominent, as in the holotype of *B. bondoc*, possibly even more so. Distally, it thins and becomes less pronounced, until it finally merges with the body of the bone near the distal end. Distal to the web, there is a small lateral extension, corresponding to the area of contact with the distal part of metacarpal III, as seen in the holotype of *B. bondoc*. Ventral to the web (in the flexor direction), the lateral edge of the flexor surface the shaft is marked by a less well developed, but still clearly marked, ridge, which extends from the area of sutural contact with metacarpal III to the proximal edge of the flexor surface of the lateral condyle distally. The area between this ridge and the overhanging dorsal web—the lateral surface of metacarpal II—is unevenly concave and rugose, and is distally excavated by a teardrop-shaped depression that marks the

contact with the medial margin of the distal metacarpal III.

The flexor surface of the shaft is widely exposed in lateral view proximally, but reorients to face only ventrally (i.e., in the flexor direction) distally. The laterally exposed portion is positioned between the lateral edge of the flexor surface and an oblique ridge crossing the flexor surface. This ridge corresponds to, but is significantly more pronounced than, the slight longitudinal prominence present on the holotype metacarpal II of *B. bondoc*. A thin, longitudinal ridge dissects this laterally facing part of the flexor surface, extending somewhat less than halfway along the preserved length of the shaft. Distal to this point, the lateral exposure of the flexor surface diminishes rapidly, so that the flexor surface is only ventrally exposed, while also becoming widely concave transversely.

The medial edge of the extensor surface of the shaft is slightly raised as a ridge, and, as a result, the extensor surface is slightly depressed between the elevated lateral and medial edges. The raised medial edge flattens out at midlength of the shaft, but continues as a barely visible, thin ridge onto the distal portion of the medial surface of the bone. On the medial surface, a short, flat, triangular area faces ventromedially along the proximal region of the bone; it is bordered ventrally (in the flexor direction) by an oblique and subtly pronounced ridge ending at approximately the same level as the ridge that bisects the portion of the flexor surface that is exposed laterally (see above). The subtle ridge on the medial surface begins in a ventral position proximally and extends toward the midline of the medial surface as it continues distally, before eventually terminating in a small protuberance. Based on comparisons with the holotype metacarpus, the flat triangular facet on the medial surface is an articulation site for metacarpal I. Due to the ventromedial orientation of this articular surface, the line of contact between the two metacarpals would have been more laterally displaced on the flexor surface, as metacarpal II has a wider exposure in extensor view than in flexor view; this condition is also seen in the articulated carpometacarpus of the holotype of *B. bondoc*. Distal to the triangular contact facet for metacarpal I, the medial surface of metacarpal II is mildly convex with a small prominence distally, near the proximal edge of the flexor surface of the medial condyle.

In distal view, the articular surface is comprised of two widely separated condyles that diverge from each other ventrally (i.e, in the flexor direction). The lateral condyle is slightly narrower than the medial condyle and has a laterally concave outline in distal view, due to the presence of a well-developed lateral ligament pit that deeply excavates the lateral margin of the condyle and is opened distally. The medial ligament pit, on the other hand, is less developed, fully closed distally, and placed at approximately midheight of the condyle. As in the holotype of *B. bondoc*, the distal articular surface is continuous across the two condyles (i.e., not divided by a trochlear groove), and is essentially flat in flexor and extensor views. The condyles are proximally separated on the flexor surface by a wide and deep flexor groove, which is clearly separated from the articular surface itself. It is not possible to ascertain whether the condyles were also separate on the extensor surface, due to abrasion in this region. However, the presence of an extensor pit or groove is hinted at by a slight depression in the damaged area.

Manual Digits: The complete array of phalanges is preserved in both the left and right hands of the holotype (figs. 17, 21–25). As preserved, the phalangeal formula is 2-3-1, which is autapomorphic among dromaeosaurids due to the atrophied digit III (see below). In general, the lateral ligament pits are deeper and larger than the medial pits on all phalanges, and deep flexor grooves and the great extent of the distal condyles onto the flexor surface of the phalanges is indicative of substantial manual flexion abilities. On the contrary, the lack of deep extensor pits and the absence of any migration of the distal articular surface onto the extensor surface of the phalanges suggest that manual extension was limited relative to that of other dromaeosaurids (e.g., Ostrom, 1969; Norell and Makovicky, 1999). However, the ability to extend the individual elements of the manus may have become progressively greater distally along each digit, judging by the increasingly deeper extensor pits (although

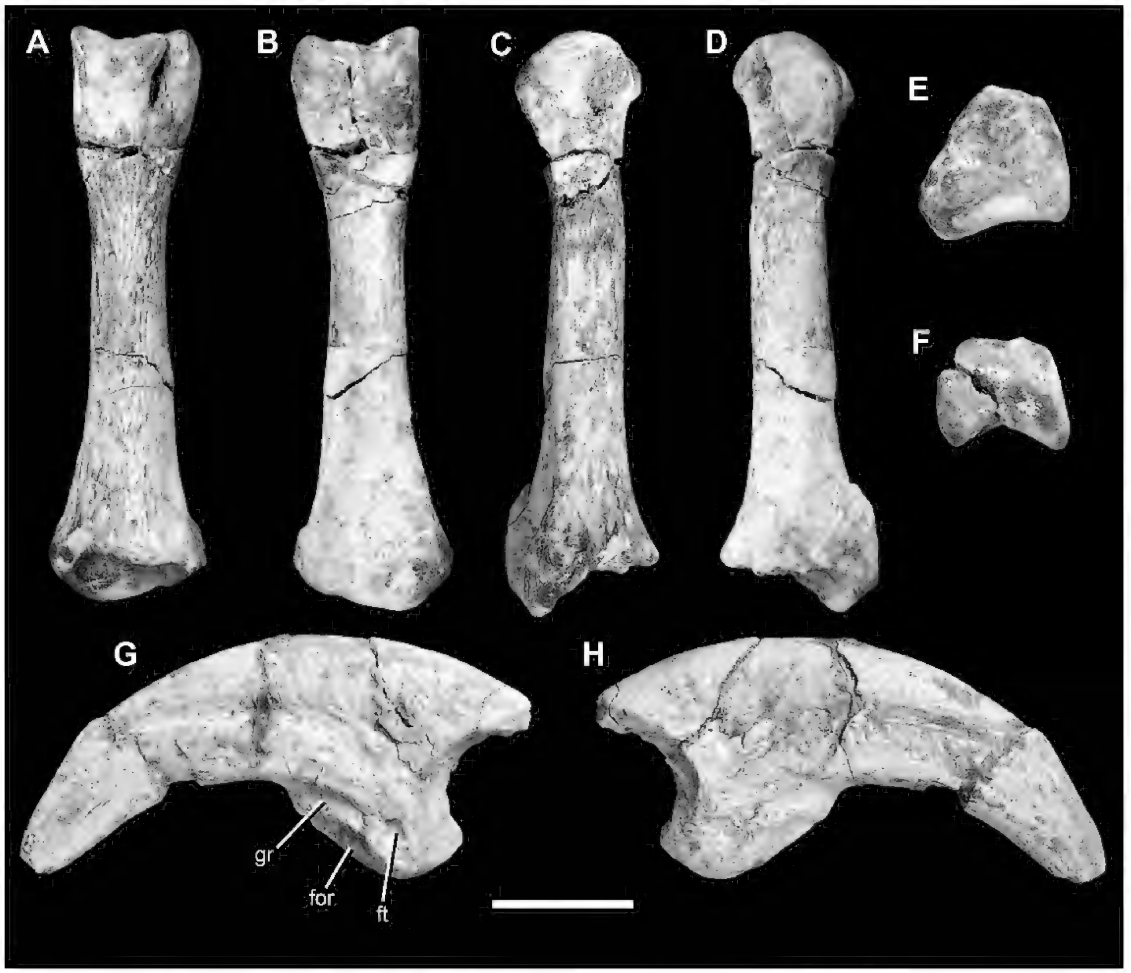

Fig. 21. Left manual digit I of *Balaur bondoc* (EME PV.313). Left phalanx I-1 (**A–F**) and left phalanx I-2 (**G–H**) in extensor (**A**), flexor (**B**), lateral (**C, G**), medial (**D, H**), proximal (**E**), and distal (**F**) views. Abbreviations: **for,** foramen; **ft,** flexor tubercle; **gr,** groove separating flexor tubercle from ventral surface of ungual. Scale bar equals 1 cm.

this is a tentative interpretation, because some extensor muscles do not have bony insertions). This is especially evident in digit II, as metacarpal II lacks an extensor pit, phalanx II-1 has a small extensor pit, and phalanx II-2 has a larger and deeper extensor pit, although it is still quite shallow compared to the condition in closely related taxa.

Manual Digit I: Digit I is approximately 72% of the length of digit II, but the two digits are essentially equally robust (table 2) (figs. 21–22). **Phalanx I-1** is the largest phalanx in the hand, and has a triangular proximal articular surface that is depressed and saddle shaped to receive the distal condyles of the first metacarpal (figs. 21–22, A–F). The saddle is asymmetrical to match the condyles of the metacarpal: the lateral portion is deeper to accept the more convex lateral condyle of metacarpal I, and the two lateral and medial portions are oriented obliquely to each other. The long axis of the proximal surface is dorsomedially oriented, such that it appears twisted relative to the long axis of the phalanx itself. There are no flexor or extensor tubercles on the proximal surface, but there is a pronounced lip surrounding the entire proximal region, which is especially prominent ventrally (in the flexor direction).

Fig. 22. Right manual digit I of *Balaur bondoc* (EME PV.313). Right phalanx I-1 (**A–F**) and right phalanx I-2 (**G–H**) in extensor (**A**), flexor (**B**), lateral (**C, H**), medial (**D, G**), proximal (**E**), and distal (**F**) views. Abbreviations: **for,** foramen; **ft,** flexor tubercle. Scale bar equals 1 cm.

The flexor surface of phalanx I-1 is concave, defined laterally and medially by longitudinal ridges on the edges of the shaft. The concavity is most pronounced proximally and distally adjacent to the articular ends. The extensor surface of the phalanx is convex and the lateral and medial surfaces are subtly convex but nearly flat. Distally there are ligament pits on both sides, unlike metacarpal I, which possesses only a lateral pit. The pits are extensively visible in extensor view because the distal end is expanded relative to the shaft.

The distal end is divided into two pronounced condyles posteriorly, which are approximately equal in size and extend to the same posterior (= flexor) level. They are separated by a deep groove and form an acute angle to each other. The groove continues ventrally as the flexor groove and also slightly onto the extensor surface, unlike metacarpal I which autapomorphically lacks any continuation of the groove dorsally (toward the extensor direction). Therefore, unlike the condition in the metacarpal, the separate condyles of phalanx I-1 are visible in

Fig. 23. Left manual digit II of *Balaur bondoc* (EME PV.313). Left phalanx II-1 (**A–F**), left phalanx II-2 (**G–L**), and left phalanx II-3 (**M–N**) in extensor (**A, G**), flexor (**B, H**), lateral (**C, I, M**), medial (**D, J, N**), proximal (**E, K**), and distal (**F, L**) views. Abbreviations: **ygr,** proximal bifurcations of the Y-shaped groove. Scale bar equals 1 cm.

Fig. 24. Right manual digit II of *Balaur bondoc* (EME PV.313). Right phalanx II-1 (**A–F**), right phalanx II-2 (**G–L**), and right phalanx II-3 (**M–N**) in extensor (**A, G**), flexor (**B, H**), lateral (**C, I, N**), medial (**D, J, M**), proximal (**E, K**), and distal (**F, L**) views. Scale bar equals 1 cm.

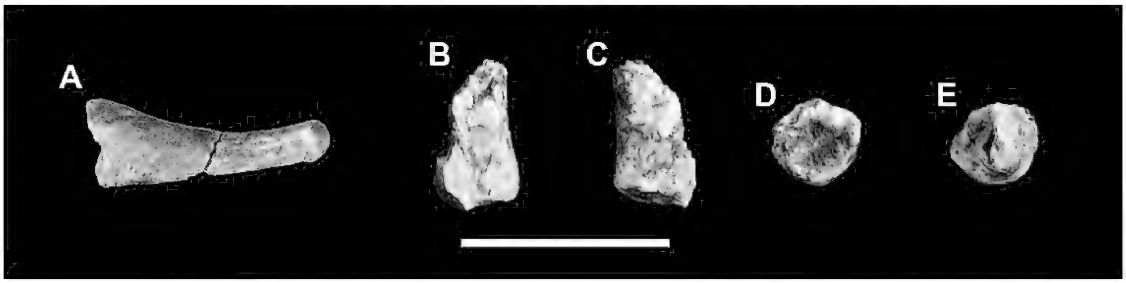

Fig. 25. Manual digit III of *Balaur bondoc* (EME PV.313). Single phalanx of the right (**A**) and left (**B–E**) manual digit III. The right phalanx is figured in extensor view, with its proximal articular surface to the left. The left phalanx is figured in flexor (**B**), extensor (**C**), proximal (**D**), and distal (**E**) views. Scale bar equals 1 cm.

extensor view, separated by the concave trace of the flexor groove.

The ungual of digit I, **phalanx I-2**, is the largest claw in the hand (table 2) (figs. 21–22, G–H). It is recurved, although not as strongly as in *Deinonychus* (Ostrom, 1969) and *Velociraptor* (IGM 1000/982), and is excavated by a single groove on the lateral and medial sides. The groove begins at the midpoint of the phalanx, curves as it continues distally, and terminates at the distal margin of the bone, slightly dorsal to the distal tip. The proximal articular surface is saddle shaped to match the distal condyles of phalanx I-1 and is surrounded by a pronounced lip, which is especially prominent along the lateral and medial edges. Ventrally there is a large, swollen flexor tubercle (fig. 21: ft), whose proximal base is penetrated by two small foramina, one on each side of the midline (fig. 21: for). The foramina are approximately 1.5 mm in diameter and are visible in both lateral and flexor views. It is possible that these are unique features of *Balaur* because they are absent in *Velociraptor* (IGM 100/982), but we hesitate to regard them as autapomorphic since the corresponding ungual of most other dromaeosaurids is not known or, if known, not well preserved. Anterior to the foramina, and separated from them, is a curved groove that divides the flexor tubercle from the flexor surface of the ungual (fig. 21: gr). This deep groove is also absent in *Velociraptor* and may be a unique feature of *Balaur*.

Manual Digit II: Digit II is the longest in the hand (table 2) (figs. 23–24). **Phalanx II-1** has a proximal surface that is triangular in shape and only weakly depressed to articulate with the distal condyles of metacarpal II (figs. 23–24, A–F). A pronounced lip surrounds the entire proximal surface and is especially prominent ventrally (i.e., toward the flexor direction), where it extends much farther proximally than the dorsal lip. As a result, the ventral lip is visible in extensor view. The flexor surface of the phalanx is concave, which is deepest distally as a large flexor pit. The distal articular surface is divided into two condyles, of which the lateral is larger, more bulbous, and extends further distally. It is nearly circular in shape, with a long axis that is approximately dorsoventrally (extensor-flexor) oriented, whereas the smaller medial condyle is aligned ventromedially. The two condyles are separated by an obtuse angle and a deep groove, which continues onto the extensor and flexor surfaces of the bone. The lateral ligament pit is large and deep, but the medial pit is absent and the corresponding surface is flat and smooth.

The proximal surface of **phalanx II-2** is saddle shaped and asymmetric to match the condyles of II-1 (figs. 23–24, G–L). The flexor surface is concave, but much more subtly than in phalanx II-1 or I-1. However, as in these other phalanges, the concavity on the flexor surface is deepest proximally and distally. The distal end is separated into two condyles of approximately the same size. Both are remarkably thin and sheetlike, as a result of the deep and wide groove between them. This groove forms an enormous trochlea and extends far onto the extensor and flexor surfaces of the bone. The extensor

(dorsal) extent is especially extensive relative to all other phalanges of the hand and would have permitted more extension than most other joints of the manus. However, since the groove is raised above the rest of the extensor surface of the phalanx and is not bordered by an extensor pit proximally, the amount of extension was still quite limited. Lateral and medial ligament pits are present and both are placed along the extensor surface of the bone, unlike the more central pits of the other phalanges. The lateral pit is larger and deeper.

The ungual, **phalanx II-3**, is broken distally but appears to be slightly smaller than the ungual of the first digit (figs. 23–24, M–N). The flexor tubercle is smaller than that of the first ungual, and the presence or absence of the ventral foramina cannot be assessed due to breakage and poor preservation. One notable difference with the first ungual is that the lateral and medial grooves are Y-shaped, as the single groove that is present across most of the length of the bone bifurcates proximally into two short grooves that are oriented obliquely to each other (fig. 23: ygr). This feature is not present in *Deinonychus* (Ostrom, 1969) or *Velociraptor* (IGM 100/982; Norell and Makovicky, 1999), which possess a standard single groove on each surface, and is therefore an autapomorphy of *Balaur*.

Manual Digit III: Digit III is autapomorphically reduced in *Balaur*, both in the size and shape of individual elements and the total number of phalanges (figs. 17, 25). Theropods generally possess four phalanges in digit III, but *Balaur* preserves only a single small phalanx (**phalanx III-1**) on both the left and right hands, the latter of which is complete. This bone is reduced to a vestigial nubbin and indicates that digit III was probably nonfunctional in life, which is also suggested by the atrophied, splintlike metacarpal III. Proximally phalanx III-1 is ovoid in cross section, with a dorsoventrally (extensor-flexor) oriented long axis. The articular surface itself is a shallow, simple concave pit, which matches the single bulbous distal articular surface of metacarpal III. The flexor surface of the bone is concave and penetrated by two small foramina, one proximal to the other. The phalanx tapers distally and then expands slightly at its terminus, where the distal articular surface is a suboval, single convexity. It is possible that another small phalanx may have articulated here, since the distal surface does appear to be articular. However, if present, this phalanx must have been very small, and it may not have been ossified.

Referred Phalanges: Three incomplete phalanges were recovered from the same site that yielded the referred humerus, ulna, and metacarpal (fig. 26). These phalanges are referred to *Balaur* sp. based on general morphological similarity with the holotype of *B. bondoc*, the likelihood that they belong to the same individual as the other referred forelimb bones (which possess clear autapomorphies of *Balaur*), and due to the presence of wrinkled surface texture, an autapomorphy of *Balaur* well expressed in the holotype. Based on comparison with the complete hand of the holotype of *B. bondoc*, these referred phalanges can be identified as the right? phalanx I-1 (LPB [FGGUB] R.1583) (fig. 23A–E), left? phalanx II-1 (LPB [FGGUB] R.1582), and left phalanx II-2 (LPB [FGGUB] R.1584) (fig. 23F–J), respectively. Both R.1582 and R.1583 are proximal phalangeal fragments. Of these, R.1582 is the more complete, whereas R.1583 is better preserved. Fortunately, in R.1582 the dimensions and the shape of the flexor aspect of the distal articular end can be reliably reconstructed using the recovered impression of the distal, missing part on the matrix. The same holds for R.1584, a distal phalangeal fragment whose proximal extent and shape of its flexor surface are revealed by a similar impression. All phalanges are relatively long, slender, weakly arched dorsally (in the extensor direction), and internally hollow (due to a large medullary cavity).

Manual phalanx I-1 (LPB [FGGUB] R.1583) is elongate, with a roughly square-shaped proximal articular surface that is excavated by a single (undivided) depression for the reception of the distal condyles of metacarpal I (fig. 26A–E). The ventral lip delimiting the proximal articular surface is well developed and extends slightly more proximally on the left side; a similar asymmetry is also evident on the dorsal lip. In flexor view, the phalanx is transversely

Fig. 26. Referred manual digits of *Balaur* sp. ?Right manual digit I-1 (LPB [FGGUB] R.1583) in extensor (**A**), flexor (**B**), lateral (**C**), medial (**D**), and proximal (**E**) views. Left manual phalanx II-2 (LPB [FGGUB] R.1584) in extensor (**F**), flexor (**G**), lateral (**H**), medial (**I**), and distal (**J**) views. Scale bar equals 1 cm. Proximal end toward top in lateral, medial, anterior, and posterior views.

concave between the raised lateral and medial margins. The concavity is especially deep proximally and distally. Far proximally, underneath the ventral lip of the articular surface, the concavity grades into a nearly flat platform. This platform is bounded laterally and medially by small, moundlike prominences, which are the proximal terminations of the raised lateral and medial edges of the flexor surface. Immediately above the medial prominence there is a smooth, teardrop-shaped pit that excavates the medial

surface of the phalanx. The medial surface is marked by an angular ridge along its midline; this ridge begins dorsal to the teardrop-shaped pit (i.e., further in the extensor direction) and extends longitudinally to approximately the midpoint of the shaft, where it is most prominent. The extensor surface is marked by another angular longitudinal ridge that begins at the halfway point of the dorsal lip of the proximal articular surface and flattens as it extends distally to a point slightly beyond the middle of the bone. The more proximally extended and thickened dorsolateral corner of the dorsal lip gives the proximal end of the bone a markedly asymmetrical shape, and also makes it appear as if the proximal region is offset laterally from the longitudinal midline of the shaft. Distally, despite poor preservation, it is apparent that similarly sized distal condyles are divided by a flexor groove that appears to extend onto the distal articular surface, identical to the condition in the holotype phalanx I-1 of *B. bondoc*.

The preserved distal portion of manual phalanx II-2 (LPB [FGGUB] R.1584) is similar in most respects to those of the *B. bondoc* holotype (fig. 26: F–J). Both the referred and holotype material exhibit thin, sheetlike distal condyles; a well-developed groove separating the condyles in flexor, distal, and extensor views; and dorsally displaced ligament pits. In the referred material, the lateral ligament pit is deeper but the medial pit larger in area. In medial and lateral views the distal articular surface is conspicuously asymmetrical: the articular surface of the condyles extends far proximally on the flexor surface and cleanly merges with the shaft proximally, whereas on the extensor surface the condyles rise high above the shaft but their articular surfaces end abruptly, and in a more distal position than those on the flexor surface. There is no flexor pit, but a small extensor pit is notched between the proximal ends of the condyles.

Pelvic Girdle

One large block contains the pelvis, sacrum, caudosacral vertebra, and first two caudal vertebrae (figs. 27–31). Parts of all three pelvic bones are preserved on both sides, although both ilia are heavily eroded and missing substantial portions. The ischium and pubis are nearly complete and well preserved on the left side and the pubis is complete on the right side, but only the acetabular region of the right ischium remains. The pelvic bones are all tightly fused to one another and sutures between individual bones are obliterated. This is an unusual feature among dromaeosaurids, but is similar to the condition in the microraptorine *Hesperonychus*, in which the ilium and pubis are fused to each other while the ischium apparently remains unfused (Longrich and Currie, 2009). In contrast, the pelvic bones of close relatives of *Balaur* are unfused (e.g., *Adasaurus*: IGM 100/20; *Bambiraptor*: Burnham et al., 2000; *Deinonychus*: Ostrom, 1969; *Velociraptor*: Norell and Makovicky, 1997, 1999), as are those of other dromaeosaurids (e.g., Novas and Puerta, 1997; Forster et al., 1998; Xu et al., 1999; Hwang et al., 2002; Makovicky et al., 2005; Turner et al., 2007a).

Pelvic Crushing: The block containing the holotype pelvis and sacrum of *Balaur* is dorsoventrally crushed (fig. 27). Additional preparation after the original description of the specimen (Csiki et al., 2010a), along with detailed reexamination undertaken as part of this monograph project, reveals that this crushing is more extensive than originally appreciated. On both sides, crushing has cracked the pelvis along the dorsal and posterior bounding ridges of the cuppedicus fossa on the pubic peduncle (these pronounced ridges seem to have acted as local strong points). The deformation appears to be stronger on the left side, however, as there are several noticeable breaks on the left ilium and pubis, and because the left sacral rib is noticeably displaced ventrally relative to the right sacral rib (both ribs are in articulation with the ilium). This extreme deformation explains two supposed autapomorphies described by Csiki et al. (2010a), which we here consider invalid.

First, the cuppedicus fossa, which would have faced laterally in life, now faces almost entirely ventrally because of the crushing. The crushing is so extensive that Csiki et al. (2010a) mistook the broken dorsal bounding ridge of the cuppedicus fossa (which in life

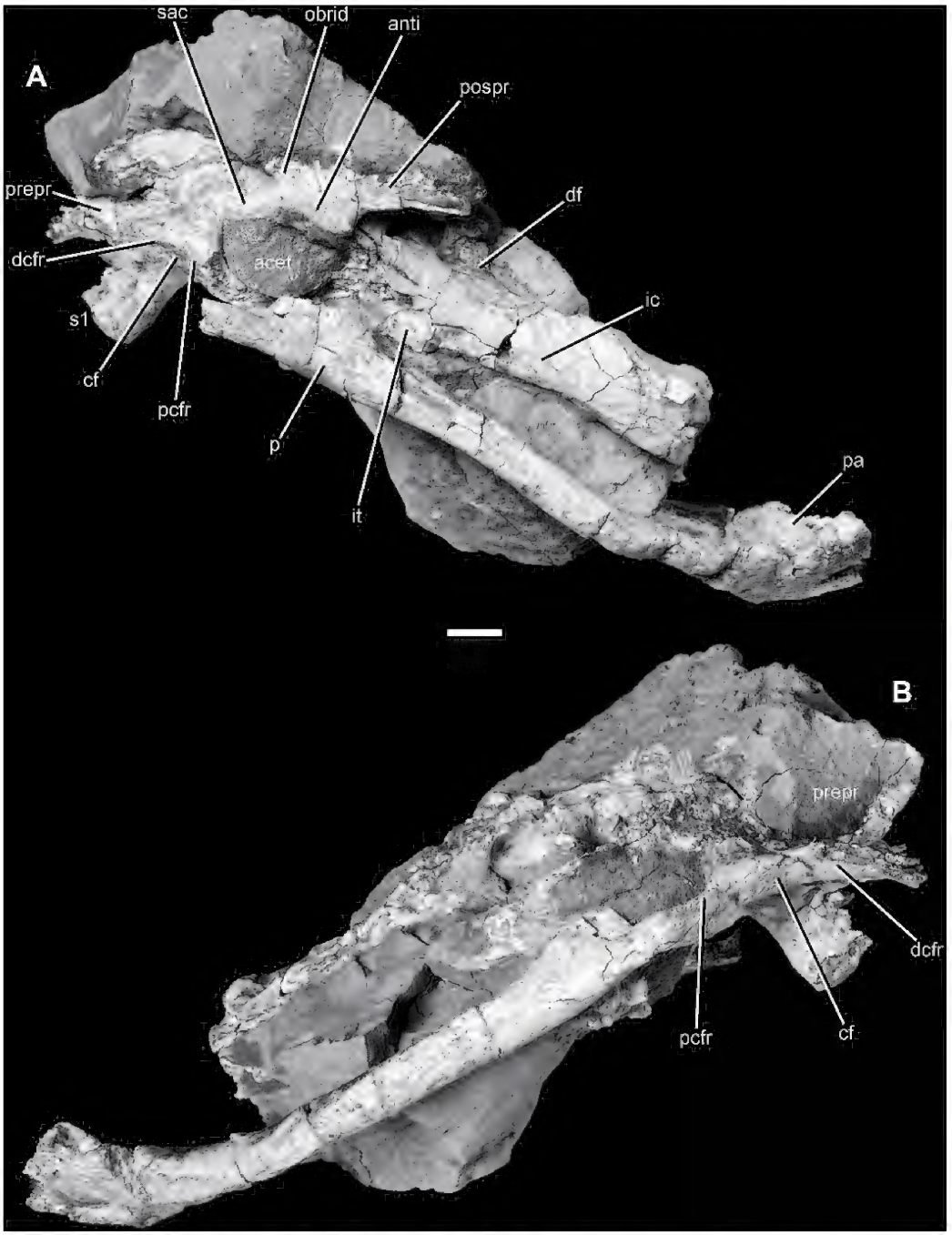

Fig. 27. Pelvis and sacrum of *Balaur bondoc* (EME PV.313) in left lateral (**A**) and right lateral (**B**) views. Photographs taken before final preparation. Abbreviations: **acet,** acetabulum, **anti,** antitrochanter; **cf,** cuppedicus fossa; **dcfr,** ridge demarcating dorsal edge of cuppedicus fossa; **df,** dorsal flange of proximal ischium; **ic,** ischial crest; **it,** ischial tubercle; **obrid,** oblique ridge extending anterodorsally from the antitrochanter; **p,** pubis; **pa,** pubic apron; **pcfr,** ridge demarcating posterior edge of cuppedicus fossa; **pospr,** postacetabular process of ilium; **prepr,** preacetabular process of ilium; **s1,** first sacral vertebra; **sac,** supraacetabular crest. Scale bar equals 1 cm.

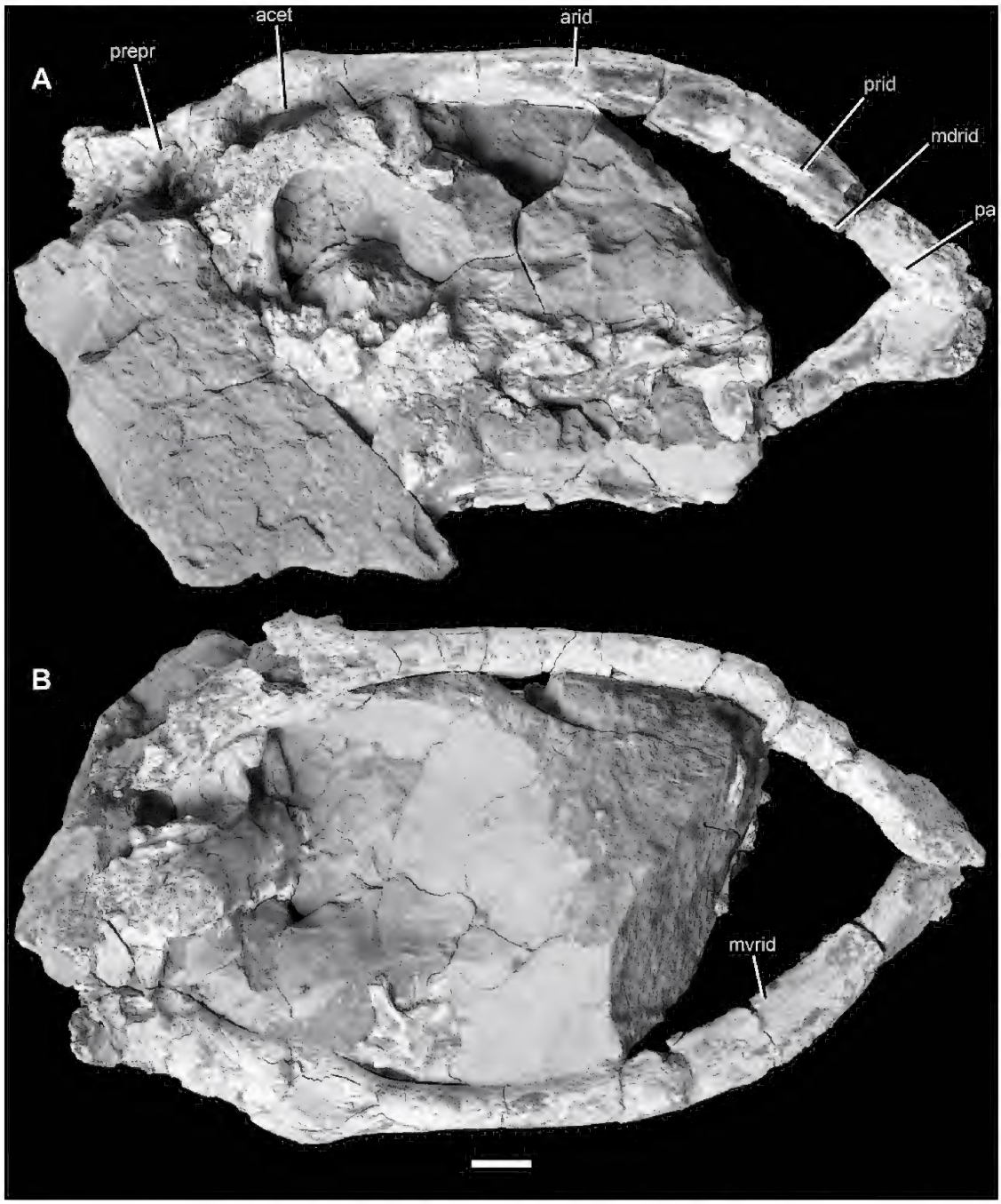

Fig. 28. Pelvis and sacrum of *Balaur bondoc* (EME PV.313) in oblique posterodorsal (**A**) and anteroventral (**B**) views. Photographs taken before final preparation (see fig. 29 for photographs taken after additional preparation). Abbreviations: **acet,** acetabulum; **arid,** anterior ridge on dorsal surface of pubic shaft; **mdrid,** medial ridge on dorsal surface of pubis that contributes to pubic apron; **mvrid,** medial ridge on ventral surface of pubis that contributes to pubic apron; **pa,** pubic apron; **prepr,** preacetabular process; **prid,** posterior ridge on dorsal surface of pubic shaft. Scale bar equals 1 cm.

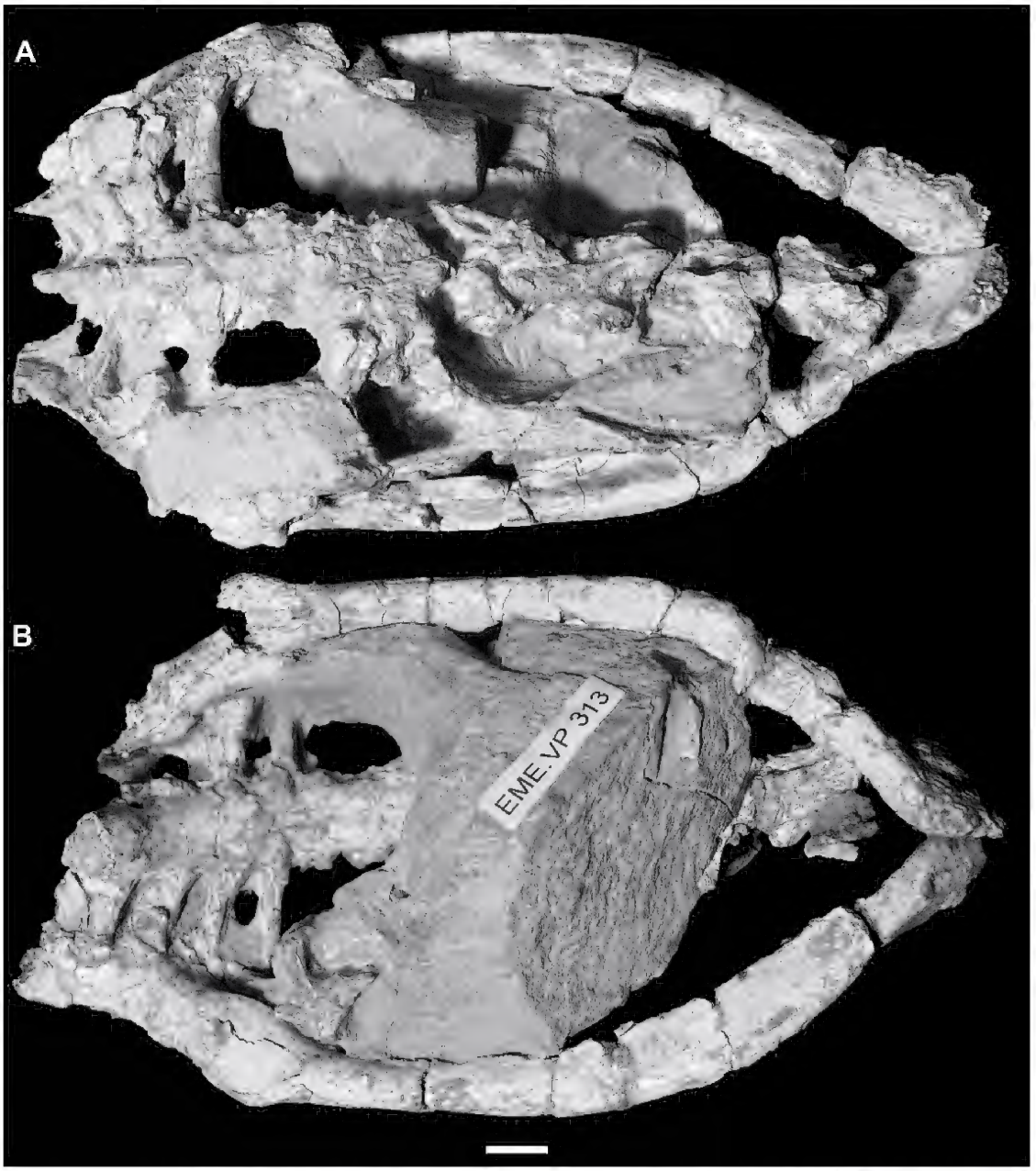

Fig. 29. Pelvis and sacrum of *Balaur bondoc* (EME PV.313) in oblique posterodorsal (**A**) and anteroventral (**B**) views. Photographs taken after final preparation (see fig. 28 for photographs taken before final preparation). Scale bar equals 1 cm.

also defines the ventral margin of the iliac preacetabular process; fig. 27: dcfr) to be the ventral margin of the pubic peduncle. As a result, they misidentified the preacetabular process as the pubic peduncle, and the fossa covering it as the cuppedicus fossa, and regarded the laterally projecting nature of this part of the ilium to be autapomorphic.

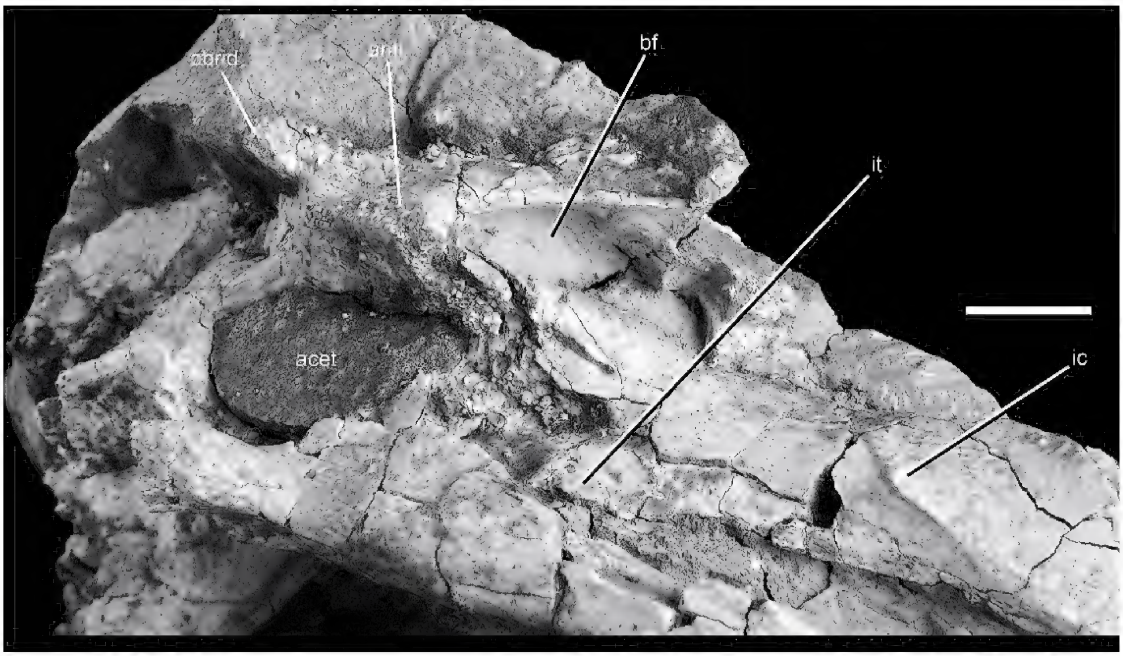

Fig. 30. Left side of pelvis of *Balaur bondoc* (EME PV.313) in posterior ventral oblique view. Abbreviations: **acet,** acetabulum; **anti,** antitrochanter; **bf,** brevis fossa; **ic,** ischial crest; **it,** ischial tubercle; **obrid,** oblique ridge extending anterodorsally from the antitrochanter. Scale bar equals 1 cm.

Fig. 31. Closeup of pubic apron of *Balaur bondoc* (EME PV.313) in dorsal view (anterior toward top). Scale bar equals 1 cm.

Indeed, a laterally (instead of ventrally) projecting pubic peduncle would be unusual, but the ventral portion of the preacetabular process does project laterally as a sheetlike flange in other dromaeosaurids (e.g., *Velociraptor*: IGM 100/986). Therefore, the condition in *Balaur* is similar to that in close relatives and is not autapomorphic. Csiki et al. (2010a) interpreted the supposed autapomorphy of *Balaur* as an attachment site for increased femoral extensor musculature, but our reinterpretation confirms that there was nothing unusual about the size or position of this muscle attachment site (at least compared to closely related dromaeosaurids such as *Velociraptor* and *Adasaurus*).

Second, on the left side of the pelvis the crushing of the posterior bounding ridge of the cuppedicus fossa (fig. 27: pcfr) was so extreme that the pubis was plastically deformed and snapped in two along the pubic peduncle. The break appears to occur slightly proximal to where the pubic peduncle of the ilium and the pubis are fused together. After the pubis was detached, it then rotated somewhat ventrally, such that its lateral surface now faces primarily ventrally. Csiki et al. (2010a) considered this to be a genuine feature of the anatomy, and hence an autapomorphy, but we here reinterpret it as an artifact of crushing, due to the obvious break in the pubis on the left side and the more traditional orientation of the pubis (lateral surface facing more strongly laterally) on the right side.

ILIUM: Only the acetabular region and the ventral portions of the pre- and postacetabular processes are present on both left and right ilia of the holotype, the former of which is better preserved and more complete. The left ilium is 75 mm long anteroposteriorly as preserved, but would have been much longer in life because it is broken both anteriorly and posteriorly (table 2). The preserved regions are enough to indicate that the two ilia did not approach each other and make contact with the sacral neural spine apron, but rather diverged from each other laterally, as is the case in all dromaeosaurids (Norell and Makovicky, 1997; Turner et al., 2007a).

The most prominent feature of the acetabular region of the ilium is the laterally extensive and swollen antitrochanter. This is eroded laterally and consequently would have been even more pronounced in life (fig. 27, 30: anti). A large antitrochanter is normal for dromaeosaurids (Norell and Makovicky, 1997; Turner et al., 2007a; Brougham and Brusatte, 2010; contra Alexander et al., 2010). Anterior to the antitrochanter is a thin supraacetabular crest (fig. 27: sac), which is subtle and overhangs the acetabulum only slightly, as is normal for dromaeosaurids and many other coelurosaurs (e.g., Norell and Makovicky, 1997, 1999; Turner et al., 2007a). The delicate morphology of the supraacetabular crest has been described as permitting a greater ranger of femoral abduction (Longrich and Currie, 2009; Alexander et al., 2010), but the large antitrochanter of *Balaur* and other dromaeosaurids would in fact have precluded extreme lateral movement of the femur (Brougham and Brusatte, 2010). In lateral view, the supraacetabular crest of *Balaur* is nearly horizontal, and is not as arched as in *Bambiraptor* (Burnham et al., 2000), *Deinonychus* (Ostrom, 1969), *Velociraptor* (Norell and Makovicky, 1997, 1999), and other dromaeosaurids (e.g., Novas and Puerta, 1997; Hwang et al., 2002; Turner et al., 2007a; Longrich and Currie, 2009). In concert with the shape of the crest, the acetabulum of *Balaur* has more of an anteroposteriorly elongated oval shape, compared with the more circular acetabula of other dromaeosaurids. This may be an unusual feature of *Balaur*, but we suspect that it is largely, or entirely, an artifact of dorsoventral crushing, and do not interpret it as an autapomorphy.

Only a small region of the lateral surface of the ilium immediately above the acetabulum is preserved on the left side. Most of this region is smooth and slightly depressed, but posteriorly there is a pronounced oblique ridge extending anterodorsally from the antitrochanter; this ridge is mostly eroded on the specimen and only its ventral base is preserved (figs. 27, 30: obrid). This ridge is extremely well developed and much larger than similar oblique ridges present in *Mahakala* (Turner et al., 2011), *Unenlagia* (MCF PVPH-78), and *Rahonavis* (US 8656). In these dromaeosaurids, the oblique ridge terminates dorsally in a large supratrochanteric process. Therefore, given the size of the

ridge in *Balaur*, it is likely that an enlarged supratrochanteric process (relative to closely related taxa such as *Velociraptor* and *Adasaurus*) would have been present at the eroded dorsal end of the ridge.

Posterior to the acetabulum and antitrochanter is the shallow brevis fossa, which faces completely ventrally and is entirely concealed in lateral view (fig. 30: bf). The medial shelf defining this fossa, the brevis shelf, projects nearly straight medially, and as a result the fossa is broad mediolaterally but is not particularly deeply inset ventrally. Unfortunately, fine details of the pubic and ischial peduncles are not observable due to poor preservation, crushing, and complete fusion of the pelvic bones. It is clear, however, that the anterior region of the acetabulum is not open, but rather formed by an enlarged, anterposteriorly extensive fossa, which would have formed part of the articulation with the femur. This fossa is located on the posterior portion of the pubic peduncle, as in *Velociraptor* and other dromaeosaurids (e.g., Norell and Makovicky, 1997, 1999; Novas and Puerta, 1997; Turner et al., 2007a, 2012). It is separated from the more anterior cuppedicus fossa (fig. 27: cf) by the dorsoventrally trending ridge on the lateral surface of the pubic peduncle (the "posterior bounding ridge" of the cuppedicus fossa, described above; fig. 27: pcfr). Unfortunately, the posterior fossa is largely covered by unremovable matrix on both sides of the pelvis, so it is not visible in the figures.

Anterior to the acetabulum, the lateral surface of the pubic peduncle is excavated by a deep and anteroposteriorly expansive cuppedicus fossa, which artificially faces mostly ventrally due to crushing (as described above) (fig. 27: cf). An expansive cuppedicus fossa that faces mostly laterally is present in other dromaeosaurids and other coelurosaurs more generally, contrasting with the deeply inset fossae of basal tetanurans that face strongly anteriorly and ventrally and are restricted to the corner where the preacetabular process and pubic peduncle meet (Norell and Makovicky, 1997, 1999; Hutchinson, 2001). The dorsal ridge defining the cuppedicus fossa is dorsally convex and extensive (fig. 27: dcfr), and it continues posteriorly to become confluent with the supraacetabular crest, as in *Rahonavis* (Forster et al., 1998), *Unenlagia* (Novas and Puerta, 1997), *Velociraptor* (Norell and Makovicky, 1997, 1999), and *Adasaurus* (IGM 100/20).

PUBIS: At first glance, the most remarkable feature of the pubis, which is also true of the ischium, is the extreme degree of retroversion (fig. 27). With the iliac blade held horizontal for reference, the pubis and ischium are oriented at more than 55° from the vertical, and the ischium in particular appears to nearly parallel the long axis of the ilium. Although all dromaeosaurids and other basal paravians have a retroverted pubis, it is usually oriented at 10°–20° from vertical (e.g., Ostrom, 1969; Novas and Puerta, 1997; Forster et al., 1998; Longrich and Currie, 2009). *Velociraptor* exhibits the most extreme retroversion of any other dromaeosaurid, with a pubis backswept at a 35° angle (Norell and Makovicky, 1997, 1999), but this is still far less extreme than the condition in *Balaur*. Therefore, the pronounced retroversion of the pubis and ischium is considered an autapomorphy of *Balaur*, although some degree of increased retroversion may be shared by *Balaur* and *Velociraptor*, which are sister taxa, due to common ancestry. However, we consider this autapomorphy only tentative, because it is likely that the extreme degree of retroversion in *Balaur* is at least partially due to dorsoventral crushing. That said, we do not completely dismiss this character as artifactual. Two lines of evidence suggest that at least some degree of greater-than-average retroversion is present: (1) the pubis is still extremely retroverted on the less deformed right side; and (2) the shape of the left ischium (also highly retroverted) appears to be less affected by crushing.

The more complete right pubis is 146 mm long as preserved, but the posterior margin is eroded, and comparison with close relatives suggests that several centimeters are missing. Therefore, based on these comparisons, the pubis would probably have been at least 170 mm long in life (table 2). Distal to the acetabular region the pubis tapers into an elongate, thin shaft. At its midsection the shaft is ovoid in cross section and measures 11 mm in mediolateral width by 9 mm in dorsoventral depth. The shaft is strongly

curved when seen in dorsal or ventral view, with a convex lateral margin and a concave medial surface. The two pubes eventually meet on the midline and together define a wide region between them. Anteriorly, there is a pronounced ridge on the dorsal surface of the shaft, which dissipates posteriorly as the bone becomes wider mediolaterally and thinner dorsoventrally (fig. 28: arid). Farther distally, approximately 20 mm before the two pubes meet, another ridge emerges (fig. 28: prid), which becomes more prominent as it continues distally and forms the lateral bounding wall of the dorsally concave pubic apron (fig. 28: pa; fig. 31).

Only the anterior portion of the pubic apron is preserved, and this region corresponds well with the morphology of *Velociraptor* (Norell and Makovicky, 1997, 1999) and *Adasaurus* (IGM 100/20). The apron is separated from the shaft by a distinct change of curvature, and its ventral surface is nearly horizontal. Further distally, however, the ventral surface curves upward such that it also faces posteriorly, and based on the shape of the broken posterior surface it is likely that the distalmost portion of the ventral pubis would have faced almost entirely posteriorly. The apron is wider than the remainder of the pubis and the actual contact between the pubes is made by two discrete ridges of bone. The medial surface of the shaft is marked by a thin ridge, which begins immediately posterior to the acetabulum and becomes thinner as it continues distally, before meeting its counterpart to form the apron (fig. 28: mdrid). This ridge is centered on the medial surface proximally, but migrates further dorsally as it extends distally. On the ventral surface, there is a ridge that begins at approximately midshaft, becomes more prominent distally, and eventually curves medially and migrates dorsally to join with the medial ridge forming the apron (fig. 28: mvrid).

The space between the pubes is proportionally wider than in close relatives such as *Velociraptor* (IGM 100/985, 986; Norell and Makovicky, 1997, 1999), and is indicative of an autapomorphically wider-barreled abdominal and pelvic region (somewhat similar to the condition in therizinosauroids). The greatest interpubic width occurs slightly posterior to the acetabulum, where the two bones are separated by 72 mm. The intervening space remains wide for a considerable distance distally, in concert with the strongly laterally bowed pubes. Because each pubis is bowed to such a pronounced degree, the interpubic distance only begins to narrow at approximately 2/3 of the length of the bone. The narrowing occurs abruptly once it begins, unlike the condition in *Velociraptor* where the narrowing between the two pubes is more gradual over a long distance (IGM 100/986; Norell and Makovicky, 1999: fig. 17).

Csiki et al. (2010a) described the pubic tubercle as located directly below the acetabulum, as a result of the supposed rotation of the pubis. As described above, this rotation is entirely due to postmortem crushing and does not reflect original morphology. The structure Csiki et al. (2010a) originally identified as the pubic tubercle is in fact a broken and swollen portion of the posterior bounding ridge of the cuppedicus fossa on the pubic peduncle of the ilium, proximal to the pubis itself. Reexamination of the specimen indicates that the true pubic tubercle is a subtle structure, visible only in ventral view due to crushing, whose size, shape, and position are similar to that in *Velociraptor* (IGM 100/986).

ISCHIUM: The ischium is nearly complete on the left side, and only a small portion is missing posteriorly (table 2) (fig. 27). It is 70 mm long as preserved and 15 mm deep dorsoventrally near its midpoint. Although both ischia are broken posteriorly, it can be inferred that they did not make broad contact at a symphysis, as there is no room for such a contact due to the intervening caudal vertebrae. This is also the case in most other maniraptorans, whereas in more basal theropods the ischia meet each other across a broad contact to form a symphysis (e.g., Madsen, 1976; Xu et al., 2006; Brusatte et al., 2008).

The long axis of the ischium parallels that of the pubis and the two are separated by a 12 mm gap at the midpoint of the ischium. The ischium is dorsoventrally deep proximally, where it forms the posteroventral corner of the acetabulum, due to dorsal and ventral expansions. The ventral expansion is formed by a greatly enlarged ischial tubercle, whose

size and morphology are autapomorphic for *Balaur* (figs. 27, 30: it). A tubercle is present in *Deinonychus* (Hutchinson, 2001) and *Velociraptor* (Norell and Makovicky, 1997, 1999), and is a synapomorphy that unites *Balaur* and these genera as a dromaeosaurid subclade. However, in these other taxa, the tuber is expressed as a small, discrete, rugose bulge (e.g., Norell and Makovicky, 1997, 1999). In *Balaur*, in contrast, it takes the form of a large, thin flange that projects ventrally and nearly contacts the pubis. Since the ventral surface of the tuber is broken, it is possible that this flange actually did contact the pubis in life, which would comprise a further autapomorphy of *Balaur*. The dorsal expansion of the proximal region is formed by a separate flange, which is thin and concave laterally (fig. 27: df). It is not present in *Velociraptor*, but is seen in an undescribed dromaeosaurid (Norell and Makovicky, 1999: fig. 24; Montanari and Norell, in prep.). Between the dorsal and ventral expansions, the lateral surface of the ischium is deeply convex and smooth.

In dorsal view, the lateral margin of the ischium has a sinusoidal shape: it is laterally convex anteriorly, then concave, and then sweeps out again posteriorly. The posterior expansion is due to a reorientation of the lateral surface, which here curves ventrally such that it now faces both ventrally and laterally. A similar, although less striking, twisting of the lateral surface is present in *Velociraptor* (IGM 100/986). The middle and posterior region of the ischium has a strongly rugose lateral surface, which is bisected by a crest that begins on the dorsal surface of the ischium near its midpoint, migrates posteroventrally up to a sharp inflection point, and then extends posteriorly along a nearly horizontal trend (figs. 27, 30: ic). The crest is most prominent at the inflection point, which forms a discrete corner. This ridge is present in many, but not all, dromaeosaurids, including *Deinonychus* and *Velociraptor* (Norell and Makovicky, 1997, 1999; Turner et al., 2007a), *Buitreraptor* (Makovicky et al., 2005), and *Sinornithosaurus* (Xu et al., 1999).

Distally, the ischium thins such that its posterior preserved edge is only 1.5 mm thick. There is no clear obturator process along the ventral margin, which is straight anteriorly and changes to a posteroventral orientation posteriorly at an inflection point. However, it is possible that the obturator process was present but located far distally on the bone, and thus is missing due to erosion. Along the dorsal margin there is clearly no median posterior process, which is present in *Rahonavis* (Forster et al., 1998) and several other basal dromaeosaurids (Turner et al., 2007a).

Hind Limb

A nearly complete specimen comprising the distal portion of the left hind limb is preserved in articulation on a single block, and includes the tibia, fibula, tarsals, metatarsals, and phalanges of all digits (table 2) (fig. 32–36, 38). The right hind limb, in contrast, is represented only by a fragmentary metatarsus (fig. 37). The distal portion of the hind limb of *Balaur* is substantially modified relative to other dromaeosaurids (and indeed all other dinosaurs) in regards to fusion, size, shape, and the development of the digits. The tibia, fibula, and proximal tarsals are fused into a tibiotarsus and sutures between individual bones have mostly been obliterated, although they can be traced in some places as raised ridges. The distal tarsals and metatarsals II–V are fused into a stout tarsometatarsus, which is proportionally short in comparison to the metatarsus of closely related taxa such as *Velociraptor* (Norell and Makovicky, 1997, 1999).

Tibiotarsus: Although fused, the tibia and fibula are recognizable as distinct bones proximally, but distally the tibia, fibula, and proximal tarsals are indistinguishably fused and sutures between them are impossible to distinguish. The tibiotarsus has a straight shaft (figs. 32–33). In contrast, the shaft is somewhat curved, due to a concave medial margin, in *Velociraptor* (IGM 100/986; Norell and Makovicky, 1999). Comparisons between the hind-limb ratios of *Balaur* and other dromaeosaurids are provided in table 6 (see also figs. 45–46).

The proximal surface of the **tibia** is heavily eroded, but much of the cnemial crest is preserved (fig. 33: cn). The crest is prominent, 10 mm wide mediolaterally by 10 mm

Fig. 32. Overview photograph of the articulated left lower hind limb, metatarsus, and foot of *Balaur bondoc* (EME PV.313). Scale bar equals 1 cm.

Fig. 33. Left tibia and fibula of *Balaur bondoc* (EME PV.313) in anterior (**A**) and medial (slightly anteromedial) view (**B**). Abbreviations: **cn,** cnemial crest; **cr,** crest on medial surface of proximal end; **fc,** fibular crest; **fo,** fossa between cnemial crest and crest on medial surface. Scale bar equals 1 cm.

Fig. 34. Closeup photo of left ankle region of *Balaur bondoc* (EME PV.313) before final preparation. See figure 35 for abbreviations. Scale bar equals 1 cm.

long anteroposteriorly as preserved, and curves laterally as it continues anteriorly, as is normal for dinosaurs (Gauthier, 1986; Novas, 1996; Brusatte et al., 2010; Nesbitt, 2011). The proximal surface of the crest slopes laterally, and as a result the medial region of the crest is higher than the lateral region, suggesting that the lateral condyle of the femur extended further distally than the medial condyle. Distally, the cnemial crest gradually merges with the shaft, and in doing so twists medially such that it terminates along the anteromedial edge of the shaft. Posteriorly, the proximal surface separates into lateral and medial condyles, both of which are heavily eroded. The incisura tibialis, the notch between the cnemial crest and lateral condyle along the lateral surface

Fig. 35. Left ankle region of *Balaur bondoc* (EME PV.313) in lateral (**A**), medial (**B**), and posterior (**C**) views. Photographs taken after final preparation. Abbreviations: **arid,** anterior ridge; **lrid,** lateral ridge; **lt,** lateral tubercle; **mp,** medial pit; **mt,** metatarsals; **vk,** ventral kink at the midpoint of the lateral ridge. Scale bar in A equals 1 cm.

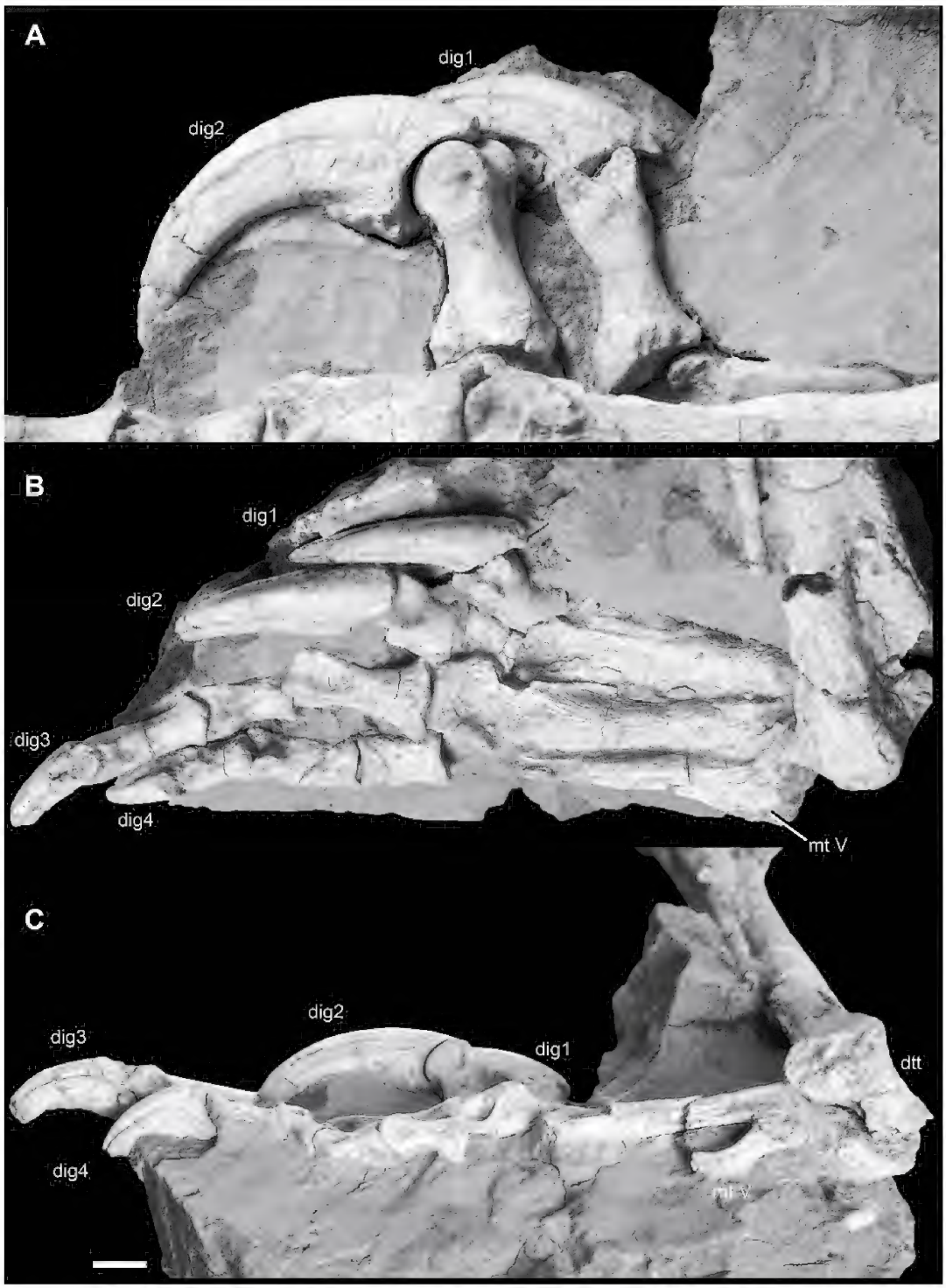

Fig. 36. Left metatarsus and foot of *Balaur bondoc* (EME PV.313) in lateral closeup (**A**), extensor (**B**), and lateral (**C**) views. Abbreviations: **dig,** individual digits; **dtt,** distal tibiotarsus, **mt V,** metatarsal V. Scale bar in C equals 1 cm.

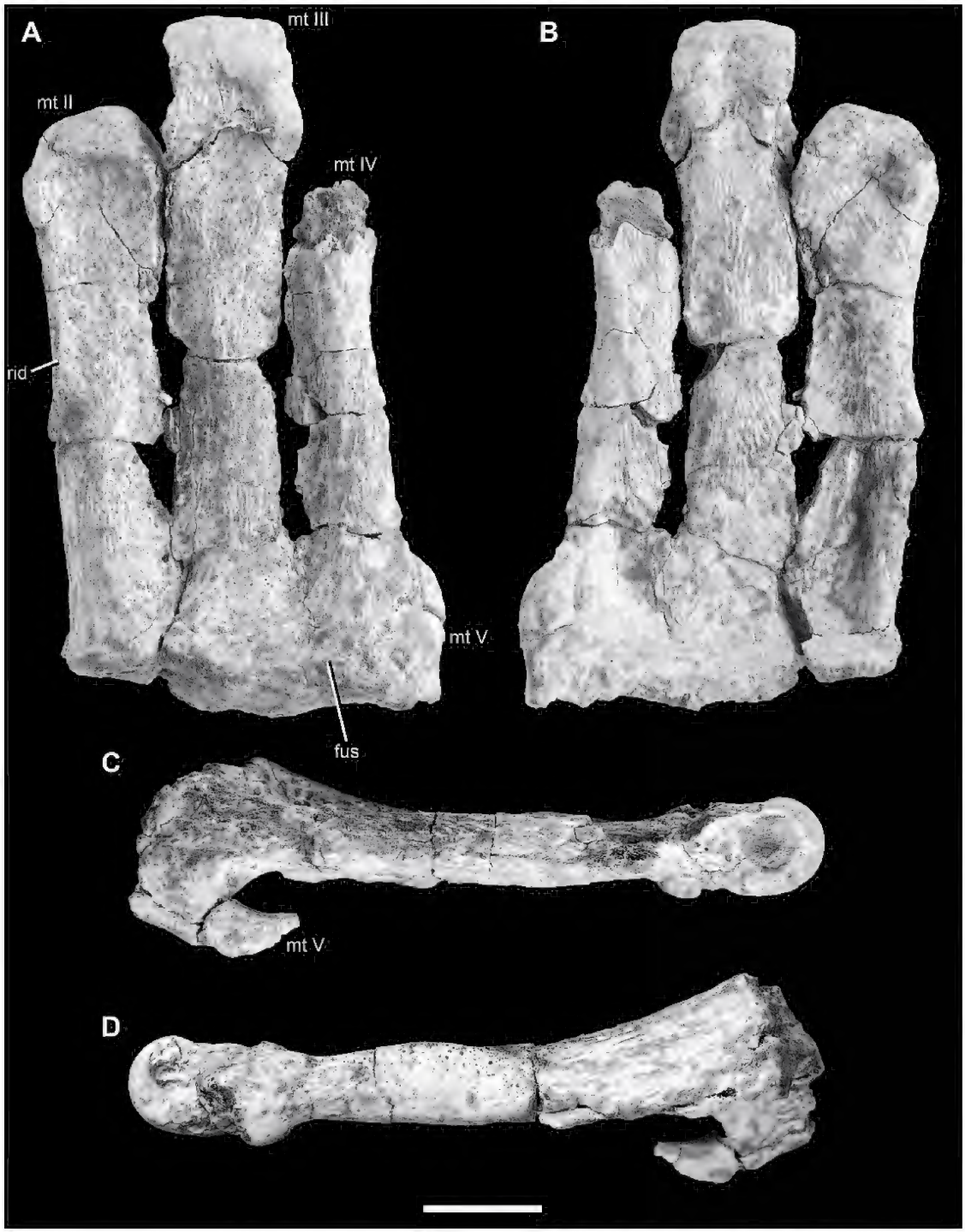

Fig. 37. Right metatarsus of *Balaur bondoc* (EME PV.313) in extensor (**A**), flexor (**B**), lateral (**C**), and medial (**D**) views. Abbreviations: **fus,** line of fusion between metatarsals and proximal tarsals; **mt,** individual metatarsals; **rid,** ridge along medial margin of extensor surface of metatarsal II. Scale bar equals 1 cm.

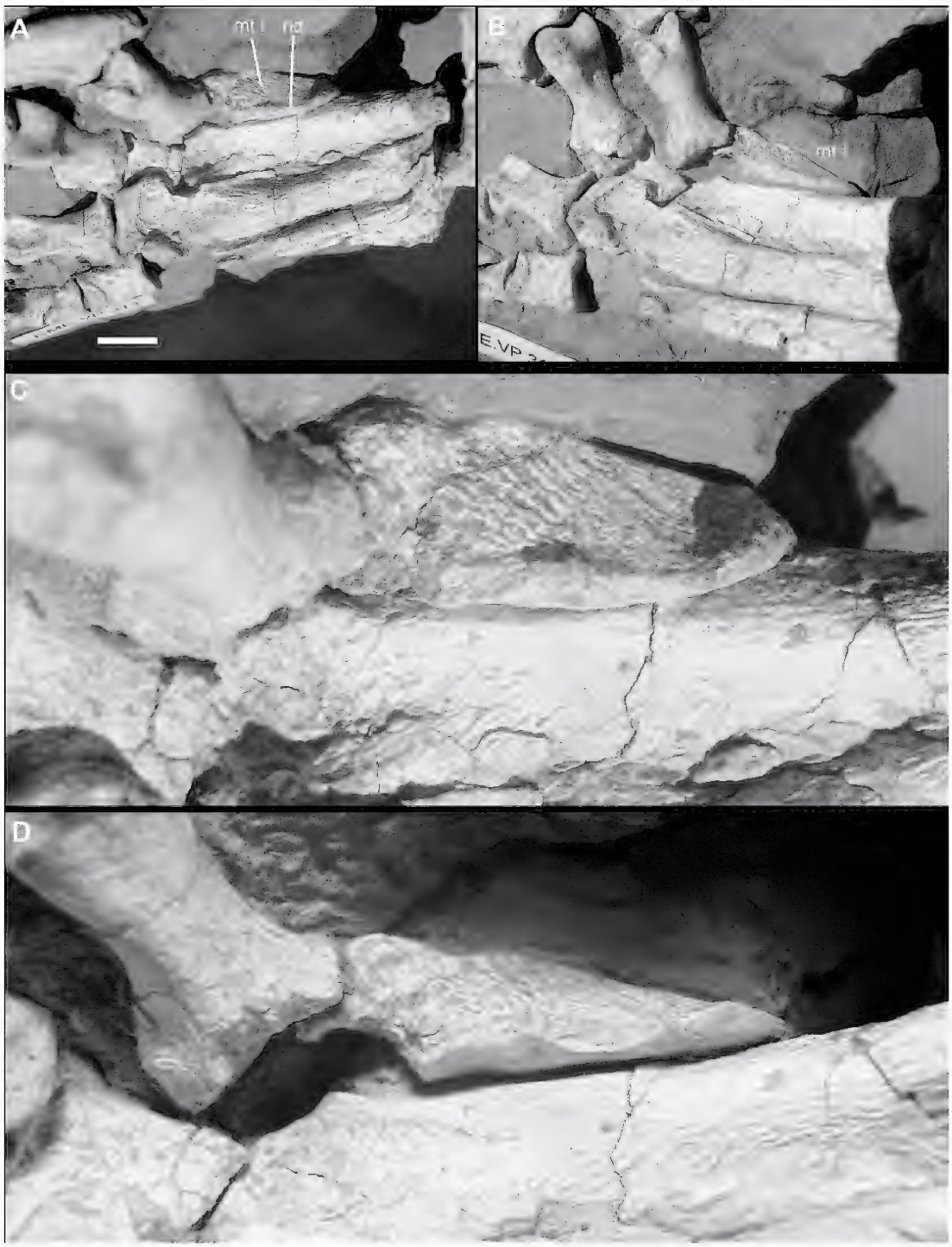

Fig. 38. Closeup of left metatarsal I of *Balaur bondoc* (EME PV.313) in extensor (**A, C**), oblique extensor-lateral (**B**), and lateral (slightly oblique to the extensor direction) (**D**) views. Abbreviations: **mt I,** metatarsal I; **rid,** ridge along lateral edge of extensor surface. Scale bar in A equals 1 cm.

of the tibia, is visible as a concave margin in proximal view. This notch is moderate in size, 6 mm long anteroposteriorly and inset 2 mm into the lateral surface. Both the cnemial crest and lateral condyle project to the same level laterally, and as a result the incisura tibialis opens only laterally and is not visible in anterior or posterior views.

On the medial surface of the proximal end is a distinct rounded crest, which is thick and prominent before gradually merging with the shaft distally (fig. 33: cr). The crest begins at, or immediately ventral to, the proximal articular surface and curves slightly anteriorly, while expanding in width, to nearly merge with the anterior surface of the cnemial crest. Between this crest and the cnemial crest, and facing anteriorly and medially, is a smooth fossa, which dissipates distally as both crests merge with the shaft (fig. 33: fo). The medial crest and associated fossa are unusual features that also appear to be present, albeit much more subtly, in *Deinonychus* (Ostrom, 1969), *Velociraptor* (IGM 100/986), and *Rahonavis* (UA 8656), and may be present in other taxa (but perhaps sometimes are imperceptible due to the delicate nature of the crest or poor preservation in this area). The medial crest may be homologous at some level with the medial cnemial crest of alvarezsaurids, which is a unique character present in derived members of this clade (Perle et al., 1994; Turner et al., 2007a). However, the alvarezsaurid crest is positioned at the anteromedial corner of the cnemial crest itself, not on the medial surface of the tibia as in *Balaur*. Furthermore, basal alvarezsaurids lack a medial cnemial crest, as do other coelurosaurs, suggesting that the crests of derived alvarezsaurids and dromaeosaurids evolved independently (Choiniere et al., 2010).

The fibular crest is a rugose flange on the lateral surface of the proximal tibia, widely visible in anterior and posterior views (fig. 33: fc). It begins proximally immediately below the lateral condyle and extends anterodistally for 56 mm before abruptly terminating. The anterior surface of the crest is smoothly concave, and is essentially a ventral extension of the smooth incisura tibialis. This concavity faces solely laterally on the proximal portion of the fibular crest, but twists distally such that it terminates on the anterior surface of the tibial shaft. The medial surface of the shaft bordering the fibular crest is damaged, but a region of collapsed bone indicates that there may have been a fossa here, as in *Velociraptor* (IGM 100/986). Further distally on the shaft it is unclear how much contact there was between the fibula and the tibia, as the former bone is largely eroded in this area. It is clear that the fibula is separated and unfused to the tibia immediately distal to the fibular crest (up to about 2/3 of the length of the tibiotarsus), and then further distally it appears as if the two bones abut each other and fuse into a common element (with indistinguishable sutures).

The **fibula** is expanded proximally and tapers into a thin shaft distally, which is ovoid in cross section at its midpoint. The medial surface of the proximal end is smoothly concave and lacks the discrete, deep fossa present in more basal theropods, including basal coelurosaurs such as tyrannosauroids and ornithomimosaurs (e.g., Madsen, 1976; Brochu, 2003; Makovicky et al., 2004; Brusatte et al., 2008). Although the proximal region is somewhat eroded, it appears that the fibula was more expanded posteriorly than anteriorly. As seen in lateral view, the anterior margin of the shaft is approximately straight, whereas the posterior margin is concave and curves strongly posteriorly as it continues proximally, in concert with the more expanded posterior end of the proximal fibula. The iliofibularis tubercle is proximally positioned, beginning approximately 41 mm distal to the proximal end of the bone. It is expressed as a slight, convex bulge on the posterior surface of the shaft, not a large rugosity as in some basal coelurosaurs, especially tyrannosauroids (e.g., Brochu, 2003). The morphology of the distal fibula is not clear, as the tibia, fibula, and proximal tarsals are strongly fused here (fig. 34). There is a pronounced lateral tubercle on the distal end of the tibiotarsus (fig. 35: lt), which is in the same approximate position as the distal end of the fibula in *Velociraptor* (IGM 100/986) and therefore may represent the distalmost extent of the fibula.

The **astragalus** and **calcaneum** are fused to the tibia and fibula and their individual

TABLE 5
Measurements of manual phalanges (in mm) of dromaeosaurid theropods
Asterisk indicates incomplete measurement due to damage or poor preservation; curv = length measured along the outer curvature of the ungual.

Taxon	I1	I2	I2 (curv)	II1	II2	II3
Balaur bondoc EME PV.313	40	37.5	47	31	38	34.6
Balaur sp. LPB (FGGUB) (see table 3)	59.2*	–	–	–	54.5*	–
Deinonychus antirrhopus YPM 5206 (Ostrom, 1969)	74.1	62.3	100	54	76.5	66.7
Deinonychus antirrhopus MCZ 4371 (Ostrom, 1976)	77.3	–	100*	64.2	83.4	–
Deinonychus antirrhopus AMNH FARB 3015 (Ostrom, 1976)	–	–	80	62.2	70.7	–
Velociraptor mongoliensis IGM 100/982	39.9	30.2	39.9	31.3	45.8	33
Velociraptor mongoliensis IGM 100/986	47.1	–	–	33.2	–	–
Saurornitholestes langstoni MOR 660	61	55	74	49	43	35
Linheraptor exquisitus IVPP V16923	47.6	–	–	32.3	53.5	–
Bambiraptor feinbergorum AMNH FARB FR 30556	33.4	26.8	40	22.1	35.6	43
Buitreraptor gonzalezorum MPCA 245	–	–	–	–	–	–
Microraptor zhaoianus CAGS 20-7-004	20.5	–	–	13.3	16.4	–
Graciliraptor lujiatunensis IVPP V13474	36	17.5	30.3	26	25.8	–
Sinornithosaurus millenii IVPP V12811	38.9	25.3	34.3	30.9	35.1	25.6
Mahakala onmogovae IGM/1033	–	–	–	–	–	–

Taxon	II3 (curv)	III1	III2	III3	III4	III4 (curv)
Balaur bondoc EME PV.313	39	11	NO	NO	NO	NO
Balaur sp. LPB (FGGUB) (see table 3)	–	–	–	–	–	–
Deinonychus antirrhopus YPM 5206 (Ostrom, 1969)	98.4	29.9	20.5	–	57.1	69.8
Deinonychus antirrhopus MCZ 4371 (Ostrom, 1976)	105	35	23.2	–	–	–
Deinonychus antirrhopus AMNH FARB 3015 (Ostrom, 1976)	–	21.7	15.5	47.3	–	–
Velociraptor mongoliensis IGM 100/982	47.5	17.6	10.1	32.2	25	32
Velociraptor mongoliensis IGM 100/986	48.8	19	11.1	33.2	–	–
Saurornitholestes langstoni MOR 660	51	13	29	40	–	–
Linheraptor exquisitus IVPP V16923	–	15.5	12	33	–	–

TABLE 5
(Continued)

Taxon	II3 (curv)	III1	III2	III3	III4	III4 (curv)
Bambiraptor feinbergorum AMNH FARB FR 30556	–	16.9	5.4	18.6	–	–
Buitreraptor gonzalezorum MPCA 245	–	–	–	–	–	–
Microraptor zhaoianus CAGS 20-7-004	10.3	10.1	4.1	10.4	–	–
Graciliraptor lujiatunensis IVPP V13474	–	11.6	6.8	18.6	–	–
Sinornithosaurus millenii IVPP V12811	36.5	17.9	8.8	23.1	15.2	22
Mahakala onmogovae IGM/1033	–	–	–	–	–	–

shapes are obscured due to this fusion (fig. 34). Complete fusion between the proximal tarsals and the tibia and fibula is rare among coelurosaurs, present otherwise only in *Buitreraptor* (Makovicky et al., 2005) and *Graciliraptor* (Xu and Wang, 2004) among dromaeosaurids (see Norell and Makovicky, 1997; Turner et al., 2007a). Because fusion is so extreme in this region, it is possible to describe only the various surfaces of the distal tibiotarsus without reference to the individual bones.

The distal surface of the tibiotarsus is saddle shaped, comprised of medial and lateral condyles that are separated by a wide and deep sulcus, which continues onto the posterior surface of the bone as a flexor groove. The anterior surface is deeply notched at its center as an extensor groove, which is visible in distal view as an inset, concave margin. This groove is inset approximately 8 mm into the bone as preserved, but was likely deeper since the anterior surfaces of the lateral and medial condyles, which define its anterior extent, are eroded. Although deep, the groove is only 5 mm wide mediolaterally. The prominent and deep extensor groove is an unusual feature among dromaeosaurids, present otherwise in *Buitreraptor* (Makovicky et al., 2005). Other dromaeosaurids, including *Velociraptor* (IGM 100/986; Makovicky and Norell, 1999) have a much shallower groove, which is considerably wider than deep. A deep groove is present, however, in some alvarezsaurids, troodontids, and basal avialans (Turner et al., 2007a), and therefore is homoplastic within coelurosaurs.

Approximately 10 mm proximal to the distal end of the bone, the lateral surface of the tibiotarsus is marked by a pronounced, curved ridge, which is oriented anteroposteriorly (fig. 35: lrid). The ridge is most pronounced anteriorly, where it terminates at a discrete rounded tubercle (fig. 35: lt) located at the point where the lateral condyle merges with the shaft of the tibiotarsus. This ridge may represent the line of fusion between the calcaneum and tibia, as its shape and position approximates the trace of this suture in many theropods (e.g., *Velociraptor*: IGM 100/986). If this is the case, then the fibula would contact these bones on, or near, the discrete tubercle, suggesting that the tubercle itself may represent the distal end of the fibula. Ventral to the ridge, the lateral surface of the tibiotarsus is smoothly concave. However, the ridge is kinked at its midpoint (fig. 35: vk), forming another small tuber that projects ventrally. Additionally, there is a sharp ridge along the anterior margin of the lateral surface, which forms the anterolateral corner of the bone (fig. 35: arid). This ridge begins at the proximal tip of the large tuberosity and extends proximally until it terminates against a broken surface. It is most pronounced distally and becomes less prominent and thinner as it continues proximally. It is likely that this crest represents the portion of the fibula that tapers distally before slightly expanding to articulate with the tarsus.

The medial surface of the distal tibiotarsus (presumably formed by the medial condyle of the astragalus) is marked by a deep, circular pit (fig. 35: mp). This feature is generally prevalent among dromaeosaurids, as it is present in *Velociraptor* (IGM 100/986), *Deinonychus* (YPM 5226), *Neuquenraptor* (MCF PVPH 77), *Microraptor* (IVPP V13352), and *Mahakala* (IGM 100/1013). The presence or absence of this feature in *Adasaurus* cannot be determined because the relevant portion of the astragalus is not sufficiently prepared. The especially deep morphology of the pit of *Balaur* may be unusual among dromaeosaurids, but the depth of this depression is variable in other taxa, and is sometimes even variable between left and right sides in individual skeletons (e.g., *Velociraptor* IGM 100/986).

TARSOMETATARSUS: The distal tarsals form a fused cap over the metatarsals, but individual tarsals are not apparent and it is difficult to determine how many tarsals were present. Fusion between the distal tarsals and metatarsals, as well as between the proximal ends of the metatarsals, is rare among nonavialan coelurosaurs. It is present in the oviraptorosaurs *Elmisaurus* (Osmólska, 1981) and *Avimimus* (Vickers-Rich et al., 2002), and the alvarezsaurid *Albinykus* (Nesbitt et al., 2011); in dromaeosaurids it is also present in *Velociraptor* (Norell and Makovicky, 1997, 1999), *Adasaurus* (IGM 100/21), and *Microraptor* (Hwang et al., 2002), albeit to a much less extensive degree, as in these taxa the sutures between elements of the tarsometatarsus are often visible. In *Balaur*, only the line of fusion between the tarsal cap and the metatarsus is visible, and it is clear that the tarsals are thickened proximodistally. The proximal surface of the tarsus is convex and smooth (fig. 36–37).

Metatarsals II–V are heavily fused to each other proximally and sutures between individual bones are not clear (figs. 36–37: fus). The fused region is approximately 8 mm in proximodistal length, and further distally the individual metatarsals separate from each other. However, it is possible that fusion continued distally, as the individual metatarsals are in close contact throughout their lengths. Furthermore, in both the left and right feet the regions between metatarsals II–IV are poorly preserved. Each metatarsal thins dramatically in dorsoventral (extensor-flexor) depth toward its lateral and medial margins, and these surfaces are largely broken. Therefore, it is possible that the broken surfaces may have contacted each other in life. Regardless, it is clear that the metatarsals were separated at their extreme distal ends, as the individual distal articular surfaces are unfused and diverge from each other.

The three central metatarsals are closely bunched to form a stout, paddlelike metatarsus. The metatarsus is 62 mm long proximodistally at its longest point, along metatarsal III, and 32 mm in mediolateral width proximally. Therefore, the metatarsus is less than twice as long as it is wide, contrasting with dromaeosaurids such as *Velociraptor,* in which the central metatarsus is more than three times longer than wide (IGM 100/985). The short and wide nature of the metatarsus is also reflected in the fact that it is more than 1.5 times as wide as the distal end of the tibiotarsus, a remarkable condition compared to other dromaeosaurids in which these two elements are approximately coequal in width (e.g., Ostrom, 1969; Norell and Makovicky, 1997, 1999; Xu et al., 1999; Hwang et al., 2002). In sum, the metatarsus of *Balaur* is autapomorphically shorter and wider compared to not only other dromaeosaurids, but all other theropods.

Although the remainder of the metatarsus and pes is heavily modified, **metatarsal I** is similar in position and morphology to the corresponding bone in other dromaeosaurids (fig. 38). As in most other theropods, including all other dromaeosaurids, this bone is a small, wedgelike element with a flat lateral surface that articulates along the midpoint of the medial surface of metatarsal II (e.g., Ostrom,1969; Forster et al., 1998; Norell and Makovicky, 1997, 1999; Hwang et al., 2002; Novas and Pol, 2005). Although metatarsal I supports large and functional phalanges (see below; fig. 36), it does not reach the tarsus, as is the case in derived therizinosauroids that independently evolved a large pedal digit I (e.g., Perle, 1979; Barsbold and Perle, 1980). The enlarged nature of the first digit of *Balaur* is reflected in the size of metatarsal I, however, which although still smaller than the other metatarsals is proportionally larger

TABLE 6
Measurements of hind-limb elements (in mm) of dromaeosaurid theropods
Asterisk indicates incomplete measurement due to damage or poor preservation.

Taxon	Femur	Tibia	MTI	MTII	MTIII	MTIV	MTV
Balaur bondoc EME PV.313	–	153	36.7	52	61	53	18
Deinonychus antirrhopus YPM 5205 (Ostrom, 1969)	–	–	–	134	150	141	52.3*
Deinonychus antirrhopus MCZ 4371 (Ostrom, 1976)	336	368	45.6	144.3	164.4	150.4	78
Deinonychus antirrhopus AMNH FARB 3015 (Ostrom, 1976)	–	312	–	129	151	134	34*
Velociraptor mongoliensis IGM 100/985	–	–	21.4	71.2	86.2	78.2	31.7*
Velociraptor mongoliensis IGM 100/982	153.7	177	22.5	68.2	88.1	84.8	32.6*
Velociraptor mongoliensis IGM 100/986	238	255	27.9	84.8	99.1	91.6	40.1
Saurornitholestes langstoni MOR 660	–	301	–	112	136	123	–
Saurornitholestes langstoni TMP 88.121.39	230	300	–	101	115	107	–
Linheraptor exquisitus IVPP V16923	220	252	–	103.2	127.9	112.8	–
Bambiraptor feinbergorum AMNH FARB FR 30556	118.5	170.5	18.6	68	81.6	75.1	33.8
Adasaurus mongoliensis IGM 100/20	273	303	–	–	147	128	61
Adasaurus mongoliensis IGM 100/21	–	–	38.8	140	178	162	–
Achillobator giganticus MNU FR-15	505	490.9	–	–	234.4	209.6	–
Neuquenraptor argentinus MCF PHPH 77	250	–	30.4	147.9	172.7	149.6	–
Buitreraptor gonzalezorum MPCA 245	149.5	158.2*	–	23.9*	–	–	–
Buitreraptor gonzalezorum MPCA 238	–	–	20	90.6	99.4	90.6	–
Austroraptor cabazai MML-195	560	565*	–	–	330	–	–
Rahonavis ostromi UA 8656	87	120	9	45.4	48.2	45.3	–
Microraptor zhaoianus CAGS 20-7-004	74.3	94.2	–	44.5	47.8	46.8	22
Microraptor zhaoianus CAGS 20-8-001	74.4	94.1	8.1	45.9	49.4	48.5	24
Graciliraptor lujiatunensis IVPP V13474	–	115.1	–	–	21.8	–	–
Sinornithosaurus millenii IVPP V12811	–	–	13.7	87.1	93.2	91	45.5
Mahakala onmogovae IGM/1033	79	110	–	–	–	–	–

than in all other dromaeosaurids (e.g., *Deinonychus*: MCZ 4371, Ostrom, 1976; *Velociraptor*: IGM 100/986, Norell and Makovicky, 1999). Indeed, while in these velociraptorines the length of metatarsal I varies between 25%–28% of that of metatarsal III, in *Balaur* it reaches 60% (table 6; see also fig. 47). This ratio is well below 25% in other derived dromaeosaurids and drops below 20% in the microraptorines and unenlagiines (table 6; see also fig. 47).

One of the most prominent features of metatarsal I is a pronounced ridge along the lateral margin of the extensor surface, which helps form the articulation with metatarsal II (fig. 38: rid). A very subtle ridge is present in one specimen of *Velociraptor* (IGM 100/986), but absent in others. *Adasaurus* (IGM 100/21) also has a slight ridge in this region, but in this taxon and in the specimen of *Velociraptor* the ridge is much smaller than that in *Balaur*. Therefore, the pronounced ridge may be an autapomorphy of *Balaur*, but we hesitate to regard it as a formal autapomorphy because metacarpal I is not preserved for most other dromaeosaurid species.

Metatarsal II is dorsoventrally (extensor-flexor direction) thickened at its proximal end and remains thick distally along its medial margin. Its lateral margin, on the other hand, thins into a platelike flange that may have made contact with metatarsal III (see above). As a result of this morphology, there appears to be a strong ridge, oriented proximodistally, along the medial edge of the bone in extensor (dorsal) view (fig. 37: rid). This ridge is not a discrete structure, but rather reflects the difference between the thick medial edge and thin lateral half of the bone. Similar ridges are present on metatarsals III and IV, also a result of the thinning of the metatarsals toward one or both edges, and are autapomorphic of *Balaur*. In contrast, the metatarsals of other dromaeosaurids, including *Deinonychus* (Ostrom, 1969), *Microraptor* (Hwang et al., 2002), *Rahonavis* (Forster et al., 1998), *Unenlagia* (Novas and Pol, 2005), and *Velociraptor* (IGM 100/985) do not thin toward their edges, and hence do not appear to possess large ridges on their extensor surfaces. *Velociraptor* has an oblique ridge on metatarsal III, but this does not extend across the length of the shaft and is not associated with thin edges of the bone, nor with similar ridges on metatarsals II and IV (Norell and Makovicky, 1999). Furthermore, in some dromaeosaurids, including *Velociraptor* (IGM 100/986) and *Adasaurus* (IGM 100/21), a tubercle is present on the extensor surface just proximal to midshaft that likely corresponds to the insertion of M. tibialis cranialis. No such tubercle is present in *Balaur*.

On the extensor surface of the distal end is an enormous extensor pit that is expressed as a broad, deep fossa, one of several features that enables hyperextension of the second pedal digit. It is not a discrete pit, with distinct edges, as is usual for theropods, but rather occupies the entire extensor surface of the distal end. It is most deeply inset distally, where it is invaginated underneath the distal condyles, which extend onto the extensor surface to slightly overhang the pit. The anterior margin of the pit is smoothly convex and its lateral and medial edges are formed by thin ridges that continue proximally from the corner of each distal condyle. The flexor (ventral) surface of metatarsal II is collapsed proximally on the right metatarsus in which this surface is visible, indicating that a fossa was present in this region. Further distally, around mid-length, the flexor surface flattens out, then becomes slightly convex, and eventually is concave as a small flexor cleft where it terminates against the distal condyles. The lateral ligament pit is much larger and deeper than the medial pit, which is reduced to a small, circular foramen.

The distal articular region is large and convex, and divides into separate condyles on the flexor surface. The condyles are not apparent as discrete structures in extensor view, and as a result, metatarsal II is not ginglymoid as in all other dromaeosaurids (e.g., Norell and Makovicky, 1997, 1999; Turner et al., 2007a, 2012). This morphology is indicative of less extreme hyperextensive abilities compared to close relatives, but several troodontids also are capable of hypextension without a ginglymoid metatarsal II (e.g., Xu et al., 2002; Turner et al., 2007a). The distal condyles are, however,

separated on the flexor surface of the metatarsal. Here, the medial condyle, which is nearly circular, projects further ventrally (toward the flexor direction) than the lateral condyle, which is ovoid, larger than the medial condyle, and extends farther proximally and distally. The long axis of both condyles projects mediodistally, and as a result, digit II curves medially away from digit III, as is normal for dromaeosaurids (e.g., Ostrom, 1969; Norell and Makovicky, 1997, 1999). Unusually, the width of the distal articular surface is less than the width of the entire distal end of the metatarsal. This is especially evident in extensor view, where a large nonarticular region is present both lateral and medial to the smooth articular surface. This is not the case in other dromaeosaurids, including *Deinonychus* (Ostrom, 1969) and *Velociraptor* (Norell and Makovicky, 1997, 1999), and therefore is an autapomorphy of *Balaur*.

Metatarsal III has a pronounced ridge extending proximodistally at the center of the extensor surface, as a result of the lateral and medial thinning of the bone as described above. The ridge is a single structure across most of its length, but proximally it divides into separate ridges that are oblique to each other and distally, at approximately 2/3 of the length of the shaft, it bifurcates into two ridges that eventually merge with the lateral and medial edges of the bone. The ridge is most pronounced at the center of the shaft, and lateral and medial to it are smooth fossae that slope away from the long axis of the bone. Distally, the portion of the extensor surface between the bifurcated ridges is depressed as a shallow extensor fossa, which is deepest distally adjacent to the distal articular surface. As in metatarsal II, the fossa is invaginated due to the overhanging distal articular surface, and the articular surface itself is slightly narrower than the total mediolateral width of the distal end. Both lateral and medial ligament pits are large and deep, and positioned dorsally (toward the extensor surface) such that they abut the smooth articular surface.

The distal articular surface is not ginglymoid, which along with the same condition in metatarsal II is a unique feature among dromaeosaurids (see above; Turner et al., 2007a). However, the nonginglymoid condition of metatarsal III is more extreme than that in metatarsal II, as separate condyles are not apparent in both extensor and distal views. The articular region divides into medial and lateral condyles on the flexor surface, but these are much smaller than the corresponding condyles in metatarsal II and are only visible in flexor view. The condyles are symmetrical, extend to the same level distally, have long axes that are oriented straight proximodistally, and continue proximally as thin ridges which merge with the lateral and medial edges of the bone. They are separated by a narrow flexor cleft. Further proximally, the flexor surface flattens out and then eventually becomes concave adjacent to the proximal articular surface. The flat portion is bisected by a subtle, proximodistally extending ridge, which abruptly ends distally against the flexor cleft. Distally, the distal articular end of metatarsal II abuts the medial edge of the shaft of metatarsal III, and this contact is reinforced by a small, convex tuberosity on metatarsal III.

Metatarsal IV is approximately the same length as metatarsal II, and both are slightly shorter than metatarsal III (figs. 36–37). As in the other central metatarsals, the extensor surface is ornamented with a pronounced ridge. Here, the ridge begins proximally at the center of the bone and trends laterally as it continues distally, such that it extends along the lateral margin of the shaft. Shallow fossae border the ridge both medially and laterally, the latter of which is small and narrows in width distally in concert with the lateral migration of the ridge. There is also a thin ridge on the proximal portion of the lateral surface, which dissipates distally. The flexor surface is concave proximally and then flattens distally. Unfortunately, the distal articular region is broken in both specimens, precluding observation of the condyles and extensor pit.

Metatarsal V is a small bone that resembles a stout hook (figs. 36–37). It is vestigial as in most other theropods and does not support any phalanges. It does exhibit a unique shape among dromaeosaurids, however, as all other members of this clade possess a longer, straighter, and more gracile metatarsal V (e.g., Ostrom, 1969; Norell and

Makovicky, 1997, 1999). The hooklike morphology of this bone is the result of a concave extensor margin and convex flexor edge. Moreover, metatarsal V of *Balaur* is uniquely shortened among dromaeosaurids, at less than 30% of metatarsal III length, whereas this ratio exceeds 40% in all derived dromaeosaurids and approaches 50% in the more basal microraptorines (table 6; fig. 47). In articulation, it is positioned only slightly lateral to metatarsal IV and is displaced ventrally (toward the flexor direction) relative to the level of the other metatarsals, and as a result there is a deep notch between metatarsals IV and V. The lateral surface of the bone is smooth and the muscle attachment sites that are so apparent in many large theropods (e.g., Currie and Zhao, 1993; Brusatte et al., 2008) are not present. There does, however, appear to be a slightly convex tuber on the distal portion of the flexor margin.

Pedal Digits: The digits are complete and well preserved on the left foot (figs. 32, 26). The phalangeal formula is 2-3-4-5-x and most remarkably, digit I is large and functional. Both digit I and II are modified for hyperextension and possess large unguals, and both are preserved in the stereotypical flexed position seen in the fossils of many deinonychosaurs. Digit III is the longest in the foot, although digit IV is nearly as long.

The most unusual feature of the foot is the large **digit I**, which, unlike in all other dromaeosaurids and most other theropod dinosaurs, was fully functional and faced forward in concert with the remaining digits (figs. 32, 36). The large size of the first digit is due to enlarged individual phalanges, which are approximately the same size as the phalanges of digits II–IV. In particular, the proximal phalanx of digit I is the longest nonungual phalanx in the foot and the ungual is nearly as large as the ungual of digit II (exceeding 80%). This departs remarkably from the morphology of other dromaeosaurids, best exemplified by *Velociraptor*, in which the nonungual phalanx of digit I is approximately 30% of the length of the longest nonungual phalanx in the foot and the ungual is approximately 31% of the length of the ungual of digit II (IGM 100/985; Norell and Makovicky, 1997, 1999) (table 7). Within dromaeosaurids, only *Adasaurus* (IGM 100/21) shows a similar I2/II3 ratio to that of *Balaur*, but this is due to the autapomorphically reduced sickle claw of digit II instead of the enlargment of the ungual of digit I. Furthermore, digit I of *Balaur* exhibits the same hyperextensive capabilities of digit II, most notably a robust extensor lip overhanging the dorsal (extensor) margin of the proximal surface of the ungual. The proximal phalanx has two large distal condyles that are separated by a deep flexor groove and the ungual has a small, but discrete, flexor tubercle. The ungual is slightly less recurved than that of the second digit, but more recurved than the claws on digits III and IV, and has a single groove on its lateral and medial surfaces.

Digit II is modified for hyperextension, as in other dromaeosaurids and troodontids (Ostrom, 1969; Norell and Makovicky, 1997, 1999; Manning et al., 2006). Its ungual is the largest and most recurved in the foot, and the distal articular surfaces of individual phalanges (especially the penultimate phalanx) are ginglymoid, with enlarged and highly convex distal condyles that extend onto the extensor surface of the bone. Lateral and medial ligament pits are deep on the nonungual phalanges, which also possess deep extensor pits. The ungual has a robust flexor tubercle, which is larger and more rugose than the tubercles of the remaining unguals, and a prominent extensor lip dorsally. Compared with *Deinonychus* and *Velociraptor*, however, the second pedal digit of *Balaur* is less modified for hyperextension, as the ungual is less strongly recurved and possesses a smaller and less rugose flexor tubercle (Ostrom, 1969; Norell and Makovicky, 1997: fig. 6).

Digit III is the primary weight-bearing digit of the foot. The nonungual phalanges have extensor pits, but these are not as deep as in the hyperextendable second digit. Where observable, the distal condyles are not ginglymoid and do not extend for a great distance onto the extensor surface of the bone. Lateral and medial ligament pits are large and deep where they are exposed. The ungual is broken distally but is clearly not as large as the unguals of the first two digits. The flexor tubercle is essentially absent and the

TABLE 7
Measurements of pedal phalanges (in mm) of dromaeosaurid theropods
Asterisk indicates incomplete measurement due to damage or poor preservation; curv = length measured along the outer curvature of the ungual.

Taxon	I1	I2	I2 (curv)	II1	II2	II3	II3 (curv)
Balaur bondoc EME PV.313	23	33.7	45	13	22	41.2	53
Deinonychus antirrhopus YPM 5205 (Ostrom, 1969)	32.9	32.3	63.2	43.5	49.6	60.6	130.2
Deinonychus antirrhopus MCZ 4371 (Ostrom, 1976)	34.8	–	48	47	49.9	–	118
Deinonychus antirrhopus AMNH FARB 3015 (Ostrom, 1976)	–	–	–	37.7	42.2	–	85
Velociraptor mongoliensis IGM 100/985	16.9	17.9	20.3	23.6	24	34.3	64.8
Velociraptor mongoliensis IGM 100/982	17	16	–	19.2	19.4	38.7	59.3
Velociraptor mongoliensis IGM 100/986	16.2	–	–	26.6	28	–	–
Saurornitholestes langstoni MOR 660	–	–	–	32	30	74	103
Saurornitholestes langstoni TMP 88.121.39	–	–	–	–	31	69	89
Linheraptor exquisitus IVPP V16923	15.7	17.5	22	–	39.9	55.6	62
Bambiraptor feinbergorum AMNH FARB FR 30556	12.6	–	10.3	14	14.2	29.2	47.1
Adasaurus mongoliensis IGM 100/21	27.3	29	40.5	36	29.5	31.4	48.3
Neuquenraptor argentinus MCF PHPH 77	27	26.9	38.6	39.1	36.2	39.7	83.3
Buitreraptor gonzalezorum MPCA 245	–	–	–	22.8	19.3	–	–
Buitreraptor gonzalezorum MPCA 238	16.2	–	–	27.9	18.3	–	–
Austroraptor cabazai MML-195	–	–	–	–	–	–	–
Rahonavis ostromi UA 8656	10	10.2	14.2	13	11.4	23.1	27
Microraptor zhaoianus CAGS 20-7-004	–	–	–	6.9	7.2	–	13.2
Microraptor zhaoianus CAGS 20-8-001	5.4	–	3.34	6.9	7.6	–	16
Graciliraptor lujiatunensis IVPP V13474	–	–	–	14.1	16.5	–	–
Sinornithosaurus millenii IVPP V12811	10.6	9.2	13.9	15	16.4	–	–
Mahakala onmogovae IGM/1033	–	–	–	–	9	16	18

Taxon	III1	III2	III3	III4	III4 (curv)	IV1	IV2
Balaur bondoc EME PV.313	21	15	19	24.7	33	14	11
Deinonychus antirrhopus YPM 5205 (Ostrom, 1969)	59.4	39.9	37.6	37.9	77.9	50	36

TABLE 7
(Continued)

Taxon	III1	III2	III3	III4	III4 (curv)	IV1	IV2
Deinonychus antirrhopus MCZ 4371 (Ostrom, 1976)	64.4	44	41.3	–	75	55.5	41.8
Deinonychus antirrhopus AMNH FARB 3015 (Ostrom, 1976)	52.5	33	28	–	50*	44.7	35.9
Velociraptor mongoliensis IGM 100/985	37.6	24.9	–	–	32.3	26.8	21.3
Velociraptor mongoliensis IGM 100/982	35	24.1	–	–	–	–	–
Velociraptor mongoliensis IGM 100/986	44	27.4	12.2	–	–	30.1	23
Saurornitholestes langstoni MOR 660	–	–	–	–	–	–	–
Saurornitholestes langstoni TMP 88.121.39	–	–	–	–	–	–	–
Linheraptor exquisitus IVPP V16923	54.2	32.9	19.3	48.5	52	40	28
Bambiraptor feinbergorum AMNH FARB FR 30556	27.8	15.4	16.9	11.4	15	23.4	17.8
Adasaurus mongoliensis IGM 100/21	63.8	40.3	36.9	33.6	55.8	46.2	31.9
Neuquenraptor argentinus MCF PHPH 77	57.4	36.6	34.4	–	–	–	32.3
Buitreraptor gonzalezorum MPCA 245	–	–	–	–	–	23.9	–
Buitreraptor gonzalezorum MPCA 238	–	–	–	–	–	–	–
Austroraptor cabazai MML-195	–	–	–	–	–	–	–
Rahonavis ostromi UA 8656	19.4	12.9	10.5	–	–	14.7	9.6
Microraptor zhaoianus CAGS 20-7-004	9.9	7.7	6.13	–	9.4	7.3	5.4
Microraptor zhaoianus CAGS 20-8-001	10.1	8.2	7.9	–	9.5	8.4	6
Graciliraptor lujiatunensis IVPP V13474	15.2	–	–	–	–	16.4	10.6
Sinornithosaurus millenii IVPP V12811	24.5	17	15.9	15.1	21.1	19.6	14.4
Mahakala onmogovae IGM/1033	20	16	13	10.5	–	–	–

Taxon	IV3	IV4	IV5	IV5 (curv)
Balaur bondoc EME PV.313	11	12	18.8	19.5
Deinonychus antirrhopus YPM 5205 (Ostrom, 1969)	30.6	28.7	34.3	64.3
Deinonychus antirrhopus MCZ 4371 (Ostrom, 1976)	35.2	32.6	–	60
Deinonychus antirrhopus AMNH FARB 3015 (Ostrom, 1976)	32.2	26.3	–	42*
Velociraptor mongoliensis IGM 100/985	16.8	16.1	–	31

TABLE 7
(Continued)

Taxon	IV3	IV4	IV5	IV5 (curv)
Velociraptor mongoliensis IGM 100/982	–	–	–	–
Velociraptor mongoliensis IGM 100/986	18.6	18.6	25.6	34.5
Saurornitholestes langstoni MOR 660	–	–	–	–
Saurornitholestes langstoni TMP 88.121.39	–	–	–	–
Linheraptor exquisitus IVPP V16923	26.1	26.4	–	–
Bambiraptor feinbergorum AMNH FARB FR 30556	12.3	12.9	12.4	16.6
Adasaurus mongoliensis IGM 100/21	27.7	19.3	31.1	–
Neuquenraptor argentinus MCF PHPH 77	25.4	25.5	21.7	32.3
Buitreraptor gonzalezorum MPCA 245	–	–	–	–
Buitreraptor gonzalezorum MPCA 238	–	–	–	–
Austroraptor cabazai MML-195	–	–	–	–
Rahonavis ostromi UA 8656	7.1	–	–	–
Microraptor zhaoianus CAGS 20-7-004	5	5.4	–	9.2
Microraptor zhaoianus CAGS 20-8-001	4.2	5.9	–	9
Graciliraptor lujiatunensis IVPP V13474	7.7	9.6	–	–
Sinornithosaurus millenii IVPP V12811	10.7	11.6	15.4	20.1
Mahakala onmogovae IGM/1033	–	–	–	–

extensor lip is reduced. Notably, the distal segment of digit III is elongated relative to the proximal segment or to metatarsal III. Both phalanx III-3 and, especially, ungual III-4 are about 1.5–2× as long relative to the length of metatarsal III than in most other derived dromaeosaurids, as well as in the basal microraptorines and unenlagiines (table 7).

Digit IV is similar to digit III in the morphology of individual phalanges. Extensor pits are present, but shallow, on the non-ungual phalanges, and the distal articular surface extends only slightly onto the extensor surface of the bone. Some individual phalanges are ginglymoid, but the extensor groove between the distal condyles is shallow. The ungual is broken distally but appears to be the smallest and straightest ungual in the foot. It has a single groove on both the lateral and medial surfaces, as do the other unguals, but unfortunately its extensor lip and flexor tubercle cannot be observed due to breakage and concealing matrix, respectively.

HISTOLOGY AND GROWTH STAGE

Histological sections of *Balaur* long bones were prepared from two individuals, the *B. bondoc* holotype (EME PV.313) and the *B.* sp. referred ulna (LPB [FGGUB] R.1581). The results were used to estimate the minimal

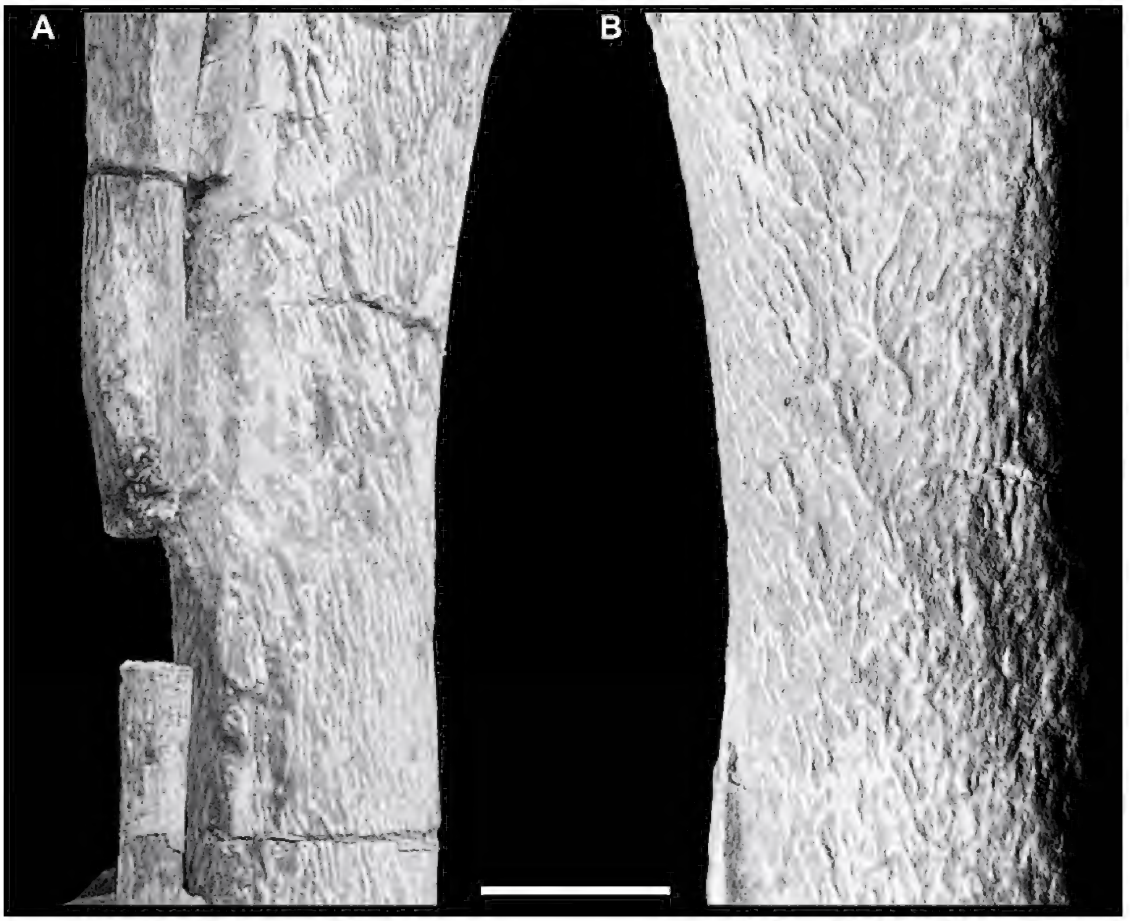

Fig. 39. The external bone surface texture on the holotype left fibula and tibia (**A**) of *Balaur bondoc* (EME PV.313) and the referred left humerus (**B**) of *Balaur* sp. (LPB [FGGUB] R.1580).

age and developmental stage of each specimen. In addition we used histological examination to infer whether the heavily sculptured external cortical texture characteristic of all the long bones is a genuine biological feature (related to osteogenesis) or the result of postmortem erosion or other taphonomic alteration (fig. 39). Histological examination was carried out by two of us (A.W. and G.M.E.).

A diaphyseal section of the left fibula of the holotype (EME PV.313, a fragment from the distalmost end of the broken shaft) and a hemisection of the isolated left ulna (LPB [FGGUB] R.1581) (48 mm from the proximal end and 83.3 mm from the incomplete distal end) were extracted and embedded in clear epoxy resin (EpoxySet: Allied High Tech Products, Inc., Rancho Dominguez, California). The segments were then serially sectioned at 1.5 mm intervals transverse to the long axes of the bones using a slow-speed bone saw fitted with a diamond-tipped blade (Isomet, 1000; Buehler Inc., Lake Bluff, Illinois). The sections were subsequenly affixed to petrographic slides using cyanoacrylate adhesive. They were then sanded on a rotary polisher (RotoPol11 polisher; Struers Inc., Cleveland, Ohio) to 60–100 μm using descending grades of silicon carbide paper with water as an irrigant. The thin sections were viewed using a polarizing petrographic microscope and the histological patterning described (cf. Francillon-Vielliot et al., 1990). Unfortunately, the microstructure of both specimens was heavily damaged by postmortem

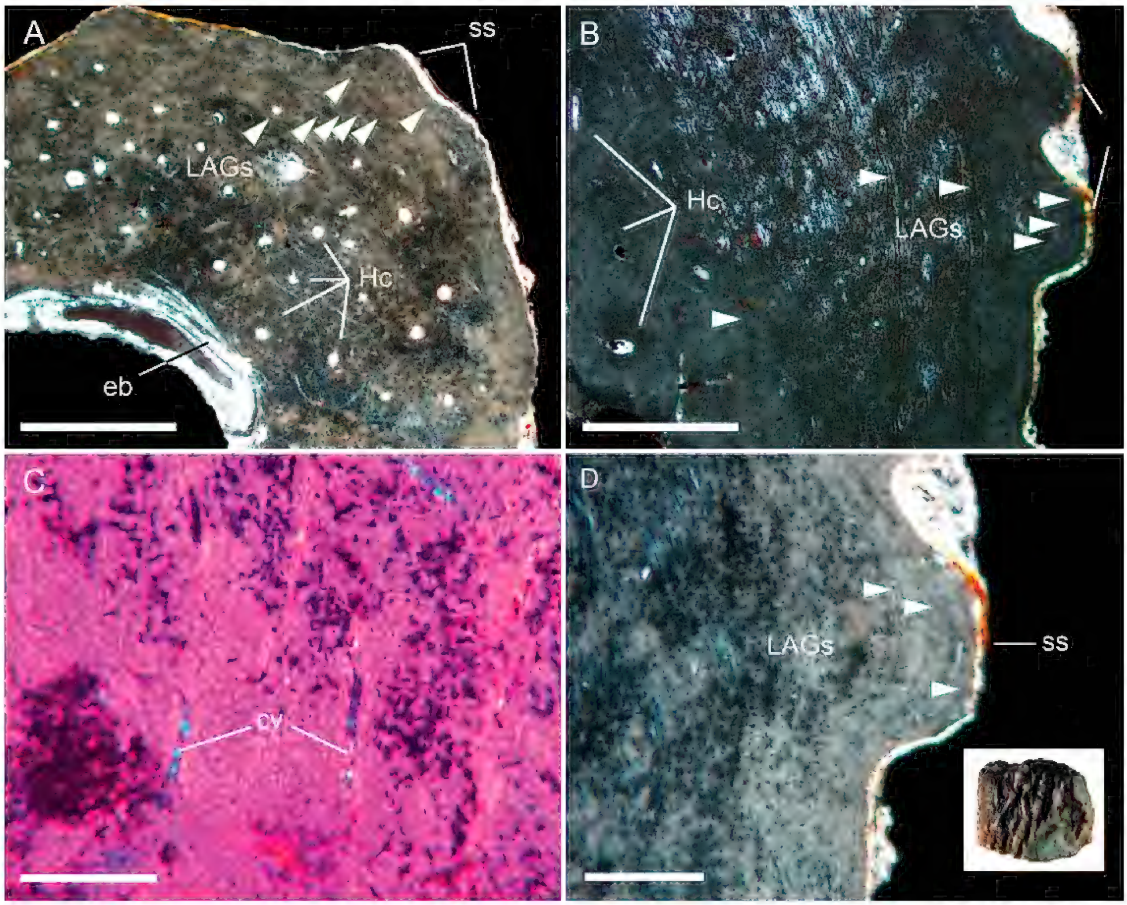

Fig. 40. Transverse histological sections of *Balaur*. (**A**) Left fibula of the *B. bondoc* holotype (EME PV.313) shown in polarized microscopy. Dense Haversian remodeling (Hc = Havesian canals), endosteal bone (eb), and weakly differentiated lines of arrested growth (LAGs) are evident (arrows). Note that deep cortical lines do not follow the prominent contours of the periosteal surface sculpturing (ss). Scale bar = 500 um. (**B**) Transverse histological section of the *B.* sp. left ulna (LPB [FGGUB R.1581] shown in polarized microscopy. Dense Haversian remodeling (Hc = Haversian canals), and weakly differentiated lines of arrested growth (LAGs) are evident (arrows). Note that deep cortical lines do not follow the prominent contours of the periosteal surface sculpturing (ss). Scale bar = 500 um. (**C**) Transverse histological section of the *B.* sp. left ulna in polarized microscopy, showing locally preserved deep cortical primary matrix. The periosteal surface is to the right (not shown). Weakly expressed deep cortical fibrolamellar bone with circumferential vascularization (cv) is preserved. Scale bar = 200 um. (**D**) Closeup histological section of the *B.* sp. left ulna showing periosteal surface sculpturing and corresponding lines of arrested growth. Note that the LAGs shown here that were deposited latest in life (arrows) follow the contours of the periosteal surface sculpturing (ss), suggesting that the sculpturing is not a diagnetic or taphonomic feature. Scale bar = 200 um.

fungal invasion. As a result, most of the histological preparations are opaque and the microstructural attributes indistinct. Nevertheless, islands of undamaged bone provided enough information to achieve our stated goals to determine growth stage and age of the two individuals and whether the bones' mottled external texture is biologically genuine (fig. 40).

HOLOTYPE SPECIMEN: The fibula of EME PV.313 shows dense Haverisan remodeling thoughout the inner two-thirds of the cortex (fig. 40A). The endosteal surface is lined with lamellar bone (fig. 40A). Because of the

extensive fungal damage, remodeling, and the hollow nature of the bone, the primary cortical bone types deposited early in ontogeny were indeterminable. The outer third of the cortex is composed of parallel-fibered matrix with sparse longitudinal vascularization. The matrix is interrupted by lines of arrested growth (LAGs). At least seven are present and their spacing diminishes nearer the periosteal surface. The deepest LAGs show negligible folding, whereas the outermost ones follow the contours of the external bone sculpturing manifest at the perisoteal surface (fig. 40A).

The results from the LAG count suggest that EME PV.313 was no less than seven years of age at the time of death. Based on the distance from the innermost preserved LAG to the centroid of the section, and the width of the deepest zone, it was likely several years older. The presence of dense Haversian bone, diminished spacing between LAGs near the periosteal surface, parallel-fibered bone deposited just prior to death, and negligible vascularization suggest that this individual is a skeletally mature individual (i.e., nearly full grown at the time of death). The extensive folding seen only in the outermost LAGs shows that the peculiar scultured texture of *B. bondoc* long bones is not a result of diagenesis or taphonomic alteration (e.g., chemical or biological erosion), but rather is a natural osteogenic developmental feature, one that manifested itself very late in the life of EME PV.313. Whether this feature is a nondebilitating or debilitating product of senescence, a response to disease, or even a functional attribute is indeterminable at this time, but is worthy of further study as new specimens are found and comparative histological datasets (of both extinct and extant taxa) are expanded.

Referred Specimen: The ulna sample from LPB (FGGUB) R.1581 shows dense Haverisan remodeling thoughout the inner third of the cortex (fig. 40B). Endosteal bone is absent. Despite extensive fungal damage, remodeling, and the hollow medullary cavity, a small section of primary bone is locally preserved deep in the cortex (fig. 40C). This shows fibro-lamellar matrix with circumferential vascularization. The outer two-thirds of the cortex is composed of parallel-fibered matrix with sparse longitudinal vascularization (fig. 40B). The matrix is interrupted by LAGs. There are at least six of these and their spacing substantially diminishes nearer the periosteal surface. As with the fibula from the holotype, the deepest LAGs show negligible folding whereas the outermost ones follow the sculpturing seen at the perisoteal surface (fig. 40B, D)

The results from the LAG count suggest that LPB (FGGUB) R.1581 was no less than six years of age at the time of death. However, based on the distance from the innermost preserved LAG to the centroid, and the sample's distance from midshaft, this individual is likely several years older. The presence of dense Haversian bone and the attenuated spacing of the outermost LAGs suggest that this individual is (like the *B. bondoc* holotype EME PV.313) skeletally mature (i.e., full or nearly full grown at the time of death). The extensive folding of only the outermost LAGs, as was also seen in EME PV.313 (see above), suggests that the peculiar sculptured texture of *Balaur* long bones is not a result of diagenesis. It is a natural late developmental osteogenic feature present on both specimens, which as discussed by Csiki et al. (2010a) are of different body size and were discovered at different localities that may be slightly different in geological age.

PHYLOGENY

In the short initial paper describing *B. bondoc*, Csiki et al. (2010a) analyzed the phylogenetic position of the new taxon by inserting it into the cladistic dataset of Turner et al. (2007a), which included 70 taxa scored for 251 characters. They recovered *Balaur* as a highly derived dromaeosaurid most closely related to *Velociraptor*, and within a larger clade of Laurasian species that lived during the middle–Late Cretaceous. Here we more fully discuss the phylogenetic position of *Balaur* based on a greatly expanded coelurosaur dataset developed by Turner et al. (2012). This dataset consists of 111 taxa and 474 characters with *Allosaurus fragilis* and *Sinraptor dongi* as outgroups used to root the most parsimonious trees. This character matrix is referred to as TWIG 2011.2. The

character list, data matrix, and supplemental analysis data are available in Turner et al. (2012) and online (http://www.morphobank.org/index.php/Projects/ProjectOverview/project_id/660).

Equally weighted parsimony analysis was implemented using TNT v. 1.0 (Goloboff et al., 2008a, 2008b) and a heuristic tree search strategy was conducted performing 1000 replicates of Wagner trees (using random addition sequences, RAS) followed by TBR branch swapping (holding 10 trees per replicate). The best trees obtained at the end of the replicates were subjected to a final round of TBR branch swapping. Zero-length branches were collapsed if they lacked support under any of the most parsimonious reconstructions (i.e., rule 1 of Coddington and Scharff, 1994). This search strategy resulted in 1190 most parsimonious trees of 2024 steps (CI = 0.300, RI = 0.740), found in 134 out of the 1000 replications of RAS+TBR. Additional TBR branch swapping of these 1190 trees found 90,970 additional optimal topologies resulting in a total of 92,160 most parsimonious topologies.

As in the initial analysis of Csiki et al. (2010a), *Balaur* was found to be a member of a monophyletic Dromaeosauridae (fig. 41). The monophyly of the clade is weakly supported (Bremer value of 1 and a Group present/Contradicted [GC] value of 16 in the reduced strict consensus cladogram). Within Dromaeosauridae, *Balaur* is placed in an unresolved position (polytomy) with *Velociraptor*, *Deinonychus*, and *Adasaurus*. This position of *Balaur* is generally consistent with the phylogenetic position recovered by the original phylogenetic analysis of Csiki et al. (2010a), which used a dataset that is a subset of the dataset employed here. Csiki et al. (2010a) found *Balaur* as the sister taxon to *Velociraptor mongoliensis*, a result that is not recovered in the strict consensus topology of the new phylogenetic analysis (but is present in many of the individual most parsimonious trees). Part of this lack of resolution in the current analysis is a result of uncertain placement of *Adasaurus mongoliensis*, but an additional source of uncertainty is from two alternate placements of *Balaur*.

One set of most parsimonious trees finds *Balaur* as the sister taxon to *Velociraptor mongoliensis* with *Adasaurus mongoliensis* the sister taxon to this clade. Two synapomorphies support this position—pneumatic foramina (pleurocoels) absent on all sacral vertebrae (char. 113.0) and the ridge bounding the cuppedicus fossa extending far posteriorly such that it is confluent, or almost confluent, with the acetabular rim (char. 163.1). The other set of most parsimonious trees finds *Balaur* as the sister taxon to a *Velociraptor mongoliensis* plus *Deinonychus antirrhopus* clade. This position is supported by pleurocoels absent on all sacral vertebrae (char. 113.0) and a pubic shaft that curves posteriorly, forming an anteriorly convex pubis (char. 180.2). Unfortunately, because skull elements of *Balaur* are currently unknown, cranial characters do not influence the phylogenetic position of this taxon. However, if cranial bones are later found, they may prove invaluable in differentiating between these two major alternative phylogenetic placements.

DISCUSSION

The European Late Cretaceous Theropod Record

Fossils of theropods are exceptionally rare in the Upper Cretaceous deposits of Europe, and as a result, little is known about the morphology, evolution, and biogeography of European Late Cretaceous carnivorous dinosaurs (Weishampel et al., 2004; Weishampel and Jianu, 2011). The holotype of *Balaur bondoc* is by far the most complete, best preserved, and diagnostic theropod specimen from the final ~50 million years of the Cretaceous in Europe, and as such, provides critical information on European dinosaur faunal evolution (see below). In contrast to the well preserved skeleton of *Balaur*, most previous records of European Late Cretaceous theropods have been limited to teeth and fragmentary, and usually disarticulated, bones. The most comparable and important of these records include a variety of specimens from the Transylvanian area of Romania (e.g., Andrews, 1913; Csiki and Grigorescu, 1998; Kessler et al., 2005), as well as

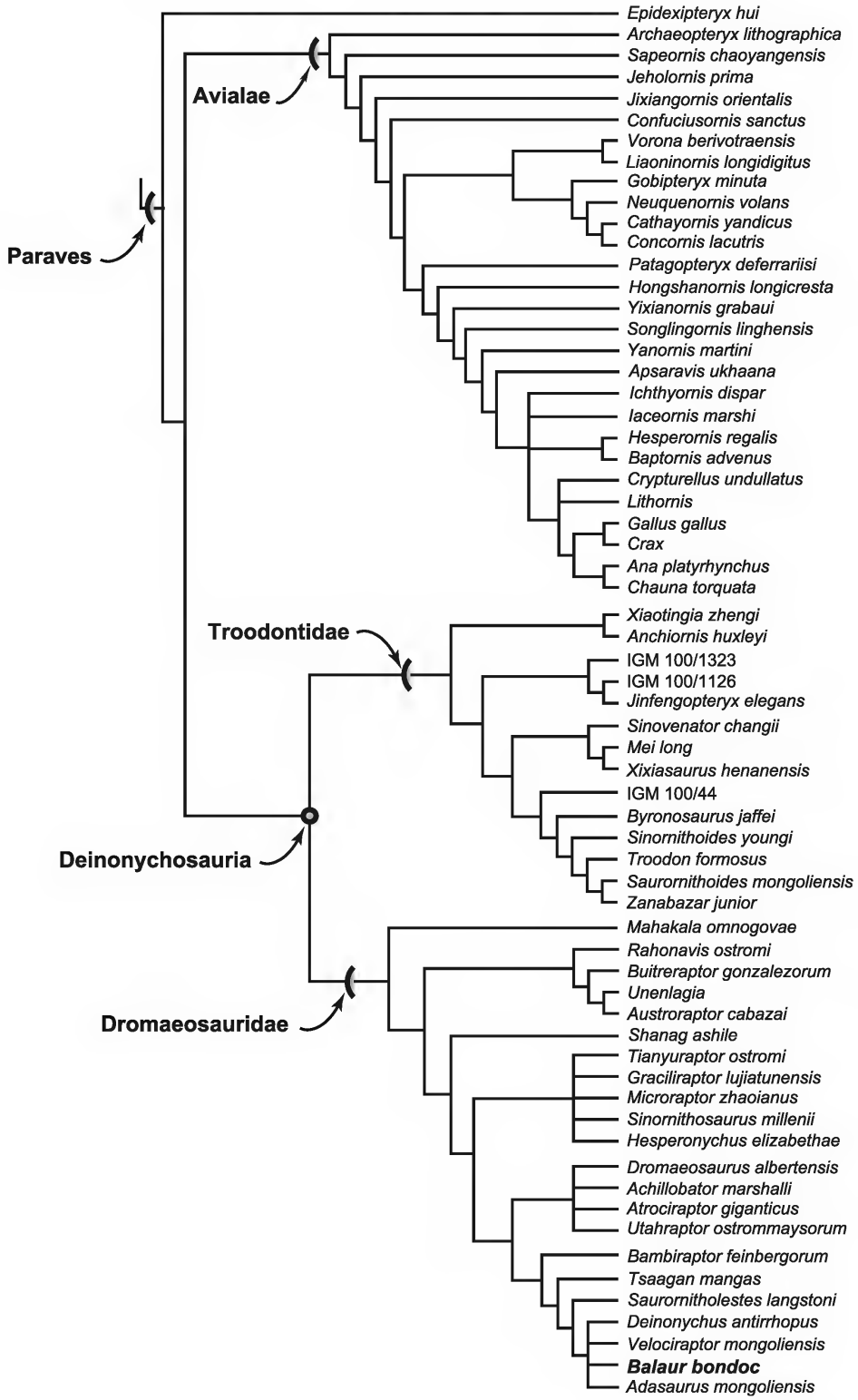
Epidexipteryx hui
Archaeopteryx lithographica
Sapeornis chaoyangensis
Jeholornis prima
Jixiangornis orientalis
Confuciusornis sanctus
Vorona berivotraensis
Liaoninornis longidigitus
Gobipteryx minuta
Neuquenornis volans
Cathayornis yandicus
Concornis lacutris
Patagopteryx deferrariisi
Hongshanornis longicresta
Yixianornis grabaui
Songlingornis linghensis
Yanornis martini
Apsaravis ukhaana
Ichthyornis dispar
Iaceornis marshi
Hesperornis regalis
Baptornis advenus
Crypturellus undullatus
Lithornis
Gallus gallus
Crax
Ana platyrhynchus
Chauna torquata
Xiaotingia zhengi
Anchiornis huxleyi
IGM 100/1323
IGM 100/1126
Jinfengopteryx elegans
Sinovenator changii
Mei long
Xixiasaurus henanensis
IGM 100/44
Byronosaurus jaffei
Sinornithoides youngi
Troodon formosus
Saurornithoides mongoliensis
Zanabazar junior
Mahakala omnogovae
Rahonavis ostromi
Buitreraptor gonzalezorum
Unenlagia
Austroraptor cabazai
Shanag ashile
Tianyuraptor ostromi
Graciliraptor lujiatunensis
Microraptor zhaoianus
Sinornithosaurus millenii
Hesperonychus elizabethae
Dromaeosaurus albertensis
Achillobator marshalli
Atrociraptor giganticus
Utahraptor ostrommaysorum
Bambiraptor feinbergorum
Tsaagan mangas
Saurornitholestes langstoni
Deinonychus antirrhopus
Velociraptor mongoliensis
Balaur bondoc
Adasaurus mongoliensis
Avialae
Paraves
Troodontidae
Deinonychosauria
Dromaeosauridae

from Hungary (e.g., Ősi and Rabi, 2006; Ősi et al., 2010a) and France (e.g., Vullo et al., 2007; Chantasit and Buffetaut, 2009). These specimens were reviewed in detail, and compared with the holotype of *Balaur*, in the supplementary information of Csiki et al. (2010a). We briefly revisit these comparisons here to reiterate that none of this material is clearly referable to *Balaur*, although some of it may belong to closely related taxa.

ROMANIAN SPECIMENS: Prior to the discovery of *Balaur*, the best-known, best-preserved, and most diagnostic theropod taxon from the Late Cretaceous of Europe was *Elopteyx nopcsai*, a small theropod named by Andrews (1913) based on two proximal femoral fragments (and possibly a distal tibiotarsus) from the Sânpetru Formation of the Haţeg Basin of Transylvania, Romania. Subsequently, various authors assigned additional material to this taxon, which usually could not be compared directly with the fragmentary type material (e.g., Lambrecht, 1929; Grigorescu and Kessler, 1981). Later workers also disagreed on the taxonomic affinities of both the *Elopteyx* type and referred material, with some authors suggesting derived avian affinities (e.g., Lambrecht, 1929; Harrison and Walker, 1975) and others arguing that some, or all, of this material belonged to small nonavian coelurosaurian theropods (e.g., Martin, 1983; Grigorescu, 1984; Le Loeuff et al., 1992; Csiki and Grigorescu, 1998; Naish and Dyke, 2004; Kessler et al., 2005; Weishampel and Jianu, 2011).

A more detailed account of the tortuous taxonomic history of *Elopteryx* is provided by Csiki et al. (2010a) and will not be repeated here. For the sake of this paper, however, it is important to point out that the holotype of *Balaur* cannot be compared to the holotype of *Elopteyx* because there is no overlapping material between the two specimens. It may be noteworthy that both *Balaur* (holotype and additional referred specimens) and the specimens referred to *Elopteryx*, as well as other isolated bones from the Late Cretaceous of Romania, possess a similar woven and rugose external bone texture (Andrews, 1913; Le Loeuff et al., 1992; Kessler et al., 2005; Csiki et al., 2010a). This may turn out to be an autapomorphy of a single species (which includes the holotypes of both *Balaur* and *Elopteryx*), but it could also represent a synapomorphy of a larger group, or perhaps an environmentally controlled feature unique to theropods living on the Late Cretaceous European archipelago. Therefore, we do not currently consider the presence of this single character as strong evidence for the synonymy of *Balaur* and *Elopteyx*.

A number of Romanian specimens besides the holotype of *Elopteryx* are preserved in collections of the Natural History Museum in London. Locality information for much of this material is uncertain (many are simply labeled "Transylvania"), and some of these are femora that, because femora are not preserved in the *Balaur* holotype, disallow direct comparison with *Balaur*. However, it is interesting to note that all these bones preserve the very unusual surface texture seen in both *Balaur* (holotype and referred specimens) and the holotype of *Elopteryx*. Although most of these specimens are referred to *Elopteryx* (both in print and in the museum's catalog) there is significant size and morphological differences among them. This suggests that there is probably more than one theropod taxon represented in this collection and that the unusual surface texture of the bones may be present on all, or many, of these small, island-dwelling theropods.

Additional theropod material from the Late Cretaceous of Romania includes isolated teeth and fragmentary cranial and postcranial

←

Fig. 41. The phylogenetic relationships of *Balaur* and other paravian theropods. Reduced strict consensus of 92,160 most parsimonious trees (CI = 0.30, RI = 0.74) recovered from a phylogenetic analysis of the Turner et al. (2012) dataset. *Pyroraptor olympius* and *Limenavis patagonicus* have been excluded from the consensus. Clades outside of Paraves are not depicted here. See text for details.

elements. Various teeth have been referred to dromaeosaurids, troodontids, and enigmatic tooth genera such as *Richardoestesia*, *Paronychodon*, and *Euronychodon* (Grigorescu, 1984; Grigorescu et al., 1985; Csiki and Grigorescu, 1998; Codrea et al., 2002; Smith et al., 2002; Vasile, 2008). Unfortunately, these teeth cannot be compared to the dentition of the *Balaur* holotype, which lacks the entire skull and dentition. Similarly, a set of putative dromaeosaurid frontals, which were described by Weishampel and Jianu (1996) and identified as belonging to a *Saurornitholestes*-like taxon, cannot be compared to *Balaur*. Finally, a sacrum mentioned in passing by Nopcsa (1915, 1923) and described in detail by Ősi and Főzy (2007) may represent an animal closely related to *Balaur*, but it is difficult to compare the two specimens (because Nopcsa's specimen is fragmentary), and our comparisons indicate that they do not share any unique derived characters. We find it likely that many of the isolated theropod remains from the Late Cretaceous of Romania do indeed belong to the same taxon as *Balaur*, but this is often difficult to test due to the lack of overlapping material, poor preservation, and the lack of clear synapomorphies.

Hungarian Specimens: Along with isolated teeth that cannot be directly compared with *Balaur* (Ősi, 2004), two peculiar specimens from the Santonian (middle Late Cretaceous) of Hungary belong to derived coelurosaurian theropods that may be close relatives of *Balaur*. First, Ősi et al. (2010a) named a new taxon, *Pneumatoraptor fodori*, based on a fused scapulocoracoid. Although *Balaur* also possesses fusion between the scapula and coracoid, these bones in the two taxa differ in detail. Most prominently, *Balaur* lacks the large pneumatic foramen on the coracoid that is an autapomorphy of *Pneumatoraptor*, whereas *Pneumatoraptor* lacks the hypertrophied coracoid tubercle that is autapomorphic of *Balaur*. It is also worth noting that other dromaeosaurids, such as *Velociraptor* and *Microraptor*, also possess fusion between the scapula and coracoid (Norell and Makovicky, 1999; Turner et al., 2007a), so it is possible that *Pneumatoraptor* may be a dromaeosaurid closely related to *Balaur*. Second, Ősi and Rabi (2006) and Ősi (2008) described a fused tarsometatarsus, which they referred to an enantiornithine bird. The various characters used to unite this specimen with enantiornithines are also present in *Balaur*, which may cast doubt on this taxonomic assignment. Regardless, it is clear that the Hungarian specimen is distinct from *Balaur* for several reasons. First, the tarsometatarsus is much shorter proximodistally relative to its mediolateral width in *Balaur*. Second, the metatarsals are more closely appressed along their shafts in *Balaur*. Third, the Hungarian specimen lacks the autapomorphic ridges on the extensor surface of metatarsals II–IV in *Balaur*. Fourth, and finally, the Hungarian specimen lacks a metatarsal V that is fused to metatarsal IV as in *Balaur*. Therefore, none of the Hungarian specimens can be assigned to *Balaur*, which is not surprising, given that these specimens are about 15–20 million years older.

French Specimens: Coelurosaurian theropod specimens have been reported from both the Cenomanian (earliest Late Cretaceous) and Campanian-Maastrichtian (latest Late Cretaceous) of France. Isolated teeth described by Vullo et al. (2007) from the Cenomanian cannot be compared directly to *Balaur*, nor can teeth from the Campanian-Maastrichtian (e.g., Buffetaut et al., 1986). However, two more complete and potentially diagnostic dromaeosaurid specimens from France can be compared to *Balaur*. The first, *Pyroraptor olympius*, is different from *Balaur* because it lacks the flat anterior surface of the ulna that is autapomorphic of *Balaur*. Furthermore, *Balaur* lacks the deep muscle attachment site on the lateral surface of the proximal ulna that Allain and Taquet (2000) described as autapomorphic of *Pyroraptor*. The second dromaeosaurid, *Variraptor mechinorum*, is also distinct from *Balaur* (Le Loeuff and Buffetaut, 1998). The humerus of *Variraptor* is more robust and straighter than that of *Balaur*, and it exhibits a prominent posteromedial tuber level with the distal end of the deltopectoral crest, which is absent in *Balaur*. Furthermore, the sacrum of *Variraptor* is marked by a ventral groove on only the fourth vertebra, whereas in *Balaur* these grooves are present on more anterior sacrals. Finally, it is worth noting that *Balaur* can be

differentiated from two more fragmentary French specimens: a manual ungual recently described by Chantasit and Buffetaut (2009) lacks the autapomorphic Y-shaped lateral and medial grooves of *Balaur*, and a caudosacral vertebra reported by Le Loeuff et al. (1992) possesses a dorsolaterally oriented transverse process that is unlike the more laterally oriented process of *Balaur*.

European Late Cretaceous Dinosaur Biogeography

The well-preserved holotype of *Balaur*, interpreted in a phylogenetic and faunal context, sheds light on the biogeographic history of Late Cretaceous European dinosaur faunas. The importance of *Balaur* in illuminating biogeographic patterns was discussed briefly by Csiki et al. (2010a) and we here review the most salient implications. *Balaur* and other Romanian Late Cretaceous dinosaurs, as well as contemporaneous European dinosaurs more broadly, inhabited a series of islands during the Cretaceous, a time of warm temperatures and high sea levels (Csontos and Vörös, 2004; Benton et al., 2010; Weishampel and Jianu, 2011). Prior to the description of *Balaur* and other recently discovered herbivorous dinosaur taxa, it was thought that the Romanian dinosaurs, and Late Cretaceous European dinosaurs in general, comprised endemic faunas that arose through a lengthy process of in situ diversification (see reviews in Weishampel et al., 1991, 2010; Ősi et al., 2010a, 2010b; Weishampel and Jianu, 2011). This hypothesis held that most Late Cretaceous island species (and not only dinosaurs) were the descendants of Late Jurassic–earliest Cretaceous lineages that were stranded in Europe for tens of millions of years as sea levels rose. Support for this scenario stemmed from the primitive phylogenetic position of many herbivorous dinosaurs, reptiles, and mammals, which were found to be members of clades that seemed to be restricted to Late Cretaceous Europe and whose closest non-European relatives were considerably older taxa (see reviews in Benton et al., 2010, Weishampel et al., 2010; Weishampel and Jianu, 2011).

The discovery of *Balaur*, however, does not synchronize with this scenario. The closest relatives of *Balaur* are primarily Asian and North American taxa of similar or slightly older age. Although the phylogenetic topology presented in this monograph differs slightly from that presented in the original description of Csiki et al. (2010a), *Balaur* is still found to occupy a derived phylogenetic position, interspersed within a clade of Laurasian (Asiamerican) taxa. It is true that there are no other European dromaeosaurids in the analysis, so given the current sample it is impossible for *Balaur* to group with other European taxa in an endemic clade. Further discoveries may show that various species of Late Cretaceous European dromaeosaurids did form a clade. What is important, however, is that *Balaur* (and by extension any undiscovered close relatives) is placed within a wider clade that contains contemporary (and near contemporary) taxa from other continental areas. *Balaur* does not group with Late Jurassic–earliest Cretaceous coelurosaurs (such as microraptorine dromaeosaurids or the *Utahraptor* clade), nor is it a basal dromaeosaurid or a basal member of a derived dromaeosaurid clade, as would be predicted if the classic scenario of long-term island endemicity was correct.

Because *Balaur* is just a single taxon, its evolutionary history may not necessarily be indicative of a wider pattern of faunal evolution. With this in mind, it is important to note that recent discoveries of hadrosaurian and ceratopsian dinosaurs in the Late Cretaceous of Europe also suggest that some herbivores were not merely endemic relicts, but rather members of clades with contemporary representatives on other landmasses, especially Asia (Dalla Vecchia, 2009; Pereda-Suberbiola et al., 2009; Prieto-Márquez and Wagner, 2009; Ősi et al., 2010b; Weishampel and Jianu, 2011). Therefore, the emerging picture of European Late Cretaceous dinosaur biogeography is a combination of island endemicity and wider interchange. There is no doubt that many Late Cretaceous European taxa were endemic to some degree, as is attested to by the basal phylogenetic positions of some taxa (herbivorous dinosaurs such as rhabdodontids, nodosaurids, and basal hadrosauroids: Benton et al., 2010) and the extreme modifications of some taxa corresponding to their island environments

(e.g., dwarfism, highly autapomorphic morphology: see below). However, not all European Late Cretaceous taxa were stranded on the European archipelago for tens of millions of years, but rather arose during periods of continued interchange between Europe and other landmasses during the Late Cretaceous.

Dromaeosaurid Limb Ratios and Skeletal Fusion

The strongly autapomorphic hand and foot skeleton of *Balaur* prompted a comprehensive survey of the limb ratios within Dromaeosauridae, in order to better understand how unusual the Romanian species is compared to its closest relatives. We assembled a large dataset, including forelimb and hind-limb lengths across the dromaeosaurid clade. Data were collected either by directly measuring the specimens or from references with published measurements, and were tabulated to allow a comparison of limb structure and ratios across Dromaeosauridae. The measurements are presented in tables 4–7 and some are shown graphically in figures 42–47. We briefly discuss some of the more salient observations gleaned from this dataset. Note that we are simply discussing raw measurements and not standardizing by body size. It is widely recognized that many limb proportions in theropods are allometric (e.g., Currie, 2003) and the influence of allometry on dromaeosaurid proportions is a fruitful area for future statistical work, which is outside of the scope of this paper and which requires a larger database than we have compiled.

A first observation concerns the relative sizes of the limbs. Excepting such outliers as *Graciliraptor* (Xu and Wang, 2004), characterized by extremely elongated forelimbs, or *Mahakala*, with a reduced forelimb (Turner et al., 2011), most other dromaeosaurids show similar values for the forelimb-to–hind limb ratio (expressed here as ratio of humerus + ulna + MC II to tibia + MT III; the femur is not included in this measure because no femur is currently known for *Balaur*). *Balaur*, however, has a slightly proportionally reduced hind limb. Unfortunately, because the femur of *Balaur* is unknown, it cannot be ascertained whether the shortening of its hind limb was restricted to the distal segment (tibia and metatarsus), or characterized the limb overall.

The distal hind-limb elements of *Balaur* are proportionally shorter than in other dromaeosaurids. Both the tibia and the metatarsus are proportionally shortened, relative to the humerus, although this reduction is more obvious in the case of the metatarsus. Within the distal hind limb, the metatarsus is proportionally short relative to the tibia in *Balaur*, although at least one specimen of each of the closely related taxa *Velociraptor* (IMG 100/986) and *Saurornitholestes* (TMP 88.121.39) appears to have similarly shortened metatarsi. The presence of a relatively short metatarsus was also noted in *Deinonychus* by Ostrom (1976). To the contrary, in the basal microraptorines and unenlangiines, the metatarsus is relatively longer than in *Balaur* and its close relatives. Therefore, some degree of metatarsal shortening, relative to other dromaeosaurid taxa, seems to characterize *Balaur* and its closest relatives. The extremely reduced condition of *Balaur* is autapomorphic, but may represent a culmination of a long-term phylogenetic trend.

The most outstanding feature of the metatarsus of *Balaur* is the autapomorphic elongation of metatarsal I, which measures approximately 60% of metatarsal III. This ratio is substantially lower in all other surveyed dromaeosaurids. There may be a progressive lengthening of metatarsal I within the dromaeosaurid clade, from the basal microraptorines toward the more derived velociraptorines, but this remains to be tested with a larger dataset and phylogenetic comparative methods, which is outside the scope of this paper. Regardless, even if such a phylogenetic trend exists, the enlarged dimensions of metatarsal I in *Balaur* represent an extreme size modification that is currently unique to this genus. A somewhat similar pattern can be noted in the case of metatarsal V, which is autapomorphically reduced to less than 30% of the metatarsal III length, whereas it exceeds 40% in all other dromaesaurids with reasonably complete fifth metatarsals.

The development of an autapomorphically enlarged, hyperextensible first pedal digit is

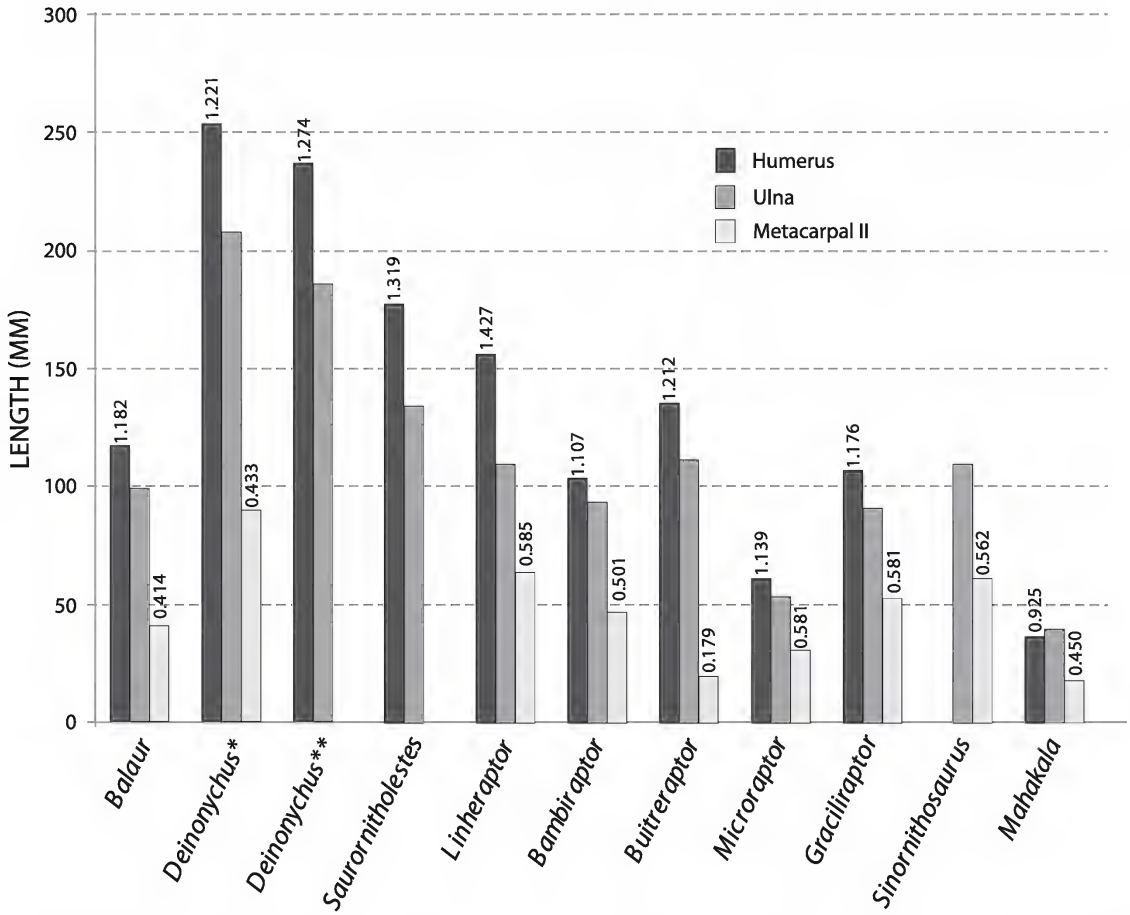

Fig. 42. Plot of absolute forelimb element lengths for various dromaeosaurid theropods (based on table 4). * = MCZ 4371, ** = AMNH FARB 3015. Numbers besides plot bars indicate the percent length of the respective element compared to the ulna, for ease of relative length comparisons between the different taxa.

probably the single most conspicuous feature of *Balaur*. This is achieved by the elongation of both metatarsal I and the individual phalanges. Based on raw proportions, the nonungual phalanx of the digit does not appear to be particularly elongated, and in fact is slightly smaller (compared to the length of the metatarsal) than the dromaeosaurid average. However, as the metatarsal itself is lenghtened, the lower values of this ratio obscure the fact that in absolute dimensions phalanx I-1 is the largest nonungual phalanx of the foot, and is substantially more elongated compared to both the entire metatarsus (as exemplified by metatarsal III) and to the tibia than in any other dromaeosaurid. Similarly, although the ungual phalanx of the first digit is relatively smaller (compared to metatarsal I) than in many dromaeosaurids, it is clearly enlarged relative to the length of the metatarsus or the tibia. Even if these ratios are partly skewed by the shortened metatarsus and tibia of *Balaur*, it is nonetheless clear that the first digit is uniquely enlarged among dromaeosaurids, even disregarding the presence of the hyperextensible sickle claw or any speculation on its function.

Unlike the first digit, digits II to IV (measured as the combined lengths of the nonungual phalanges) have approximately similar proportions in *Balaur* as compared to other dromaeosaurids. Digit III is marginally longer, and digit IV slightly shorter, than in

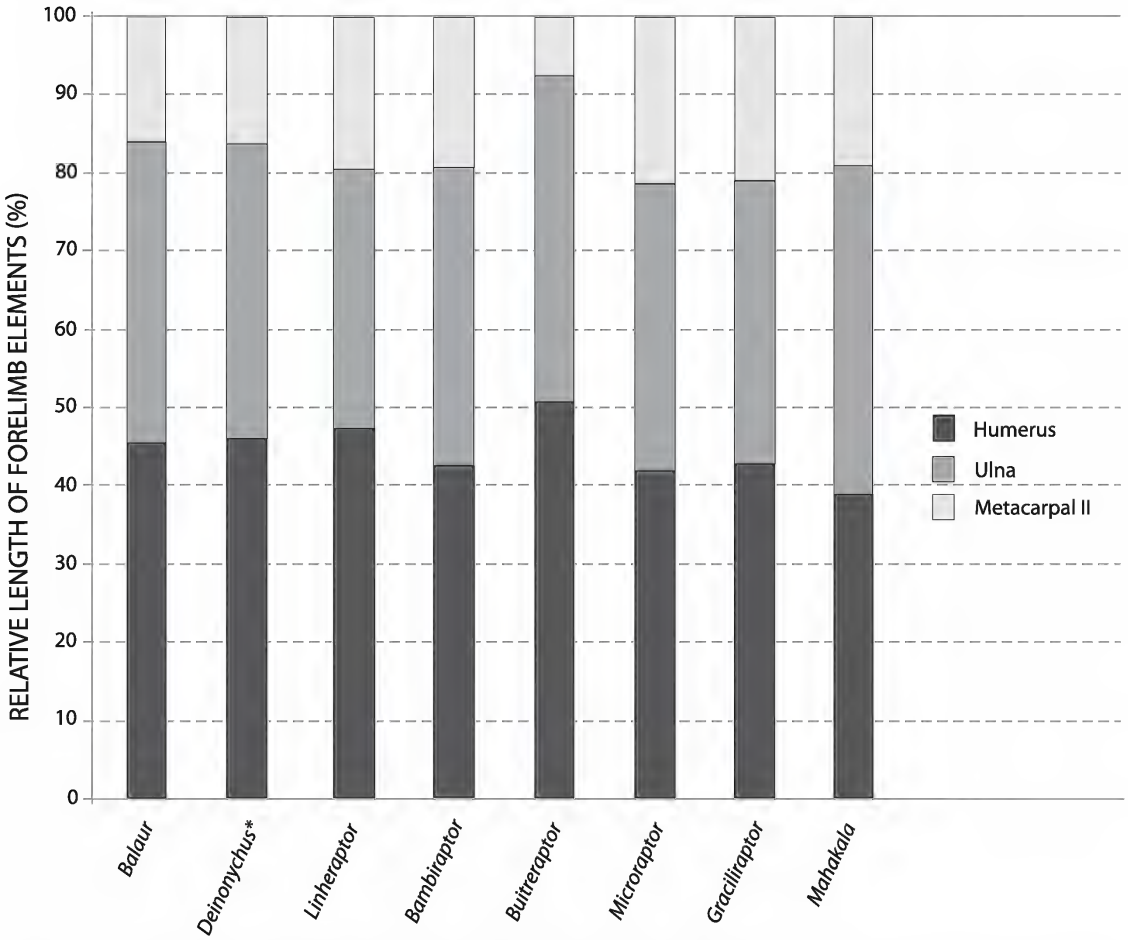

Fig. 43. Stacked plot of relative forelimb element lengths for various dromaeosaurid theropods (based on table 4). * = MCZ 4371.

most velociraptorines, but the spread of these values among the surveyed taxa does not show any clear trends. To the contrary, the unguals of these digits are all relatively longer in *Balaur* as compared to other dromaeosaurids, whether the unguals (measured as a straight line in dorsal view) are compared to their respective metatarsals, to the length of the metatarsus itself, or to the length of the tibia. Only *Linheraptor* shows a comparable relative development of the ungual and only on digit III.

The elongation of the ungual phalanges in *Balaur* appears to be associated with a similar elongation of the distal nonungual phalanges of these digits, both relative to the length of their respective metatarsals and within-digit phalangeal ratios. In digit II, the last nonungual phalanx (II-2) is substantially longer (1.7×) than the first phalanx, while this ratio is close to 1 or even lower in most other dromaeosaurids. In digit III, the penultimate phalanx (III-3) is subequal in length to the first phalanx, and substantially longer (25%) than the second phalanx (III-2), while III-3 is smaller than both the second (except in *Bambiraptor*) and, especially, the first phalanx of the digit in all other dromaeosaurids. In digit 4, the final nonungual phalanx (IV-4) is slightly longer than the third phalanx (IV-3), unlike all other velociraptorines except *Bambiraptor*; in this respect *Balaur* is more similar to microraptorines and unenlagiines. That said, the degree of the relative elongation of the phalanges increases in *Balaur* toward the tip of the toe

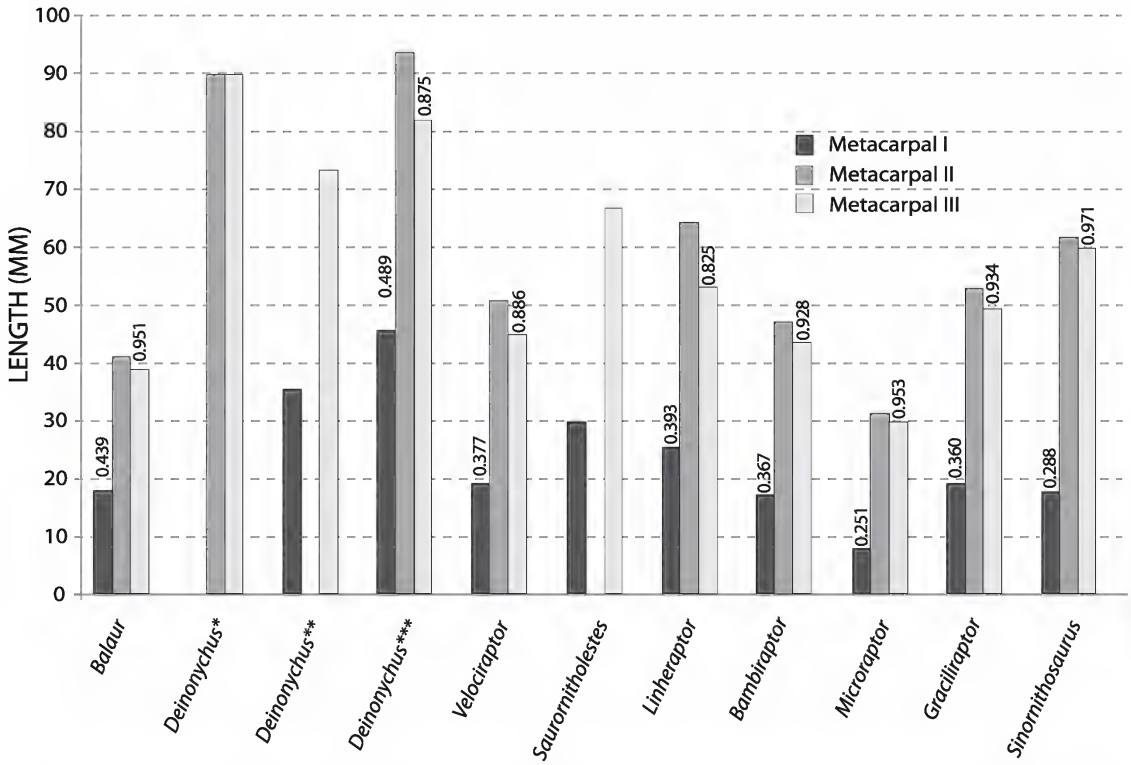

Fig. 44. Plot of absolute metacarpal lengths for various dromaeosaurid theropods (based on table 5). * = MCZ 4371, ** = AMNH FARB 3015, *** = YPM 5206. Numbers besides plot bars indicate the percent length of the respective element compared to the metacarpal II, for ease of relative length comparisons between the different taxa.

more markedly than in any other dromaeosaurid. Accordingly, the penultimate phalanx (IV-4) is almost the same length as the first phalanx (IV-1) of digit IV in *Balaur*, while there is a progressive decrease in absolute length in all other velociraptorines and a similar progressive decrease, but one that is reversed at the last nonungual, in the microraptorines and some unenlagiines. Due to these proportional trends, the distal segments of the hind limb in *Balaur* are relatively longer (compared, for example, to the metatarsus) than in any other dromaeosaurid.

One final outstanding feature of the hind limb of *Balaur* regards the association between high degrees of fusion in the metatarsus and its short, wide morphology. In other theropods, advanced fusion in the metatarsus appears in taxa with an arctometatarsalian pes (i.e., metatarsal III pinched between metatarsals II and IV) and a relatively elongated, gracile foot (see above, and Nesbitt et al., 2011, for examples). *Balaur*, therefore, is the first example of a theropod with a highly fused metatarsus that is short, robust, wider than the distal tibiotarsus, and non-arctometatarsalian.

Some unusual proportional features of the manus of *Balaur* also deserve comment. The most notable features include the relatively well-developed metacarpal I, the long and narrow metacarpal III, and the fusion of the proximal end of the bones into a fuctional carpometacarpus. The first metacarpal amounts to almost half of the length of metacarpal II, whereas this percentage is less than 40% in all other dromaeosaurids (except in *Deinonychus*: YPM 5206). In *Balaur*, the enlarged metacarpal I supports a similarly enlarged digit, in which both the first phalanx and the ungual are relatively longer than in other dromaeosaurids (the first phalanx is of similar proportions in some microraptorines: *Microraptor*, *Sinornithosaurus*). Manual digit

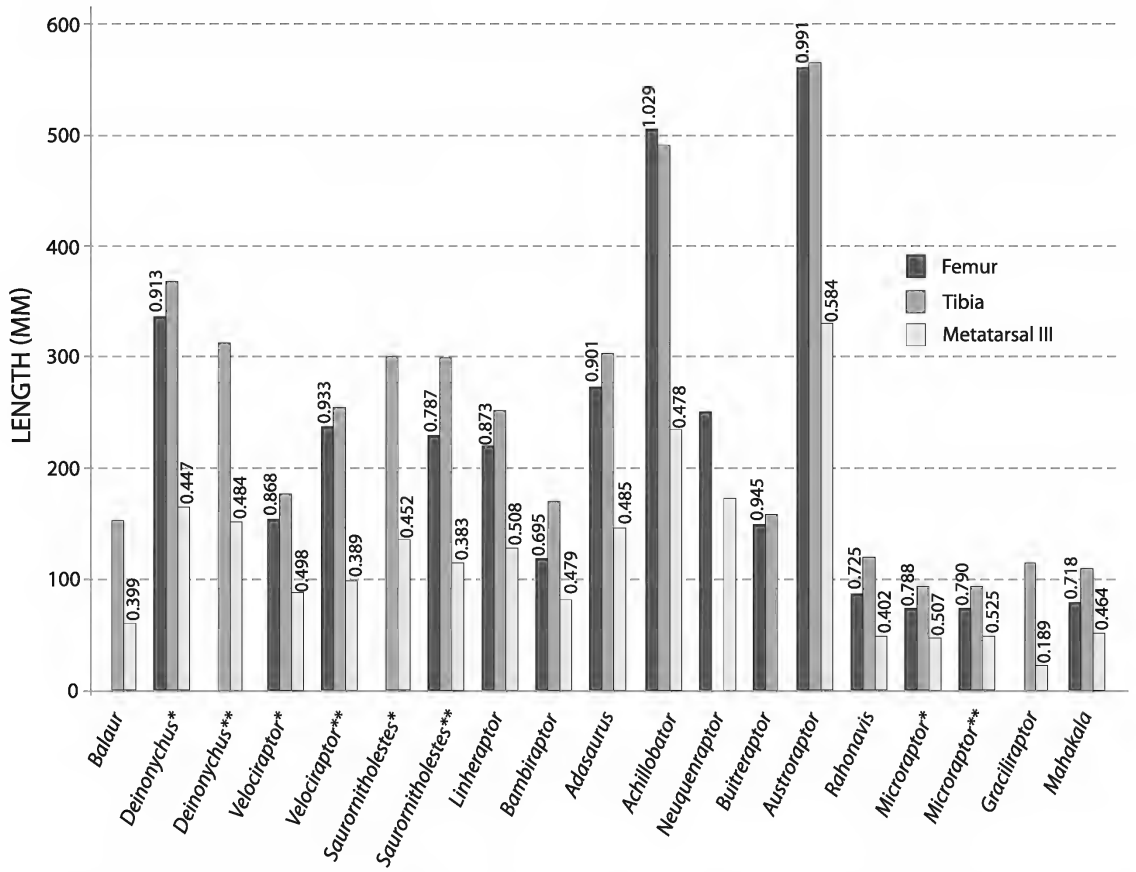

Fig. 45. Plot of absolute hind-limb element lengths for various dromaeosaurid theropods (based on table 6). For *Deinonychus*: * = MCZ 4371, ** = AMNH FARB 3015; for *Velociraptor*: * = IGM 100/982, ** = IGM 100/986; for *Saurornitholestes*: * = MOR 660, ** = TMP 88.121.39; for *Microraptor*: * = 20-7-004, ** = 20-8-001. Numbers besides plot bars indicate the percent length of the respective element compared to the tibia, for ease of relative length comparisons between the different taxa.

I of *Balaur* is relatively longer than in any other dromaeosaurid, with the nonungual phalanx almost as long as metacarpal I. Digit II is also more elongated relative to the metacarpus than in other dromaeosaurids, especially compared to the microraptorines.

In summary, besides its autapomorphic and highly fused hands and feet, *Balaur* is also remarkable in that, despite its relatively shortened main distal limb segments (metacarpus, metatarsus), the distalmost elements (distal phalanges, including unguals) are elongated. These unusual proportions comprise part of the highly aberrant Bauplan of *Balaur*, which we discuss in detail below and hypothesize is due to the "island effect."

Balaur: An Island-Dwelling Theropod

Regardless of whether they become stranded on an island for a long period of time, or arrive as later immigrants, island-dwelling taxa often possess important skeletal and behavioral modifications well suited to their unusual habitat (the so-called island effect). This phenomenon has been widely noted in many modern and recently extinct island-dwelling taxa (e.g., Sondaar, 1977; Azzaroli, 1982; Palombo, 2008). These modifications might include some or all of the following: size changes (either dwarfing or gigantism: e.g., Foster, 1964; Case, 1978; Lomolino, 1985), morphological changes to the overall

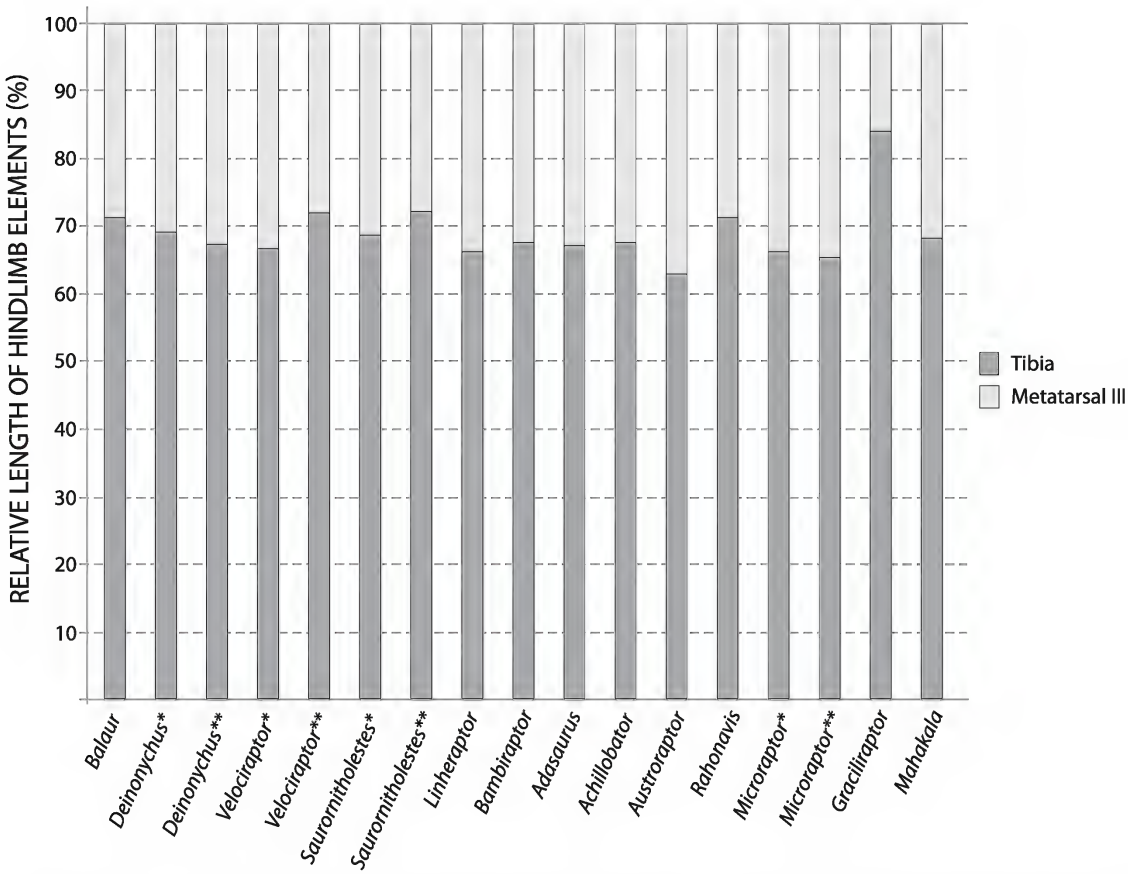

Fig. 46. Stacked plot of relative lower hind-limb element lengths for various dromaeosaurid theropods (based on table 6). For *Deinonychus*: * = MCZ 4371, ** = AMNH FARB 3015; for *Velociraptor*: * = IGM 100/982, ** = IGM 100/986; for *Saurornitholestes*: * = MOR 660, ** = TMP 88.121.39; for *Microraptor*: * = 20-7-004, ** = 20-8-001.

body plan, locomotory and feeding apparatus, or body parts used in intraspecific signalling (e.g., Köhler and Moyà-Solà, 2001; Van der Geer et al., 2006a), neurological changes (e.g., Köhler and Moyà-Solà, 2004; Weston and Lister, 2009), shifts in behavior or ecology (e.g., Van der Geer, 2008; Van der Geer et al., 2006b), or even shifts in life history traits and metabolism (e.g., McNabb, 2002; Raia et al., 2003; Palkovacs, 2003; Köhler and Moyà-Solà, 2009).

These modifications are well documented in mammals, both extant (e.g., Case, 1978; Lomolino, 1985) and extinct (see Van der Geer et al., 2010, for a recent review), but have yet to be widely recognized in other island-dwelling fossil vertebrates, including dinosaurs. Although inferred previously based on size-related and phylogenetic arguments in the case of several Late Cretaceous Romanian dinosaurs (e.g., Nopcsa, 1923; Weishampel et al., 1993, 2003; Weishampel and Jianu, 2011), the first well-supported report of insular habit-related modifications in dinosaurs was presented by Sander et al. (2006), who noted the occurence of dwarfing and related life history shifts in the Late Jurassic basal macronarian sauropod *Europasaurus*, which lived on islands that comprised some of the land of present-day Germany. More recently, similar island-related life-history modifications were described in the titanosaur *Magyarosaurus* from the Late Cretaceous of the Haţeg Basin (Romania), a contemporary and sympatric

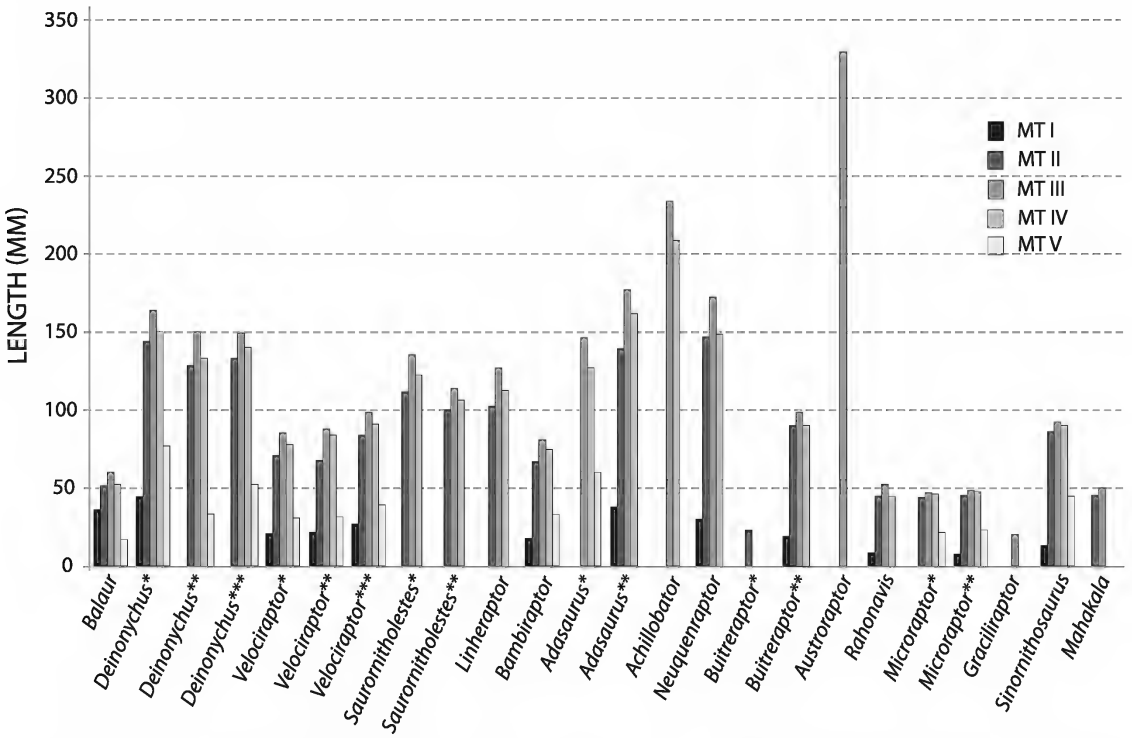

Fig. 47. Plot of absolute metatarsal lengths for various dromaeosaurid theropods (based on table 7). For *Deinonychus*: * = MCZ 4371, ** = AMNH FARB 3015, *** = YPM 5206; for *Velociraptor*: * = IGM 100/985, ** = IGM 100/982, *** = IGM 100/986; for *Saurornitholestes*: * = MOR 660, ** = TMP 88.121.39; for *Adasaurus*: * = IGM 100/20, ** = IGM 100/21; for *Buitreraptor*: * = MPCA 245, ** = MPCA 238; for *Microraptor*: * = 20-7-004, ** = 20-8-001.

taxon of *Balaur* (Stein et al., 2010; see also Jianu and Weishampel, 1999). From within the same Late Cretaceous Haţeg assemblage, island dwarfing was also suggested to be present in the basal euornithopod *Zalmoxes* and the non-hadrosaurid hadrosauroid *Telmatosaurus* (Weishampel et al., 1993, 2003; Benton et al., 2010; Weishampel and Jianu, 2011; but see Osi et al. 2012). Other than this handful of cases, the presence of insular habitat-related modifications in dinosaurs and other Mesozoic vertebrates remains poorly documented, especially among carnivores. In fact, prior to the discovery of *Balaur*, island-related modifications were unknown for any nonavian theropod dinosaurs.

The strikingly autapomorphic body plan of *Balaur* (figs. 48–49) shows a marked departure from the common dromaeosaurid Bauplan, and as pointed out in the original description of the taxon (Csiki et al., 2010a), it is most likely another result of the island effect that is present in the Haţeg assemblage. The aberrant nature of *Balaur* is even more noteworthy because it represents the first instance of distinct island-related morphological change (other than dwarfism) that can be identified in a dinosaur, and indeed, in any other island-dwelling predatory vertebrate taxon.

It has long been debated whether the island effect influences predators as well as herbivores. Changes in body size are considered to be the most pervasive reaction to an island environment (Foster, 1964; Van Valen, 1973), but Case (1978) documented no unique trend of body size changes in island-dwelling predators. Some predators, such as foxes, raccoons, and snakes, were reported to develop smaller sizes on islands, whereas others, such as bears and some mustelids, apparently increased in size. Moreover, Meiri et al. (2004) found no general size differences between island-dwelling carnivorous

Fig. 48. Life reconstruction of *Balaur bondoc* preying on a dwarf hadrosauroid dinosaur in the Late Cretaceous Haţeg Island ecosystem of present-day Romania. Illustration by Mihai Dumbrava.

mammals and their mainland relatives, whereas in a later study, Meiri (2007) showed that carnivorous lizards exhibit different size trends on islands, with small species becoming smaller than mainland relatives but larger species growing relatively larger. Subsequently, using a phylogenetically controlled dataset, Meiri et al. (2008) demonstrated the tendency of certain recent mammalian island carnivores (especially viverrids and herpestids) to undergo size reduction compared to their mainland relatives, and similar trends have been noted for some, but not all, Pio-Pleistocene insular canids and hyaenids (Lyras et al., 2010; see also: Gompper et al., 2006; Van der Geer et al., 2010). Recently, it has even been suggested that while insular dwarfing might be widespread in large-bodied mammal clades, it is largely absent in lizards or birds (Meiri et al., 2011), which are more closely related to nonavian dinosaurs than are mammals (and, therefore, perhaps more applicable comparisons).

In summary, therefore, there is some evidence that vertebrate predators might be expected to respond to an insular habitat through body-size reduction, but trends in body-size evolution among living island-dwelling carnivores are complex, and there is little evidence that living sauropsid carnivores (except for snakes; e.g., Boback, 2003; Keogh et al., 2005; Meik et al., 2010) exhibit island dwarfism. Furthermore, even among mammals, it has been suggested that carnivore body-size evolution on islands is dependent mainly on prey abundance and size, and therefore is not necessarily controlled by an overarching "rule" of size increase or decrease (Raia and Meiri, 2006).

With this information from living taxa in mind, what may *Balaur* indicate about body-size changes in insular carnivorous dinosaurs? Csiki et al. (2010a) argued that *Balaur* does not provide evidence for any clear body-size changes, especially dwarfism, among island-dwelling theropods, because it is of the same general size as closely related dromaeosaurids such as *Velociraptor*. This argument was based on both the holotype and referred specimens of *Balaur*, which at the time were considered to belong to a single species. We do note here, however, that the

Fig. 49. Life reconstruction of a group of *Balaur* bondoc individuals attacking a dwarf hadrosauroid dinosaur in the Late Cretaceous Haţeg Island ecosystem of present-day Romania. Illustration by Demetrios Vital.

holotype and referred specimens are both skeletally mature individuals but drastically differ in body size (see above). The holotype specimen is somewhat smaller in size than closely related and contemporaneous (or near contemporaneous) dromaeosaurids; it is between 66% and 75% of the size of these other taxa, based on the length of the humerus (table 4). However, it is not clear whether humerus length is a meaningful proxy for overall body size. Femur length and circumference, which are known to be tightly correlated to body size in theropod dinosaurs (Christiansen and Fariña, 2004), cannot currently be measured in either of the *Balaur* specimens because the femora are missing. Therefore, the question of whether *Balaur* (and perhaps other theropod dinosaurs) exhibited some type of island dwarfism remains open, although we note that if dwarfism in *Balaur* was present then it was of a smaller magnitude than in contemporaneous herbivorous dinosaurs (Benton et al., 2010; Weishampel and Jianu, 2011).

Whether or not it is an island dwarf, *Balaur* exhibits numerous morphological modifications that are probably related to its island environment. Such modifications, other than body-size changes, are seldom noted in extant and recently extinct island-dwelling carnivores, most of which are anatomically similar (perhaps slightly larger or smaller) to their mainland ancestors or sister taxa (e.g., Gompper et al., 2006; Theodorou et al., 2007). Minor changes in morphology have been noted in fossil insular otters (Van der Geer et al., 2010), but such changes are not unlike those known in certain mainland taxa and suggest only slight shifts in ecological traits such as feeding preferences. Therefore, nothing as extreme as the aberrant morphology of *Balaur* has been reported to occur in insular carnivores of any kind (mammals, squamates, birds), neither recent nor fossil.

Unexpectedly, however, morphological changes comparable to those found in the hind limb of *Balaur* (shortening and increased

robustness, as well as occasional fusion, of distal-limb elements) are widely documented in fossil insular herbivores (see Sondaar, 1994; Caloi and Palombo, 1994, 1995; Van der Geer et al., 2010), including cervoids (e.g., Matsumoto and Otsuka, 2000; Van der Geer et al., 2005, 2006; Van der Geer, 2008), suids (e.g., Van der Geer et al., 2010), and bovids (e.g., Köhler and Moyà-Solà, 2001; Croft et al., 2006). Comparable adaptations of the limbs, although different in detail, were reported recently in the gigantic insular rabbit *Nurolagus* (Quintana et al., 2011). Most of these taxa, however, are obligate quadrupeds, and therefore under different locomotory constraints than *Balaur*. With that in mind, it may be noteworthy that somewhat similar modifications, including shortening of the lower limb segment and the relatively long feet, are also known in the small island-dwelling human *Homo floresiensis* (Jungers et al., 2009; see also Meijer et al., 2010; van Heteren, 2012), which was probably an insular obligate biped (e.g., Brown et al., 2004; Blaszczyk and Vaughan, 2007).

Such skeletal modifications are usually interpreted as adaptations to locomotion over rugged, uneven terrain, often described as "low-gear locomotion" (Leinders and Sondaar, 1974), and considered as potentially advantageous while moving in environmental conditions where the need for stability and energy-saving supersedes the need for speed. In all of the above reported cases of island herbivores, development of a low-gear locomotion style is thought to have been linked to their restrictive insular habitat, characterized by a lack of predators to avoid (by fast locomotion), as well as a (relative) shortage of food resources that favored energy-saving locomotory adaptations. Moreover, shortening, increased robustness, and stabilization of the lower limb through fusion of the bones is thought to be instrumental in achieving stability during locomotion across rocky, uneven terrain, which is often widespread in insular environments. Stability during locomotion was also enhanced by lowering the center of gravity by means of the shortened and more robust limbs, as well as of a relatively wide pelvis, as described in *Homo floresiensis* (see Van Heteren, 2012). It appears, therefore, that *Balaur* exhibits a widespread morphological complex characteristic of insular taxa, but to our knowledge so far reported to occur only in herbivorous or omnivorous mammals. If insular mammals are a relevant comparison, the hind-limb modifications of *Balaur* may have been driven by the functional need for stability during locomotion, and not other factors such as release from predatory pressure. Empirical biomechanical studies are needed, however, to test whether *Balaur* did move in a substantially different fashion than close relatives such as *Velociraptor*.

It should be pointed out that the unique, fused, and reduced hand morphology of *Balaur* is unparalleled in known island-dwelling species, and thus it is unclear whether the development of this second autapomorphic character complex is related somehow to the insular nature of the Romanian dromaeosaurid, to the modifications seen in the hind limb, or to another functional or ecological demand (e.g., diet, flight or flightlessness, feather function and distribution). The entire skeleton of *Balaur* is remarkably divergent from other dromaeosaurids, as attested to by the presence of nearly 20 autapomorphies. We hope that future discoveries, especially of other island-dwelling predatory dinosaurs and close relatives of *Balaur*, will help further reveal which features of *Balaur* may relate to its island environment and help better understand the peculiar anatomy (and perhaps biology) of insular theropods.

ACKNOWLEDGMENTS

We are especially grateful to Akiko Shinya for her skillful on site preparation of the specimen and Mick Ellison for his meticulous work photographing the material (all photos by M. Ellison, except for: photos in figures 2, 3, 8, 29, 35, and 38 by M. Vremir and photos in figure 13 by Z. Csiki-Sava). Corwin Sullivan, Nick Longrich, and Federico Gianechini are thanked for sharing information, photographs, and data on *Graciliraptor*, *Linheraptor* and *Sinornithosaurus* (C.S.), *Deinonychus* (N.L.), and *Buitreraptor* and *Neuquenraptor* (F.G.), respectively. David Weishampel and an anonymous reviewer are thanked for helpful comments on the

ms. This project is supported by a National Science Foundation Graduate Research Fellowship and National Science Foundation Doctoral Dissertation Improvement Grant (DEB 1110357) to S.L.B., a National Science Foundation Assembling the Tree of Life Grant (0228693) to M.A.N., and a National Scientific Research Council grant (CNCSIS 1930/2009 IDEI-PCE) to Z.C.-S. The Research Foundation of Stony Brook University provided support for AHT. The histological analysis was funded by NSF grant EAR 0959029 presented to G.M.E. and M.A.N. and an NSF Graduate Research Fellowship presented to A.W. Further support was provided by the American Museum of Natural History Division of Paleontology and Columbia University Department of Earth and Environmental Sciences.

REFERENCES

Alexander, D.E., E. Gong, L.D. Martin, D.A. Burnham, and A.R. Falk. 2010. Model tests of gliding with different hindwing configurations in the four-winged dromaeosaurid *Microraptor gui*. Proceedings of the National Academy of Sciences of the United States of America 107 (7): 2972–2976.

Allain, R., and P. Taquet. 2000. A new genus of Dromaeosauridae (Dinosauria: Theropoda) from the Upper Cretaceous of France. Journal of Vertebrate Paleontology 20: 404–407.

Andrews, C.W. 1913. On some bird remains from the Upper Cretaceous of Transylvania. Geological Magazine 10: 193–196.

Azzarolli, A. 1982. Insularity and its effects on terrestrial vertebrates: evolutionary and biogeographic aspects. *In* E.M. Gallitelli (editor), Palaeontology, essential of historical geology, 193–213. Modena: S.T.E.M. Mucchi.

Barsbold, R., and A. Perle. 1980. Segnosauria, a new infraorder of carnivorous dinosaurs. Acta Palaeontol. Polonica 25: 185–195.

Benson, R.B.J., R.J. Butler, M.T. Carrano, and P.M. O'Connor. 2012. Air-filled postcranial bones in theropod dinosaurs: physiological implications and the 'reptile'-bird transition. Biological Reviews 87: 168–193.

Benton, M.J., et al. 2010. Dinosaurs and the island rule: the dwarfed dinosaurs from Haţeg Island. Palaeogeography, Palaeoclimatology, Palaeoecology 293: 438–454.

Blaszczyk, M.B., and C.L. Vaughan. 2007. Reinterpreting the evidence for bipedality in *Homo floresiensis*. South African Journal of Science 103: 409–414.

Boback, S.M. 2003. Body size evolution in snakes: evidence from island populations. Copeia 2003: 81–94.

Bojar, A.-V., D. Grigorescu, F. Ottner, and Z. Csiki. 2005. Palaeoenvironmental interpretation of dinosaur- and mammal-bearing continental Maastrichtian deposits, Haţeg basin, Romania. Geological Quarterly 49: 205–222.

Bojar, A.-V., S. Halas, H.-P. Bojar, D. Grigorescu, and Ş. Vasile. 2011. Upper Cretaceous volcanoclastic deposits from the Haţeg Basin, South Carpathians (Romania): K-Ar ages and intrabasinal correlation. Geochronometria 3: 182–188.

Brochu, C.A. 2003. Osteology of *Tyrannosaurus rex*: insights from a nearly complete skeleton and high-resolution computed tomographic analysis of the skull. Society of Vertebrate Paleontology Memoir 7: 1–138.

Brougham, J., and S.L. Brusatte. 2010. Distorted *Microraptor* specimen is not ideal for understanding the origin of avian flight. Proceedings of the National Academy of Sciences 107 (40): E155 pp.

Brown, P., et al. 2004. A new small-bodied hominin from the Late Pleistocene of Flores, Indonesia. Nature 431: 1055–1061.

Brusatte, S.L., R.B.J. Benson, and S. Hutt. 2008. The osteology of *Neovenator salerii* (Dinosauria: Theropoda) from the Wealden Group (Barremian) of the Isle of Wight. Monograph of the Palaeontographical Society 162 (631): 1–166.

Brusatte, S.L., M.J. Benton, J.B. Desojo, and M.C. Langer. 2010. The higher-level phylogeny of Archosauria (Tetrapoda: Diapsida). Journal of Systematic Palaeontology 8: 3–47.

Buffetaut, E., B. Marandat, and B. Sigé. 1986. Découverte de dents de deinonychosaures (Saurischia, Theropoda) dans le Crétacé supérieur du sud de la France. Comptes Rendus de l'Académie des Sciences (Série 3) Sciences de la Vie 303: 1393–1396.

Bunce, M., et al. 2003. Extreme reversed sexual size dimorphism in the extinct New Zealand moa *Dinornis*. Nature 425: 172–175.

Burnham, D.A. 2004. New information on *Bambiraptor feinbergi* (Theropoda: Dromaeosauridae) from the Late Cretaceous of Montana. *In* P.J. Currie, E.B. Koppelhus, M.A. Shugar, and J.L. Wright (editors), Feathered dragons: studies on the transition from dinosaurs to birds, 67–111. Bloomington: Indiana University Press.

Burnham, D.A., et al. 2000. Remarkable new birdlike dinosaur (Theropoda: Maniraptora) from the Upper Cretaceous of Montana.

University of Kansas Paleontological Contributions 13: 1–14.

Caloi, L., and R.M. Palombo. 1994. Functional aspects and ecological implications in Pleistocene endemic herbivores of Mediterranean islands. Historical Biology 8: 151–172.

Caloi, L., and R.M. Palombo. 1995. Functional aspects and ecological implications in Pleistocene endemic cervids of Sardinia, Sicily and Crete. Géobios 28: 247–258.

Calvo, J.O., J.D. Porfiri, and A.W. Kellner. 2004. On a new maniraptoran dinosaur (Theropoda) from the Upper Cretaceous of Neuquen, Patagonia, Argentina. Revista Museo Argentino de Ciencias Naturales 62: 549–566.

Carpenter, K., C. Miles, and K. Cloward. 2005. New small theropod from the Upper Jurassic Morrison Formation of Wyoming. *In* K. Carpenter (editor), The carnivorous dinosaurs, 23–48. Bloomington: Indiana University Press.

Case, T.J. 1978. A general explanation for insular body size trends in terrestrial vertebrates. Ecology 59: 1–18.

Chanthasit, P., and E. Buffetaut. 2009. New data on the Dromaeosauridae (Dinosauria: Theropoda) from the Late Cretaceous of southern France. Bulletin de la Société Géologique de France 180: 145–154.

Choiniere, J.N., et al. 2010. A basal alvarezsauroid theropod from the Early Late Jurassic of Xinjiang, China. Science 327: 571–573.

Christiansen, P., and R.A. Fariña. 2004. Mass prediction in theropod dinosaurs. Historical Biology 16: 85–92.

Clarke, J.A., and M.A. Norell. 2002. The morphology and phylogenetic position of *Apsaravis ukhanna* from the Late Cretaceous of Mongolia. American Museum Novitates 3387: 1–46.

Clarke, J.A., Z. Zhou, and F. Zhang. 2006. Insight into the evolution of avian flight from a new clade of Early Cretaceous ornithurines from China and the morphology of *Yixianornis grabaui*. Journal of Anatomy 208: 287–308.

Coddington, J., and N. Scharff. 1994. Problems with zero-length branches. Cladistics 10: 415–423.

Codrea, V., et al. 2002. Dinosaur egg nests, mammals and other vertebrates from a new Maastrichtian site of the Haţeg Basin (Romania). Comptes Rendus Palevol 1: 173–180.

Codrea, V., et al. 2010. More than just Nopcsa's Transylvanian dinosaurs: a look outside the Haţeg Basin. Palaeogeography, Palaeoclimatology, Palaeoecology 293: 391–405.

Colbert, E.H. 1989. The Triassic dinosaur *Coelophysis*. Bulletin, Museum of Northern Arizona 57: 1–160.

Colbert, E.H., and D.A. Russell. 1969. The small Cretaceous dinosaur *Dromaeosaurus*. American Museum Novitates 2380: 1–49.

Croft, D.A., L.R. Heaney, J.J. Flynn, and A.P. Bautista. 2006. Fossil remains of a new, diminutive *Bubalus* (Artiodactyla: Bovidae: Bovini) from Cebu Island, Philippines. Journal of Mammalogy 87: 1037–1051.

Csiki, Z., and D. Grigorescu. 1998. Small theropods of the Late Cretaceous of the Haţeg Basin (western Romania) – an unexpected diversity at the top of the food chain. Oryctos 1: 87–104.

Csiki, Z., M. Vremir, S.L. Brusatte, and M.A. Norell. 2010a. An aberrant island-dwelling theropod dinosaur from the Late Cretaceous of Romania. Proceedings of the National Academy of Sciences of the United States of America 107 (35): 15357–15361.

Csiki, Z., D. Grigorescu, V. Codrea, and F. Therrien. 2010b. Taphonomic modes in the Maastrichtian continental deposits of the Haţeg Basin, Romania—palaeoecological and palaeobiological inferences. Palaeogeography, Palaeoclimatology, Palaeoecology 293: 375–390.

Csontos, L., and A. Vörös. 2004. Mesozoic plate tectonic reconstruction of the Carpathian region. Palaeogeography, Palaeoclimatology, Palaeoecology 210: 1–56.

Currie, P.J. 2003. Allometric growth in tyrannosaurids (Dinosauria: Theropoda) from the Upper Cretaceous of North America and Asia. Canadian Journal of Earth Sciences 40: 651–665.

Currie, P.J., and P. Chen. 2001. Anatomy of *Sinosauropteryx prima* from Liaoning, northeastern China. Canadian Journal of Earth Sciences 38: 1705–1727.

Currie, P.J., and Z.-M. Dong. 2001. New information on Cretaceous troodontids (Dinosauria, Theropoda) from the People's Republic of China. Canadian Journal of Earth Sciences 38: 1753–1766.

Currie, P.J., and X.J. Zhao. 1993. A new carnosaur (Dinosauria, Theropoda) from the Jurassic of Xinjiang, People's Republic of China. Canadian Journal of Earth Sciences 30: 2037–2081.

Dalla Vecchia, F.M. 2009. *Tethyshadros insularis*, a new hadrosauroid dinosaur (Ornithischia) from the Upper Cretaceous of Italy. Journal of Vertebrate Paleontology 29: 1100–1116.

Forster, C.A., S.D. Sampson, L.M. Chiappe, and D.W. Krause. 1998. The theropod ancestry of birds: new evidence from the Late Cretaceous of Madagascar. Science 279: 1915–1919.

Foster, J.B. 1964. Evolution of mammals on islands. Nature 202: 234–235.

Fowler, D.W., H.N. Woodward, E.A. Freedman, P.L. Larson, and J.R. Horner. 2011. Reanalysis

of "*Raptorex kriegsteini*": a juvenile tyrannosaurid dinosaur from Mongolia. PLoS ONE 6 (6): e21376 pp.

Francillon-Vielliot, H., et al. 1990. Microstructure and mineralization of vertebrate skeletal tissues. *In* J.G. Carter (editor), skeletal biomineralization: patterns, processes and evolutionary trends, 471–530. New York: Van Nostrand Reinhold.

Gauthier, J. 1986. Saurischian monophyly and the origin of birds. Memoirs of the California Academy of Sciences 8: 1–55.

Gauthier, J., and K. Padian. 1985. Phylogenetic, functional, and aerodynamic analyses of the origin of birds and their flight. *In* M.K. Hecht, J.H. Ostrom, G. Viohl, and P. Wellnhofer (editors), The beginnings of birds, 185–197. Eichstatt: Freunde des Jura-Museums.

Goloboff, P.A., J.S. Farris, and K.C. Nixon. 2008a. TNT: tree analysis using new technology, vers. 1.1 (Willi Hennig Society edition). Program and documentation available online (http://www.zmuc.dk/public/phylogeny/tnt).

Goloboff, P.A., J.S. Farris, and K.C. Nixon. 2008b. TNT, a free program for phylogenetic analysis. Cladistics 24: 774–786.

Gompper, M.E., A.E. Petrites, and R.L. Lyman. 2006. Cozumel Island fox (*Urocyon* sp.) dwarfism and possible divergence history based on subfossil bones. Journal of Zoology 270: 72–77.

Grigorescu, D. 1984. New tetrapod groups in the Maastrichtian of the Haţeg Basin: coelurosaurians and multituberculates. *In* W.E. Reif and F. Westphal (editors), Short papers, third symposium on Mesozoic terrestrial ecosystems, 99–104. Tübingen: Attempo Verlag.

Grigorescu, D., and E. Kessler. 1981. A new specimen of *Elopteryx nopcsai* from the dinosaurian beds of Haţeg Basin. Révue Roumaine de Géologie Géophysique Géographie, Série de Géologie 24: 171–175.

Grigorescu, D., J.-L. Hartenberger, C. Rădulescu, P. Samson, and J. Sudre. 1985. Découverte de mammifères et dinosaures dans le Crétacé supérieur de Pui (Roumanie). Comptes Rendus de l'Académie des Sciences Paris (Série 2) Mécanique, Physique, Chimie, Sciences de l'univers, Sciences de la Terre 301 (19): 1365–1368.

Grigorescu, D., et al. 1994. Late Maastrichtian dinosaur eggs from the Haţeg Basin (Romania). *In* K. Carpenter, K.F. Hirsch, and J.R. Horner (editors), Dinosaur eggs and babies, 75–87. Cambridge: Cambridge University Press.

Grigorescu, D., G. Garcia, Z. Csiki, V. Codrea, and A.-V. Bojar. 2010. Uppermost Cretaceous megaloolithid eggs from the Haţeg Basin, Romania, associated with hadrosaur hatchlings: search for explanation. Palaeogeography, Palaeoclimatology, Palaeoecology 293: 360–374.

Harrison, C.J.O., and C.A. Walker. 1975. The Bradycnemidae, a new family of owls from the Upper Cretaceous of Romania. Palaeontology 18: 563–570.

Huene, F. von. 1914. Das natürliche System der Saurischia. Zentralblat fur Mineralogie, Geologie, Palaeontologie B 1914: 154–158.

Hutchinson, J.R. 2001. The evolution of pelvic osteology and soft tissue on the line to extant birds (Neornithes). Zoological Journal of Linnean Society 131: 123–168.

Hwang, S.H., M.A. Norell, Q. Ji, and K.-Q. Gao. 2002. New specimens of *Microraptor zhaoianus* (Theropoda: Dromaeosauridae) from northeastern China. American Museum Novitates 3381: 1–44.

Jianu, C.M., and D.B. Weishampel. 1999. The smallest of the largest: a new look at possible dwarfing in sauropod dinosaurs. Geologie en Mijnbouw 78: 335–343.

Jungers, W.L., et al. 2009. The foot of *Homo floresiensis*. Nature 459: 81–84.

Keogh, J.S., I.A.W. Scott, and C. Hayes. 2005. Rapid and repeated origin of insular gigantism and dwarfism in Australian tiger snakes. Evolution 59: 226–233.

Kessler, J., D. Grigorescu, and Z. Csiki. 2005. *Elopteryx* revisited—a new bird-like specimen from the Maastrichtian of the Haţeg Basin (Romania). Acta Palaeontologica Romaniae 5: 249–258.

Köhler, M., and S. Moyà-Solà. 2001. Phalangeal adaptations in the insular fossil goat *Myotragus*. Journal of Vertebrate Paleontology 21: 621–624.

Köhler, M., and S. Moyà-Solà. 2004. Reduction of brain size and sense organs in the fossil insular bovid *Myotragus*. Brain, Behavior and Evolution 63: 125–140.

Köhler, M., and S. Moyà-Solà. 2009. Physiological and life history strategies of a fossil large mammal in a resource-limited environment. Proceedings of the National Academy of Sciences of the United States of America 106: 20354–20358.

Lambrecht, K. 1929. Mesozoische und tertiare Vogelreste aus Siebenbürgen. *In* E. Csiki (editor), X^{e} Congrès International de Zoologie, 1262–1275. Budapest: Stephaneum.

Leinders, J.J.M., and P.Y. Sondaar. 1974. On functional fusions in footbones of ungulates. Zeitschrift für Säugetierkunde 39: 109–115.

Le Loeuff, J., and E. Buffetaut. 1998. A new dromaeosaurid theropod from the Upper Cretaceous of southern France. Oryctos 1: 105–112.

Le Loeuff, J., E. Buffetaut, P. Mechin, and A. Mechin-Salessy. 1992. The first record of

dromaeosaurid dinosaurs (Saurischia, Theropoda) in the Maastrichtian of southern Europe: palaeobiogeographical implications. Bulletin de la Société Géologique de France 163: 337–343.

Lomolino, M.V. 1985. Body size of mammals on islands: the island rule re-examined. American Naturalist 125: 310–316.

Lomolino, M.V. 2005. Body size evolution in insular vertebrates: generality of the island rule. Journal of Biogeography 32: 1683–1699.

Lomolino, M.V., D.F. Sax, B.R. Riddle, and J.H. Brown. 2006. The island rule and a research agenda for studying ecogeographical patterns. Journal of Biogeography 33: 1503–1510.

Longrich, N.R., and P.J. Currie. 2009. A microraptorine (Dinosauria-Dromaeosauridae) from the Late Cretaceous of North America. Proceedings of the National Academy of Science of the United States of America 106: 5002–5007.

Lyras, G.A., A.A.E. Van der Geer, and L. Rook. 2010. Body size of insular carnivores: evidence from the fossil record. Journal of Biogeography 37: 1007–1021.

McNab, B.K. 2002. Minimizing energy expenditure facilitates vertebrate persistence on oceanic islands. Ecology Letters 5: 693–704.

Madsen, J.H. 1976. *Allosaurus fragilis*: a revised osteology. Utah Geological Survey Bulletin 109: 1–163.

Madsen, J.H., and S.P. Welles. 2000. *Ceratosaurus* (Dinosauria, Theropoda) – a revised osteology. Utah Geological Survey, Miscellaneous Publication 00–2: 1–80.

Makovicky, P.J., Y. Kobayashi, and P.J. Currie. 2004. Ornithomimosauria. *In* D.B. Weishampel, P. Dodson, and H. Osmolska (editors), The Dinosauria (2nd ed.), 137–150. Berkeley: University of California Press.

Makovicky, P.J., S. Apesteguía, and F.L. Agnolín. 2005. The earliest dromaeosaurid theropod from South America. Nature 437: 1007–1011.

Manning, P.L., D. Payne, J. Pennicott, P.M. Barrett, and R.A. Ennos. 2006. Dinosaur killer claws or climbing crampons? Biology Letters 2: 110–112.

Marsh, O.C. 1881. Principal characters of American Jurassic dinosaurs. Part V. American Journal of Science (Series 3) 21: 417–423.

Martin, L. 1983. The origin and early radiation of birds. *In* A.H. Brush and G.A. Clark, Jr (editors), Perspectives in Ornithology, 291–338. Cambridge: Cambridge University Press.

Martin, J.E., M. Rabi, and Z. Csiki. 2010. Survival of *Theriosuchus* (Mesoeucrocodylia: Atoposauridae) in a Late Cretaceous archipelago: a new species from the Maastrichtian of Romania. Naturwissenschaften 97: 845–854.

Matsumoto, Y., and H. Otsuka. 2000. Morphotypes of fossil deer (*Cervus astylodon*) and its miniaturization process in the Ryukyu Islands. Tropics 10: 155–164.

Matthew, W.D., and B. Brown. 1922. The family Deinodontidae, with notice of a new genus from the Cretaceous of Alberta. Bulletin of the American Museum of Natural History 46 (6): 367–385.

Meijer, H.J.M., L.W. Van den Hoek Ostende, G.D. van den Bergh, and J. de Vos. 2010. The fellowship of the hobbit: the fauna surrounding *Homo floresiensis*. Journal of Biogeography 37: 995–1006.

Meik, J.M., A.M. Lawing, and A. Pires-daSilva. 2010. Body size evolution in insular speckled rattlesnakes (Viperidae: *Crotalus mitchellii*). PLoS ONE 5 (3): e9524 pp.

Meiri, S. 2007. Size evolution in island lizards. Global Ecology and Biogeography 16: 702–708.

Meiri, S., T. Dayan, and D. Simberloff. 2004. Body size of insular carnivores: little support for the Island Rule. American Naturalist 163: 469–479.

Meiri, S., N. Cooper, and A. Purvis. 2008. The island rule: made to be broken? Proceedings of the Royal Society of London Series B Biological Sciences 275: 141–148.

Meiri, S., P. Raia, and A.B. Phillimore. 2011. Slaying dragons: limited evidence for unusual body size evolution on islands. Journal of Biogeography 38: 89–100.

Naish, D., and G.J. Dyke. 2004. *Heptasteornis* was no ornithomimid, troodontid, dromaeosaurid or owl: the first alvarezsaurid (Dinosauria: Theropoda) from Europe. Neues Jahrbuch für Geologie und Paläontologie Monatshefte 2004: 385–401.

Nesbitt, S.J. 2011. The early evolution of archosaurs: relationships and the origin of major clades. Bulletin of the American Museum of Natural History 352: 1–292.

Nesbitt, S.J., J.A. Clarke, A.H. Turner, and M.A. Norell. 2011. A small alvarezsaurid from the eastern Gobi Desert offers insight into evolutionary patterns in the Alvarezsauroidea. Journal of Vertebrate Paleontology 31: 144–153.

Nopcsa, F. 1905. Zur Geologie der Gegend zwischen Gyulafehérvár, Déva, Ruszkabánya und der Rumänischen Landesgrenze. Mitteilungen aus dem Jahrbuche der Königlisch Ungarischen Geologische Reichsanstalt 14: 93–279.

Nopcsa, F. 1914. Über das Vorkommen der Dinosaurier in Siebenbürgen. Verhandlungen der Zoologische-botanischen Gesellschaft in Wien 54: 12–14.

Nopcsa, F. 1915. Die Dinosaurier der siebenbürgischen Landesteile Ungarns. Mitteilungen aus

dem Jahrbuche der Königlisch Ungarischen Geologische Reichsanstalt 24: 1–24.

Nopcsa, F. 1923. On the geological importance of the primitive reptilian fauna of the uppermost Cretaceous of Hungary; with a description of a new tortoise (*Kallokibotium*). Quarterly Journal of the Geological Society of London. 79: 100–116.

Norell, M.A., and P.J. Makovicky. 1997. Important features of the dromaeosaur skeleton: information from a new specimen. American Museum Novitates 3215: 1–28.

Norell, M.A., and P.J. Makovicky. 1999. Important features of the dromaeosaur skeleton II: information from newly collected specimens of *Velociraptor mongoliensis*. American Museum Novitates 3282: 1–45.

Norell, M.A., et al. 2006. A new dromaeosaurid theropod from Ukhaa Tolgod (Omnogov, Mongolia). American Museum Novitates 3545: 1–51.

Novas, F.E. 1996. Dinosaur monophyly. Journal of Vertebrate Paleontology 16: 723–741.

Novas, F.E., and D. Pol. 2005. New evidence on deinonychosaurian dinosaurs from the Late Cretaceous of Patagonia. Nature 433: 858–861.

Novas, F.E., and P.F. Puerta. 1997. New evidence concerning avian origins from the Late Cretaceous of Patagonia. Nature 387: 390–392.

Novas, F.E., D. Pol, J.I. Canale, J.D. Porfiri, and J.O. Calvo. 2009. A bizarre Cretaceous theropod dinosaur from Patagonia and the evolution of Gondwanan dromaeosaurids. Proceedings of the Royal Society of London Series B Biological Sciences 276: 1101–1107.

Ősi, A. 2004. The first dinosaur remains from the Upper Cretaceous of Hungary (Csehbánya Formation, Bakony Mts). Géobios 37: 749–753.

Ősi, A. 2008. Enantiornithine bird remains from the Late Cretaceous of Hungary. Oryctos 7: 55–60.

Ősi, A., and I. Főzy. 2007. A maniraptoran (Theropoda, Dinosauria) sacrum from the Upper Cretaceous of the Haţeg Basin (Romania)—in search of the lost pterosaurs of Baron Franz Nopcsa. Neues Jahrbuch für Geologie und Paleontologie Abhandlungen 246: 173–181.

Ősi, A., and M. Rabi. 2006. The Late Cretaceous continental vertebrate fauna from the Bakony Mountains II: crocodiles, dinosaurs (Theropoda, Aves, Ornithischia), pterosaurs. Földtani Közlöny 136: 503–526.

Ősi, A., S.M. Apesteguía, and M. Kowalewski. 2010a. Non-avian theropod dinosaurs from the early Late Cretaceous of Central Europe. Cretaceous Research 31: 304–320.

Ősi, A., R.J. Butler, and D.B. Weishampel. 2010b. A Late Cretaceous ceratopsian dinosaur from Europe with Asian affinities. Nature 465: 466–468.

Ősi, A., E. Prondvai, R. Butler, and D.B. Weishampel. 2012. Phylogeny, histology and inferred body size evolution in a new rhabdodontid dinosaur from the Late Cretaceous of Hungary. PLoS ONE 7 (9): e44318. [doi:10.1371/journal.pone.0044318]

Osmólska, H. 1981. Coossified tarsometatarsi in theropod dinosaurs and their bearing on the problem of bird origins. Palaeontologia Polonica 42: 79–95.

Ostrom, J.H. 1969. Osteology of *Deinonychus antirrhopus*, an unusual theropod from the Lower Cretaceous of Montana. Bulletin of the Peabody Museum of Natural History 30: 1–165.

Ostrom, J.H. 1976. On a new specimen of the Lower Cretaceous theropod dinosaur *Deinonychus antirrhopus*. Breviora 439: 1–21.

Palkovacs, E.P. 2003. Explaining adaptive shifts in body size on islands: a life history approach. Oikos 103: 37–44.

Palombo, M.R. 2008. Insularity and its effects. Quaternary International 182: 1–5.

Pereda-Suberbiola, X., et al. 2009. The last hadrosaurid dinosaurs of Europe: a new lambeosaurine from the uppermost Cretaceous of Aren (Huesca, Spain). Comptes Rendus Palevol 8: 559–572.

Perle, A. 1979. Segnosauridae—a new family of theropods from the Late Cretaceous of Mongolia. Transactions, Joint Soviet-Mongolian Palaeontological Expedition 15: 28–39.

Perle, A., L.M. Chiappe, R. Barsbold, J.M. Clark, and M.A. Norell. 1994. Skeletal morphology of *Mononykus olecranus* (Theropoda: Avialae) from the Late Cretaceous of Mongolia. American Museum Novitates 3105: 1–29.

Perle, A., M.A. Norell, and J.M. Clark. 1999. A new maniraptoran theropod—*Achillobator giganticus* (Dromaeosauridae)—from the Upper Cretaceous of Burkhant, Mongolia. Ulan Bator, Mongolia: Geology and Mineralogy Chair, National University of Mongolia, 105 pp.

Prieto-Márquez, A., and J.R. Wagner. 2009. *Pararhabdodon isonensis* and *Tsintaosaurus spinorhinus*: a new clade of lambeosaurine hadrosaurids from Eurasia. Cretaceous Research 30: 1238–1246.

Quintana, J., M. Köhler, and S. Moyà-Solà. 2011. *Nuralagus rex*, gen. et sp. nov., an endemic insular giant rabbit from the Neogene of Minorca (Balearic Islands, Spain). Journal of Vertebrate Paleontology 31: 231–240.

Raia, P., and S. Meiri. 2006. The island rule in large mammals: paleontology meets ecology. Evolution 60: 1731–1742.

Raia, P., C. Barbera, and M. Conte. 2003. The fast life of a dwarfed giant. Evolutionary Ecology 17: 293–312.

Sander, P.M., and N. Klein. 2005. Developmental plasticity in the life history of a prosauropod dinosaur. Science 310: 1800–1802.

Sander, P.M., O. Mateus, T. Laven, and N. Knötschke. 2006. Bone histology indicates insular dwarfism in a new Late Jurassic sauropod dinosaur. Nature 441: 739–741.

Senter, P. 2006. Comparison of forelimb function between *Deinonychus* and *Bambiraptor* (Theropoda: Dromaeosauridae). Journal of Vertebrate Paleontology 26: 897–906.

Sereno, P.C. 1997. The origin and evolution of dinosaurs. Annual Review of Earth and Planetary Science 25: 435–489.

Smith, T., et al. 2002. A new exceptional vertebrate site from the Late Cretaceous of the Haţeg Basin (Romania). Studia Universitatis Babeş-Bolyai, Geologia, Special issue 1: 321–330.

Sondaar, P.Y. 1977. Insularity and its effect on mammal evolution. *In* M.N. Hecht, P.C. Goody, and B.M. Hecht (editors), Major patterns in vertebrate evolution, 671–707. New York: Plenum.

Sondaar, P.Y. 1994. Paleoecology and evolutionary patterns in horses and island mammals. Historical Biology 8: 1–13.

Stein, K., et al. 2010. Small body size and extreme cortical bone remodeling indicate phyletic dwarfism in *Magyarosaurus dacus* (Sauropoda: Titanosauria). Proceedings of the National Academy of Sciences of the United States of America 107: 9258–9263.

Theodorou, G.E., S.I. Roussiakis, A. Athanassiou, I. Giaourtsakis, and I. Panayides. 2007. A Late Pleistocene endemic genet (Carnivore, Viverridae) from Aghia Napa, Cyprus. Bulletin of the Geological Society of Greece 40: 201–208.

Therrien, F. 2005. Palaeoenvironments of the latest Cretaceous (Maastrichtian) dinosaurs of Romania: insights from fluvial deposits and paleosols of the Transylvanian and Hateg basins. Palaeogeography, Palaeoclimatology, Palaeoecology 218: 15–56.

Turner, A.H., D. Pol, J.A. Clarke, G.M. Erickson, and M.A. Norell. 2007a. A basal dromaeosaurid and size evolution preceding avian flight. Science 317: 1378–1381.

Turner, A.H., P.J. Makovicky, and M.A. Norell. 2007b. Feather quill knobs in the dinosaur *Velociraptor*. Science 317: 1721.

Turner, A.H., D. Pol, and M.A. Norell. 2011. Anatomy of *Mahakala omnogovae* (Theropoda: Dromaeosauridae), Tögrögiin Shiree, Mongolia. American Museum Novitates 3722: 1–66.

Turner, A.H., P.J. Makovicky, and M.A. Norell. 2012. A review of dromaeosaurid systematics and paravian phylogeny. Bulletin of the American Museum of Natural History 371: 1–206.

Van der Geer, A.A.E. 2005. Island ruminants and parallel evolution of functional structures. *In* E. Crégut-Bonnoure (editor), Les ongulés holarctiques du Pliocène et du Pléistocène, 231–240. Paris: Maison de la Géologie.

Van der Geer, A.A.E. 2008. The effect of insularity on the eastern Mediterranean early cervoid *Hoplitomeryx*: the study of the forelimb. Quaternary International 182: 145–159.

Van der Geer, A., M. Dermitzakis, and J. de Vos. 2006a. Relative growth of the metapodals in a juvenile island deer: *Candiacervus* (Mammalia, Cervidae) from the Pleistocene of Crete. Hellenic Journal of Geosciences 41: 119–125.

Van der Geer, A., J. de Vos, G.A. Lyras, and M.D. Dermitzakis. 2006b. New data on the Pleistocene Cretan deer *Candiacervus* sp. II (Cervinae, Mammalia). Courier Forschnung-Institut Senckenberg 256: 131–137.

Van der Geer, A., G.A. Lyras, J. de Vos, and M.D. Dermitzakis. 2010. Evolution of island mammals: adaptation and extinction of placental mammals on islands. Oxford: Wiley-Blackwell.

van Heteren, A.H. 2012. The hominins of Flores: insular adaptations of the lower body. Comptes Rendus Palevol 11 (2–3): 169–179, [doi:10.1016/j.crpv.2011.04.001]

Van Valen, L. 1973. A new evolutionary law. Evolutionary Theory 1: 1–33.

Vasile, Ş. 2008. A new microvertebrate site from the Upper Cretaceous (Maastrichtian) deposits of the Haţeg Basin. Sargetia 21: 4–14.

Vickers-Rich, P., L.M. Chiappe, and S. Kurzanov. 2002. The enigmatic birdlike dinosaur *Avimimus portentosus*: comments and a pictorial atlas. *In* L.M. Chiappe and L.M. Witmer (editors), Mesozoic birds: above the heads of dinosaurs, 65–86. Berkeley: University of California Press.

Vremir, M. 2010. New faunal elements from the late Cretaceous (Maastrichtian) continental deposits of Sebeş area (Transylvania). Terra Sebus. Acta Musei Sabesiensis 2: 635–684.

Vullo, R., D. Neraudeau, and T. Lenglet. 2007. Dinosaur teeth from the Cenomanian of Charentes, western France: evidence for a mixed Laurasian-Gondwanan assemblage. Journal of Vertebrate Paleontology 27: 931–943.

Weishampel, D.B., and C.-M. Jianu. 1996. New theropod dinosaur material from the Haţeg Basin (Late Cretaceous, western Romania). Neues Jahrbuch für Geologie und Paläontologie Abhandlung 200: 387–404.

Weishampel, D.B., and C.-M. Jianu. 2011. Transylvanian dinosaurs. Baltimore: Johns Hopkins University Press.

Weishampel, D.B., et al. 2004. Dinosaur distribution. *In* D.B. Weishampel, P. Dodson, and H. Osmólska (editors), The Dinosauria (2nd ed.), 517–606. Berkeley: University of California Press.

Weishampel, D.B., D. Grigorescu, and D.B. Norman. 1991. The dinosaurs of Transylvania. National Geographic Research 7: 196–215.

Weishampel, D.B., D.B. Norman, and D. Grigorescu. 1993. *Telmatosaurus transsylvanicus* from the Late Cretaceous of Romania: the most basal hadrosaurid dinosaur. Palaeontology 36: 361–385.

Weishampel, D.B., C.-M. Jianu, Z. Csiki, and D.B. Norman. 2003. Osteology and phylogeny of *Zalmoxes* (n.g.), an unusual euornithopod dinosaur from the latest Cretaceous of Romania. Journal of Systematic Palaeontology 1: 65–123.

Weishampel, D.B., Z. Csiki, M.J. Benton, D. Grigorescu, and V. Codrea. 2010. Palaeobiogeographic relationships of the Haţeg biota—between isolation and innovation. Palaeogeography, Palaeoclimatology, Palaeoecology 293: 419–437.

Weston, E.M., and A.M. Lister. 2009. Insular dwarfism in hippos and a model for brain size reduction in *Homo floresiensis*. Nature 459: 85–89.

Xu, X., and X.-L. Wang. 2004. A new dromaeosaur (Dinosauria: Theropoda) from the Early Cretaceous Yixian Formation of western Liaoning. Vertebrata PalAsiatica 42: 111–119.

Xu, X., X.-L. Wang, and X.-C. Wu. 1999. A dromaeosaurid dinosaur with a filamentous integument from the Yixian Formation of China. Nature 401: 262–266.

Xu, X., Z. Zhou, and X. Wang. 2000. The smallest known non-avian theropod dinosaur. Nature 408: 705–708.

Xu, X., M.A. Norell, X.-L. Wang, P.J. Makovicky, and X.-C. Wu. 2002. A basal troodontid from the Early Cretaceous of China. Nature 415: 780–784.

Xu, X., Z. Zhou, X. Wang, X. Kuang, F. Zhang, and X. Du. 2003. Four-winged dinosaurs from China. Nature 421: 335–340.

Xu, X., et al. 2006. A basal tyrannosauroid dinosaur from the Late Jurassic of China. Nature 439: 715–718.

Xu, X., et al. 2010. A new dromaeosaurid (Dinosauria: Theropoda) from the Upper Cretaceous Wulansuhai Formation of Inner Mongolia, China. Zootaxa 2403: 1–9.

Zanno, L.E. 2006. The pectoral girdle and forelimb of the primitive therizinosauroid *Falcarius utahensis* (Theropoda, Maniraptora): analyzing evolutionary trends within Therizinosauroidea. Journal of Vertebrate Paleontology 26: 636–650.

Zhou, Z., and F. Zhang. 2002. A long-tailed, seed-eating bird from the Early Cretaceous of China. Nature 418: 405–409.

Zhou, Z., and F. Zhang. 2003. Anatomy of the primitive bird *Sapeornis chaoyangensis* from the Early Cretaceous of Liaoning, China. Canadian Journal of Earth Sciences 40: 731–747.